Covalent Surface Modification of Silicon Oxides

by

Austin Woohyuk Lee

B.A.Sc., University of Waterloo, 2012

Thesis Submitted in Partial Fulfillment of the
Requirements for the Degree of
Doctor of Philosophy

in the
Department of Chemistry
Faculty of Science

SIMON FRASER UNIVERSITY

Summer 2017

Approval

Name:	**Austin W.H. Lee**
Degree:	**Doctor of Philosophy**
Title:	***Covalent Surface Modification of Silicon Oxides***
Examining Committee:	**Chair:** Dr. Tim Storr Associate Professor

Dr. Byron Gates
Senior Supervisor
Associate Professor _____

Dr. Vance Williams
Supervisor
Associate Professor _____

Dr. Paul Li
Supervisor
Professor _____

Dr. Woo Soo Kim
Supervisor
Associate Professor _____

Dr. Gary Leach
Internal Examiner
Associate Professor _____

Dr. Tricia B. Carmichael
External Examiner
Associate Professor
Department of Chemistry
University of Windsor _____

Date Defended/Approved: August 30, 2017

Abstract

Microwave radiation was utilized as a tool to modify surface properties of silicon oxides. Covalent surface modification of silicon oxides has been widely pursued in the areas of material science, electronics, microfluidics, biology, and separation science. Chemical surface modifications are often achieved through the formation of organic monolayers, often referred to as self-assembled monolayers (SAMs). While these organic monolayers have been proposed as an effective surface modification strategy, the defects in these organic monolayers compromise the effectiveness on their ability to alter surface properties. For example, in the case of passivation of microscale electronic devices, the surfaces that are not covered by the organic monolayers are susceptible to environmental stress or corrosion, which can cause detrimental failures of the devices. Traditional methods of formation of monolayers often cause many defects including formation of multilayers or micelles, physically adsorbed organic film, and/or voids. In this thesis, microwave radiation is utilized as a tool to accelerate the formation of uniform monolayers. In particular, the formation of silane based monolayers and alcohol based monolayers on silicon oxide surfaces have been extensively studied. Microwave heating, unlike the traditional heating methods, delivers the thermal energy to the substrate surfaces. It can effectively accelerate the formation of both silane and alcohol based monolayers. Alcohol based reagents, in particular, is proposed as an alternative building blocks for their widespread availability and minimal reactivity with moisture. Tuning of surface chemistry of silicon oxides have been achieved with alcohol based regents with different functional groups. Furthermore, the formation of mixed monolayers has been proposed as means of controlling oleophobicity of the silicon oxide surfaces. Finally, the film thickness of the alcohol based monolayers has been characterized with angle-resolved X-ray photoelectron spectroscopy (ARXPS). The film thickness can be precisely tuned by choosing the alcohol based reactants with particular lengths of alkyl chains. A variety of surface chemistry can be designed towards many practical applications requiring surface functionalized silicon oxides using the research presented herein.

Keywords: Microwave, surface modification, silicon oxides, self-assembled monolayer, hydrophobicity, oleophobicity, alkylsilanes, alcohols

To my beloved family

Acknowledgements

I would like to sincerely thank my senior supervisor, Dr. Byron Gates, for providing me the opportunity to work with him. I truly appreciate his continued support and guidance throughout my graduate career.

I also thank my committee members – Dr. Vance Williams, Dr. Paul Li, Dr. Woo Soo Kim – for their valuable advice and encouragement, which greatly helped to improve my research and presentation skills.

I thank the industry collaborators, in particular the SkyTap team for their interest and support to my research. The industry sponsorship helped me greatly to think through the practical usage of my research.

I would like to thank the technicians and engineers at 4D LABS for their help on training of the tools as well as advice on interpretation of the results. I thank Dr. Rob Britton and his students for access to their microwave reactor that helped me to pursue my research.

I would also like to thank my colleagues for the opportunity to work with them at SFU. I thank for the memories that we built together not only as co-workers but also great friends whom I enjoyed talking about research, grabbing coffee or beer together.

Finally, I thank my family for their continued support and gracious love.

Table of Contents

List of Tables

List of Figures

List of Acronyms

AFM	Atomic force microscopy
ARXPS	Angle-resolved X-ray photoelectron spectroscopy
b.p.	Boiling point
CAD	Canadian dollars
c_p	Specific heat capacity
d	Film thickness
E_b	Binding energy
E_k	Kinetic energy
E_{RMS}	Root mean square value of microwave energy
f	Frequency
FDDCS	1*H*,1*H*,2*H*,2*H*-perfluorodecyldimethyl-cholorosilane
FDTS	1*H*,1*H*,2*H*,2*H*-perfluorodecyltrichlorosilane
GHz	Gigahertz
H	Hysteresis
HDPDT	(5-(hexadecyloxy)-1,3-phenylene)-dimethanethiol
h	Plank's constant
v	Photon's frequency
KPFM	Kelvin probe force microscopy
LFM	Lateral force microscopy
m	Mass
MEMS	Microelectromechanical systems
OTS	Octadecyltrichlorosilane
P	Power
PFDDT	(5-(9,9,10,10,11,11,12,12,13,13,14,14,15,15,16,16,16-heptadecafluorohexadecyloxy)-1,3-phenylene)dimethanethiol
Q	Heat energy
RMS	Root mean square
SAMs	Self-assembled monolayers
SEM	Scanning electron microscopy
SiO_x	Silicon oxide
T	Temperature

t	Time
T_0	Initial temperature
T-BAG	Tethering by aggregation and growth
W	Watts
WCA	Water contact angle
XPS	X-ray photoelectron spectroscopy
γ	Surface tension
ε	Dielectric constant
ε_0	Permittivity of free space (8.85×10^{-12} F/m)
θ_a	Advancing contact angle
θ_r	Receding contact angle
θ_Y	Young's contact angle
λ	Attenuation length of emitted photoelectrons
μ	Permeability
μ_0	Permeability of free space (1.26×10^{-6} H/m)
µCP	Microcontact printing
σ	Conductivity
ω	Angular frequency
Φ_s	Work function

Glossary

Byproduct	A secondary product from a chemical reaction.
Microwave	A form of electromagnetic radiation with frequencies between 300 MHz and 300 GHz.
Condensation reaction	A chemical reaction in which two molecules combine to form a larger molecule while producing a small molecule as a byproduct.
Dielectric heating	A form of electronic heating induced by a high-frequency alternating electric field such as microwave electromagnetic radiation. Dielectric heating is caused by molecular dipole rotation within a dielectric material.
Head group	A functional group responsible for bonding of organic monolayers to the substrate surfaces.
Tail group	A functional group located at the top of the organic monolayers. This group is also referred to as a terminal group.
Hydrophobicity	A measure of resistance to wetting water.
Lossy dielectric	A medium in which an electromagnetic wave loses power as the wave propagates the medium.
Monoreactive	Having one reactive group within a molecule for a chemical reaction.
Oleophobic	A measure of resistance to wetting oil.
Permeability	A proportionality constant between magnetic induction and magnetic field intensity. It describes the ability for a material to form magnetic fields within itself.
Permittivity	A measure of resistance encountered when forming an electric field in a medium.
p-type	A type of extrinsic semiconductor that has deficiencies of valence electrons by addition of trivalent impurities such as boron, aluminum or gallium.
Self-Assembled Monolayers	Molecular assemblies of compounds that are formed spontaneously by intermolecular interactions.
van der Waals forces	Attractive or repulsive forces between molecules, atoms, and surfaces. They also include intermolecular forces. Examples of the van der Waals forces include London dispersion and dipole-dipole forces.

Chapter 1.

Introduction

1.1. Introduction to Self-Assembled Monolayers (SAMs)

1.1.1. Motivations

Silicon oxides are one of the most widely utilized materials for their accessibility and chemical inertness. The surfaces of silicon oxides are modified using self-assembled monolayers (SAMs), which refer to a single molecule layer film that is formed by the self-assembly of organic molecules on surfaces.[1-4] The modification of silicon oxide surfaces has been of great interest and importance in many fields including electronics,[5-10] microfluidics,[11-15] printing,[16-20] passivation,[21-25] separation sciences,[26-29] electrochemical sensing,[30-35] and biological interfaces.[2, 36-45] The SAMs can effectively modify surface properties of silicon oxides without altering the properties of the underlying material. Typical thickness of SAMs range from 0.5 nm to 3 nm, and they do not play a significant role in changing the bulk properties of the underlying material. The precursors of the SAMs consist of head group, spacer group, and terminal group (Figure 1.1). Head group is responsible for covalent bonding, or similar interactions, between the organic precursor and the substrate. The spacer group typically consists of a long alkyl chain, which is responsible for driving self-assembly of the precursors via van der Waals forces. The terminal group dictates the surface properties (e.g., hydrophobic, hydrophilic, surface charge) of the resulting SAMs. The utilization of these organic monolayers has been limited in part by challenges of forming uniform monolayers with organic precursors due to their susceptibility to competing reactions (e.g., hydrolysis), intermolecular polymerization, commercial accessibility, and toxicity.[46]

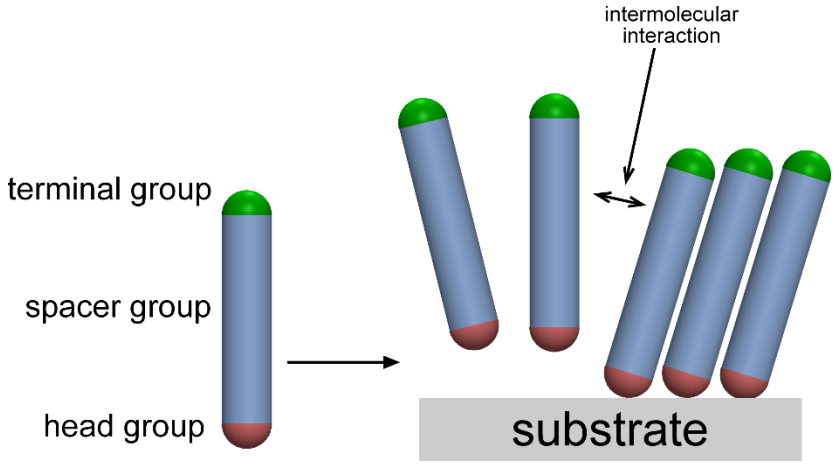

Figure 1.1. Structure of self-assembled monolayers (SAMs) and their mechanism of self-assembly on surfaces of a substrate.

Limitations of the SAMs are well pronounced in the literature for the application of passivation against etchants of an underlying material. For example, patterning of copper substrates was demonstrated using patterning thiol based SAMs (Figure 1.2).[21, 23] The SAMs are utilized for passivation of underlying copper film against wet etchants. It is important for these monolayers to be closely packed with few defects, as depicted in Figure 1.2A. In reality, these thiol based SAMs were formed with substantial amount of defects as depicted in Figure 1.2B. Such defects in the monolayers can lead to catastrophic failure for passivation of underlying film. This catastrophic failure was clearly demonstrated by scanning electron microscope (SEM) images of the defects in the copper thin film (Figure 1.2C). The quality of SAMs are affected by processing conditions as well as the type of substrate and precursors used for the process. For example, the quality of SAMs have been monitored and characterized with respect to a variety of processing parameters, such as temperature of the reaction, concentration of the reagent, solvent compositions, and the type of precursors.[1, 37, 47-50] It is generally reported that an increase in temperature will increase the rate of formation of monolayers while decreasing the ordering of the SAMs.[51-52] The rate of formation of monolayers increases as the concentration of the precursors increase.[48, 53] Also, the increase in alkyl chain length of the precursors will increase the rate of formation of SAMs due to the increase in intermolecular interactions for the SAMs that consist of linear alkyl chains.[53] These intermolecular interactions can vary depending on the functional groups.[47, 54] In summary,

many efforts have been made to study the mechanisms of the formation of SAMs towards improving the overall quality of the organic monolayers on surfaces.

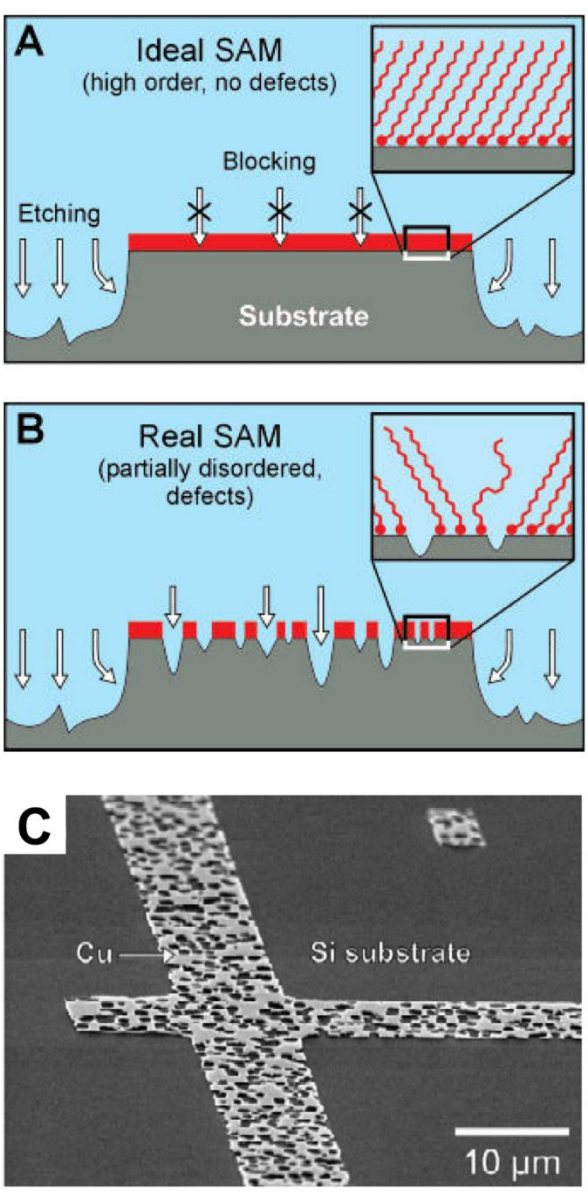

Figure 1.2. **Schematic depictions of etching of substrates patterned with (A) ideal SAMs and (B) real SAMs. Defects in the real SAMs can cause catastrophic failure in passivation of underlying material. (C) An SEM image of a copper pattern obtained from micro-contact printing (µCP) of SAMs. As depicted in the image, the copper patterns exhibit substantial amount of defects due to the production of disordered, defective SAMs. Adapted with permission from Ref. [21] ©2002 American Chemical Society and Ref. [23] ©2003 Elsevier.**

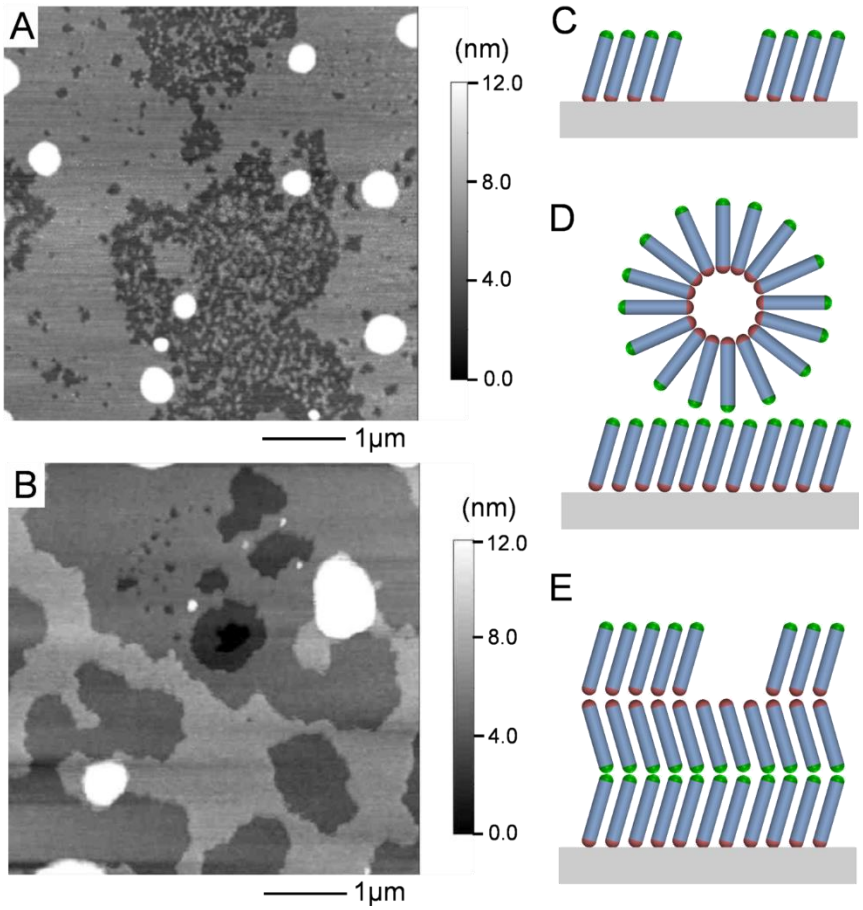

Figure 1.3. **(A,B) Atomic force microscope (AFM) images of fluoroalkylsilane-based SAMs on silicon oxide surfaces formed in toluene. (C,D,E) Schematic depictions of different types of defects observed in the organic monolayers.**

Despite the efforts to optimize the processing techniques and conditions, the formation of uniform SAMs covalently attached to silicon oxide surfaces is still a challenging task. For instance, silane based precursors need to be handled carefully because they are moisture sensitive compounds. Precise control over water content (less than a few micromoles) is important for the formation of uniform silane based monolayers.[46, 55] Upon poor management of water content, the silane based precursors cause formation of multilayers, which can be easily observed with AFM, as shown in Figure 1.3A and B. The observed defects on the substrates are described in Figure 1.3C, D, and E. Defects in the SAMs can expose surfaces of the underlying material to the environment. These are caused by non-uniform coverage of the organic molecules at the

surfaces. This type of defect can cause detrimental failure in passivation of the underlying material as shown in Figure 1.2. Another type of defect is the formation and deposition of micelles at the interface. This phenomenon is common especially if the molecular structure of the precursors is amphiphilic, with a hydrophobic tail and a polar head group. When the micelles form, they can be physically adsorbed to the surface through intermolecular interactions (Figure 1.3D). Formation of multilayers is another common defect observed in the formation of SAMs (Figure 1.3E). Layers of the organic precursors can deposit through weak interactions, causing non-uniformity in the organic monolayers and compromising the surface functionality. The properties of the organic precursors will fundamentally affect the design of experiments, such as processing conditions for the formation of SAMs. Therefore, it is necessary to understand the types of organic precursors utilized for the formation of SAMs.

1.1.2. Building Blocks for Preparing SAMs

Many types of organic precursors have been utilized to covalently modify surface properties of silicon oxides.[2] In particular, the four types of organic precursors widely studied in the literature include thiols,[1, 48, 56] phosphonic acids,[52, 57-59] silanes,[3, 6, 60] and alcohols.[2, 61-65] Figure 1.4 provides an overview of the chemical structures of these materials and their structures when they are anchored onto surfaces as they form organic monolayers. Thiols are one of the most widely studied SAMs for the modification of metal surfaces. Thiolate bonds readily form a covalent bond with metal surfaces (S–M), making them ideal to control the surface properties of a variety of metals including platinum, gold, silver, or copper.[1, 37, 66-70] On the other hand, hydrolytic or thermal stability of thiolate on these surfaces is relatively poor.[71-72] Moreover, the thiols do not covalently attach on silicon oxide surfaces,[73] and thiols on silicon oxide surfaces have not been studied extensively in the literature.[2]

Phosphonates are becoming popular as they can form uniform organic monolayers on a variety of oxide surfaces.[2, 74-77] The advantages of phosphonic acids are in the high uniformity of the resulting monolayers and the ease of processing. A variety of solvents including water can be utilized for the formation of SAMs derived from phosphonic acids. The most well-known technique for the modification of silicon oxide surfaces with

phosphonic acids is the “tethering by aggregation and growth” (T-BAG) method.[52, 78-79] This approach starts by immersion of substrates in solution containing the precursors. The solution is evaporated, while the phosphonic acids are physically adsorbed on the surfaces. The substrates are subsequently annealed for days to covalently bond the phosphonic acids with hydroxyl terminated oxide surfaces. The major drawbacks are the processing conditions and long reaction times to obtain covalently attached organic monolayers with phosphonic acids. Moreover, after the complete covalent attachment, the stability of the resulting monolayers limits their commercial viability for functionalization of oxide surfaces.[72]

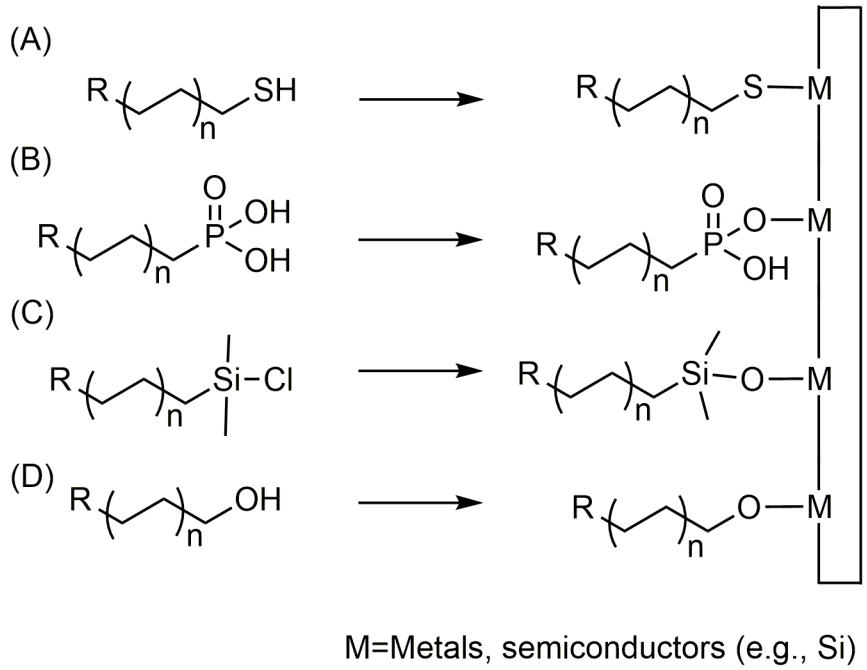

Figure 1.4. Chemical structures of precursors of SAMs (A) thiols, (B) phosphonic acids, (C) silanes, and (D) alcohols and their immobilized forms on surfaces.

Silane based precursors can be utilized to form stable organic monolayers on silicon oxide surfaces.[2-3] The silane based precursors covalently attach to hydroxyl terminated surfaces through the formation of the siloxane bond (Si–O–Si).[2] This condensation reaction can proceed in a wide range of temperatures and concentrations. The siloxane bonds have a high bonding energy and are inert to many chemicals, which make the silane based SAMs highly stable.[72] The drawback of silane based precursors is their reactivity with many hydroxyl groups, including water molecules. In the presence of

water the silane based compounds can undergo intermolecular polymerization,[46, 80] leading to formation of multilayers.[46, 55] The formation of multilayers can compromise the desired surface properties while altering the properties of the underlying materials. Moreover, the silane based compounds should be carefully handled and stored to minimize the exposure to moisture and other contaminants.

Alcohols are another candidate for surface modification of silicon oxides. Alcohols can covalently bond with hydroxyl terminated silicon oxide surfaces or hydrogenated silicon surfaces through the formation of silyl ether (Si–O–C).[81] Alcohols are attractive precursors for the formation of monolayers because they are readily accessible. They are not reactive with ambient moisture, and easy to handle, store and process without excessive environmental control. The major shortcoming of using alcohols as precursors to SAMs is their slow reaction kinetics. The covalent attachment of alcohols to silicon oxide surfaces require a substantial amount of thermal energy.[62, 65]

A summary of price, purity, bonding energy of the organic precursors utilized for the formation of some SAMs are shown in Table 1 for comparison. The precursors that consist of the head group and a long alkyl chain with 18 carbons were compared because of their widespread usage to tune properties of surfaces.[1-3] In order to create stable organic monolayers for surface modification of silicon oxides, silanes and alcohol based reagents were chosen as precursors in this thesis work. Effective methods that enable the rapid formation of uniform silane and alcohol based SAMs without forming other defects were developed and pursued throughout this thesis.

Table 1.1. Price, purity, bonding energy comparison of counterparts of different types of precursors used for formation of SAMs. Prices were acquired from Sigma-Aldrich as of date May 24, 2017 in Canadian dollars (CAD).

Types of precursors	Example	Purity	Bond energy (kJ/mol)	Price
thiols	1-octadecanethiol	98%	188	$1.09/1g
phosphonic acid	octadecylphosphonic acid	97%	334	$94.50/1g
silanes	trichloro(octadecyl)silane	>90%	452	$1.27/1g
alcohols	1-octadecanol	99%	358	$0.51/1g
alcohols	1-octadecanol	95%	358	$0.08/1g

1.2. Introduction to Dielectric Heating

1.2.1. Principle of Microwave Heating

Microwave induced heating has been widely used in food processing,[82] organic chemistry,[83-88] sintering,[89-96] and nanomaterial synthesis.[86, 94, 97-101] One of the most noteworthy benefits to microwave heating in chemistry is the speed of reaction. Microwaves can heat a system rapidly, which allows researchers to synthesize the desired material promptly. Microwave heating is also considered to be a “green” synthetic tool because the energy efficiency is considered to be higher compared to incumbent heating methods.[99] The microwave reactions can enable the design of synthetic routines that are more environmentally friendly. Another benefit of microwave heating includes its unique properties with regards to rate of heating different materials, which depends on the electromagnetic properties of the materials.

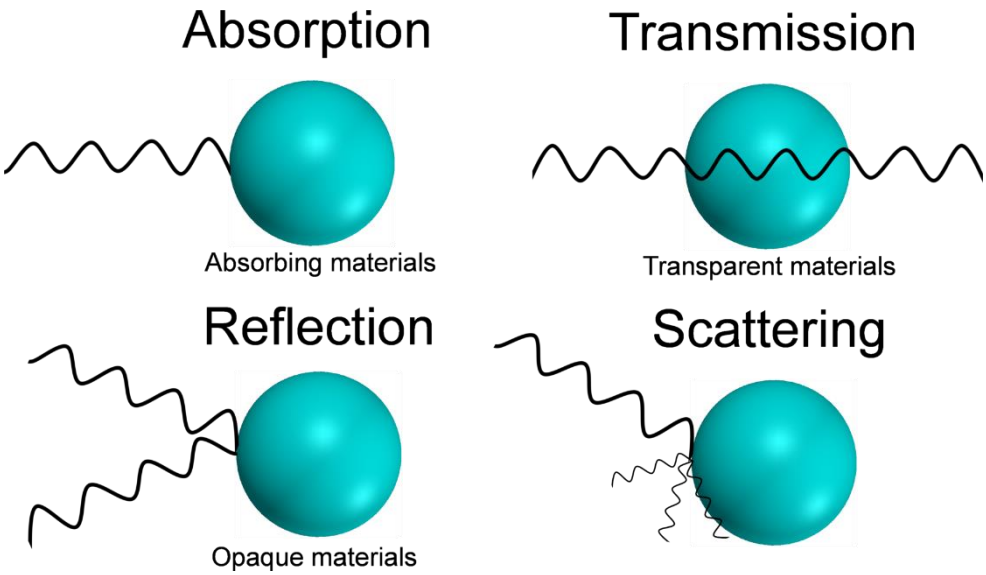

Figure 1.5. Different interactions of microwaves with a material.

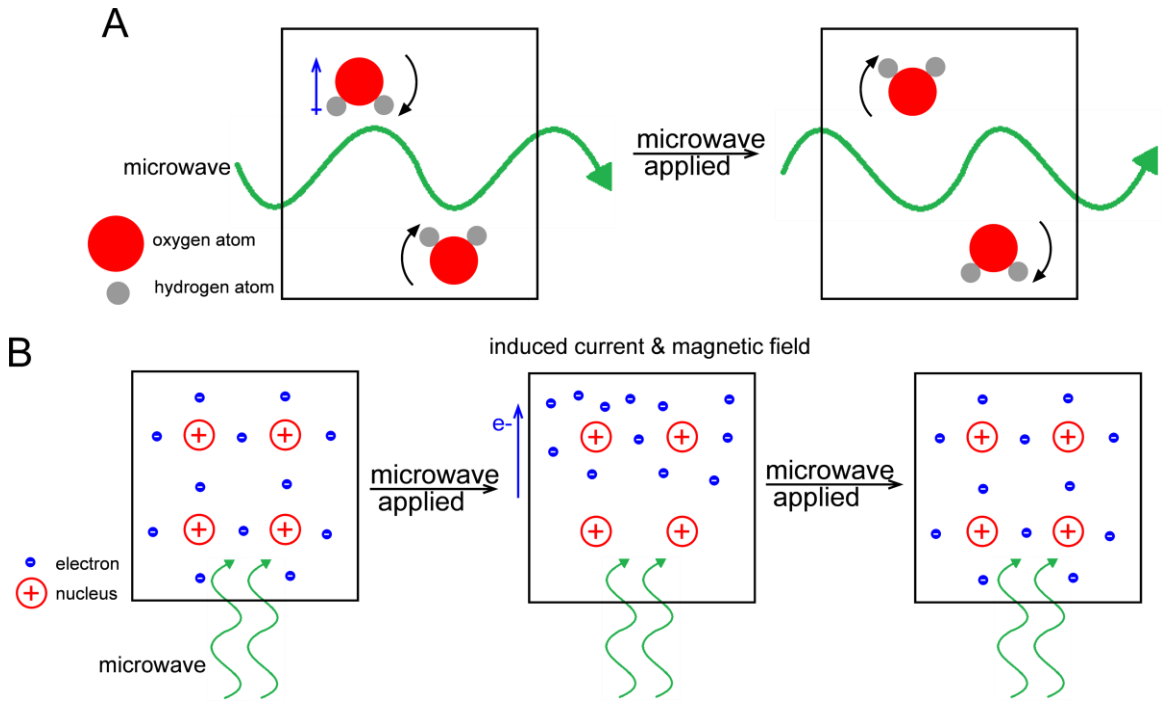

Figure 1.6. Mechanism of microwave heating through (A) dielectric loss induced by polarization of materials and (B) conduction loss induced by generation of electric current within a conductive material.

Microwaves interact with materials in many ways (Figure 1.5). Lossy dielectric materials absorb the electromagnetic energy from the microwave and covert it to heat. Transparent materials with low dielectric loss reflect or absorb electromagnetic waves to a negligible amount. These materials allow microwaves to pass through with little attenuation. Some conducting materials with free electrons can reflect or scatter electromagnetic waves, and do not allow the microwaves to pass through. Among these interactions, microwave heating occurs when the microwaves get absorbed by the material. There are many mechanisms by which the microwaves can get absorbed by a material. For instance, materials with high conductivity such as metals get heated based on conduction losses.[89, 91, 94, 102-106] Free electrons in these materials move in the direction of external electric field, inducing electric current. This current generates a magnetic field that is in the opposite direction of the external magnetic field. This induced magnetic field generates eddy currents, which generate resistive heating within the material. Dielectric insulators, including organic compounds, absorb microwave radiation via polarization of atoms and molecules in the presence of external electric fields, referred to as dielectric

loss. Atoms or molecules in the material attempt to align their dipole with the oscillating electric field.[84, 107-108] The induced molecular motion causes dielectric heating of the solution. Magnetic materials will interact with external magnetic field created from microwaves.[91, 94] The microwave heating can be further understood by estimating the amount of power dissipated from the material through conversion of electromagnetic energy to heat.

In order to describe microwave heating, one must first understand the dielectric response of a material to an alternating electric field. Dielectric constant, ε', (also known as relative permittivity) describes the ability of a material to polarize in response to the applied electric field. For heating of dielectric materials, it is assumed that the microwave absorption and heating occurs due to the alternating electric field.[109] In order to account for the losses in the response to a material exposed to electromagnetic wave, the complex permittivity, ε*, is introduced:[109]

$$\varepsilon^* = \varepsilon' - j\varepsilon'' \tag{1.1}$$

where ε" represents the dielectric loss factor. The response of a material to a magnetic field can be described with permeability, μ'. Similar to dielectric loss from microwave heating, the losses of a material due to an alternating magnetic field can be expressed with the complex permeability, μ*:

$$\mu^* = \mu' - j\mu'' \tag{1.2}$$

where μ" is a magnetic loss factor due to response under the influence of an alternating magnetic field. The power dissipated into or absorbed by the material by the conversion of microwave energy into heat is given by the following equations:[109-112]

$$P_{total} = P_{elec} + P_{mag} \tag{1.3}$$

$$P_{mag} = \omega\mu_0\mu''_{eff}E^2_{RMS} \tag{1.4}$$

$$P_{elec} = \omega\varepsilon_0\varepsilon''_{eff}E^2_{RMS} \tag{1.5}$$

where ω is the angular frequency (can be written as 2πf, where f is the frequency of microwave), E_{RMS} is the root mean square value of the electric field, $\mu"_{eff}$ is the effective relative magnetic loss factor, and $\varepsilon"_{eff}$ is the effective relative dielectric loss factor. The $\varepsilon"_{eff}$ is a summation of the effective dielectric and conduction losses. The effective conduction loss can be expressed with electric conductivity of the material (σ), angular frequency (ω), and permittivity of free space (ε_0).

$$\varepsilon"_{eff} = \varepsilon"_{polarization} + \varepsilon"_{conduction} = \varepsilon"_{polarization} + \frac{\sigma}{\varepsilon_0} \tag{1.6}$$

If we assume that there is no power dissipated due to magnetic loss, we can rewrite the equation:

$$P_{total} = P_{elec} = \omega\varepsilon_0\varepsilon"_{eff}E_{RMS}^2 = \omega\varepsilon_0(\varepsilon"_{polarization} + \frac{\sigma}{\varepsilon_0})E_{RMS}^2 \tag{1.7}$$

If we assume that all of the power dissipated is converted to heat, then we can equate the power (as denoted by P_{total} in Equation 1.8 below) to heat transfer equation (shown in Equation 1.8 below) and isolate the rate of the change in temperature of a system:

$$P_{total} = \frac{Q}{t} = \frac{mc_p(T-T_0)}{t} \tag{1.8}$$

$$\frac{\Delta T}{\Delta t} = \frac{(T-T_0)}{t} = \frac{P_{total}}{mc_p} = \frac{2\pi f\varepsilon_0 E_{RMS}^2}{mc_p}(\varepsilon"_{polarization} + \frac{\sigma}{\varepsilon_0}) \tag{1.9}$$

As shown in the equation, the change in temperature will depend on the dielectric loss factor ($\varepsilon"_{polarization}$), electric conductivity (σ), microwave power (E_{RMS}), microwave frequency (f), and specific heat capacity (c_p). In particular, the rate of microwave heating will largely depend on the dielectric loss factor. For instance, fused quartz and Teflon are insulators with low dielectric loss factor (ε"=0.001), and they will absorb little microwave energy. In contrast, distilled water possess a relatively high dielectric loss factor (ε"=12.0), and it readily absorbs the microwave. The rate of microwave heating also depends on the temperature of the material because the dielectric loss factor is a temperature dependent term. In the case of many dielectric materials in liquid state, the dielectric loss factor decreases as the temperature increases.[99] Water and many organic solvents exhibit the low rate of change in temperature as their temperatures increase. A temperature profile

portrayed in Figure 1.7 demonstrates that the rate of change in temperature of 1-octanol exposed to microwave radiation with a constant power decreases as the temperature of 1-octanol increases. In the beginning of the temperature profile, the temperature is maintained at ~20 °C while the microwave reactor is initiating the reaction, followed by a rapid increase in the reaction temperature due to the microwave heating. In some cases, dielectric loss factor may increase as the temperature of the material increases. For example, undoped silicon at 25°C has ε'=4.3 and ε"<0.05 at 1GHz, while the same material at 300°C has ε'=9 and ε"=1.3 at 1GHz.[109] It is anticipated that the rate of change in temperature will increase as the temperature of the material increases for intrinsic silicon.

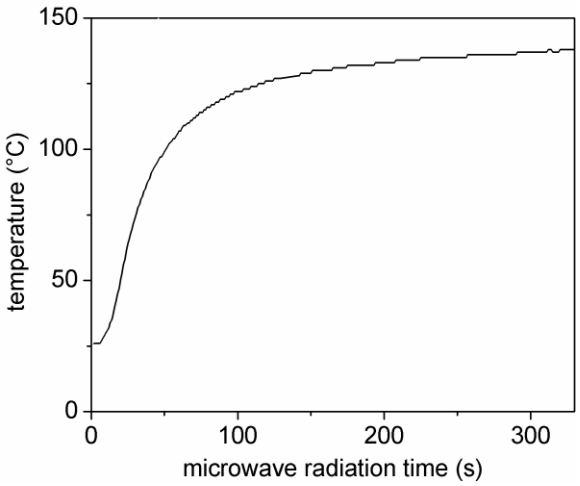

Figure 1.7. A temperature profile of 2 mL of 1-octanol exposed to 300 W microwave heating for ~5 min. The experiment was performed using CEM microwave reactor. Adapted with permission from Ref. [205] ©2016 American Chemical Society

1.2.2. Benefits of Microwave Heating in Surface Chemistry

Microwave heating has been utilized for many applications including organic material synthesis, nanomaterial synthesis, and solid state synthesis.[83-85, 89-91, 94, 98-99, 102-103, 113] Microwave heating provides several interesting traits to these applications over traditional methods of heating. First, microwave heating can facilitate the chemical reaction to reduce the reaction time.[84-85, 99, 107] The convective heating relies on the diffusion of thermal energy from the outside of the reaction vessel. In contrast, the microwave energy delivers the thermal energy directly to the molecules within the vessel.

The microwave heating is a more effective method to deliver thermal energy for the chemical reactions to occur when compared with convective heating. Second, the pressurized microwave chambers provide an environment that enables high temperature processing with little loss of solvents. Many microwave-assisted reactions are carried out at the temperature higher than the boiling points of solvents.[84] The high temperatures provided with the microwave reactors can provide more effective strategies for preparing the wide range of molecules in organic chemistry. Third, the microwaves heats different materials at different rates. As demonstrated in the previous section, the rate of microwave heating is largely dependent on the dielectric or electronic properties of material. This physical phenomenon allows the selective heating of a certain material over other materials in a given system, creating "hot spots" in the microwave heated systems.[84, 89, 91, 94, 99] For instance, doped silicon substrates will absorb microwave to generate heat due to conductive loss, while quartz substrates will not heat upon exposure to microwave as its dielectric or conduction loss will be minimal. An example thermal image of these substrates after exposure to microwave radiation at 900 W for 15 s clearly demonstrates the hot spot is being generated from the heating of doped silicon substrate (Figure 1.8A and B). This unique characteristic is also shown in the temperature profile of microwave reactions that proceeded either with or without a doped silicon substrate (Figure 1.8C). Difference in the reaction temperature over the microwave-assisted reaction at constant power and time is attributed to the hot spot generated from microwave heating of a doped silicon substrate.

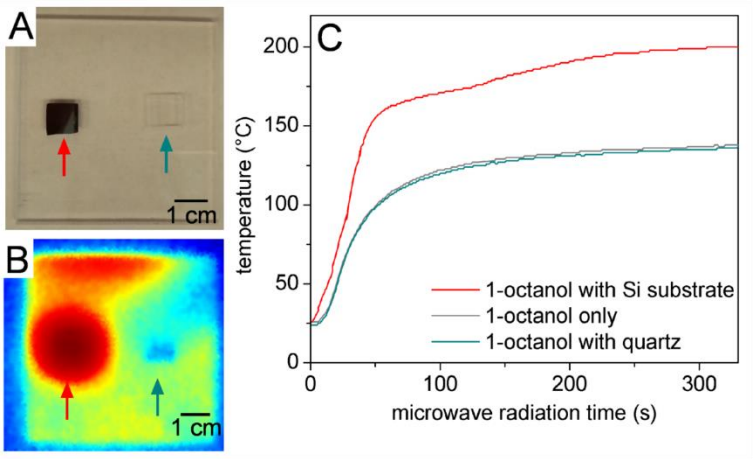

Figure 1.8. **Microwave heating effect – (A) Visible light and (B) infrared images of the silicon and quartz substrates supported on an acrylic plate obtained after direct exposure to microwave radiation for 15 s. (C) Temperature profiles recorded in a 1-octanol solution during exposure to microwave radiation at 300 W for up to 5 min in the presence of either a silicon or quartz substrate as well as in the absence of either substrate. Adapted with permission from Ref. [205] ©2016 American Chemical Society.**

1.3. Characterization Methods

1.3.1. Contact Angle Measurements

One of the most common techniques to evaluate organic monolayers on surfaces is through contact angle measurements.[1-3, 72, 114] The results obtained in these measurements are relevant to fundamental physical characteristics of surfaces, as well as applied sciences. Contact angle measurements can provide information about interfacial properties of surfaces, such as wettability, surface energy, or surface roughness. The information obtained from contact angle studies can be relevant to applications related to lubrication,[59, 115] oil separation and recovery,[116-118] and printing.[16-17] For these reasons, contact angle measurements are one of the most popular methods to assess surface properties of materials, including those coated with organic monolayers.

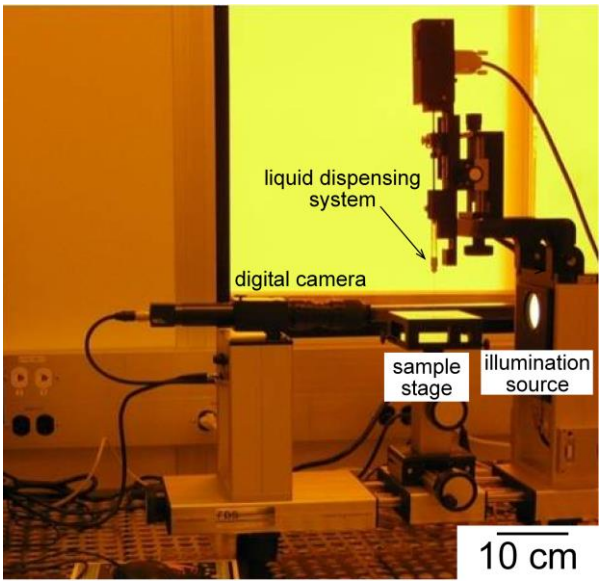

Figure 1.9. A picture of contact angle goniometer. A modern contact angle goniometer consists of a light source, sample stage, a liquid dispensing system (e.g., syringe), and a digital camera or a protractor eyepiece.

To obtain contact angle values, the angle between the air-liquid interface and the solid-liquid interface of a droplet on a solid substrate is measured. The contact angle is measured using a contact angle goniometer (Figure 1.9). The equipment consists of an illumination source, a horizontal stage to mount a solid sample, and a telescope with either a digital camera or a protractor eyepiece.[114] The most widely used technique for measuring contact angle involves the formation of a sessile droplet (i.e. stationary) on a solid surface.[119] This technique starts by dispensing a small volume (typically between 2 to 10 µL) of a liquid onto the surfaces of a substrate using either a liquid dispensing system or a microliter pipette. The angle between the air-liquid interface and the solid-liquid interface of a droplet on a solid substrate is measured with a protractor. This direct optical method is simple and it requires only a few microliters of liquid. On the other hand, the technique can have shortcomings for its accuracy and reproducibility as the measurement relies on the consistency of the operator in the assignment of the tangent line. The direct goniometer method suffers from another limitation – less accuracy in small contact angles (below 20°) due to uncertainty of assigning a tangent line when the droplet profile is almost flat. For surfaces with a high chemical heterogeneity or high roughness in surface topography, the contact angle values can widely vary depending on the location and the

size of the droplet, which results in inconsistencies of the measurements. In case of organic monolayers deposited on flat surfaces, this can largely be ignored as the surfaces should be relatively homogenous and flat. It is generally recognized that such direct measurements of sessile drop contact angles can yield an accuracy of approximately ±2°.[114]

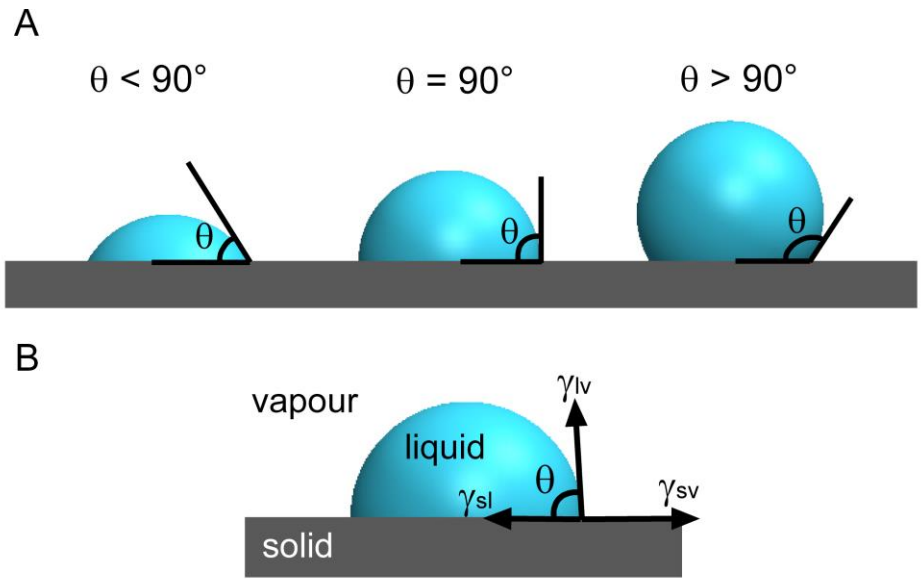

Figure 1.10. (A) Depiction of sessile liquid droplets formed on a smooth, homogeneous surface. In case of water contact angle, hydrophilic surface is defined by θ < 90°, while hydrophobic surface is defined by θ > 90°. (B) Depiction of a stationary liquid droplet showing the surface tensions in the Young equation.

Despite the limitations in accuracy of contact angle measurements, SAMs on flat surfaces are commonly assessed through contact angle measurements (Figure 1.10A).[1-3] The most common liquid used for contact angle studies is water because information on surface hydrophobicity can be obtained from these measurements. Water contact angle (WCA) values of 0° indicate that the surfaces are completely wetted, and is referred to as a hydrophilic state. Surfaces exhibiting WCA values between 0° to 90° are considered hydrophilic, while those exhibiting the values over 90° are considered hydrophobic.[114] Alkyl-terminated organic monolayers on smooth surfaces are evaluated through WCA measurements.[1, 47-48] In the case of organic monolayers on silicon oxide surfaces, hydrophobicity of those coated with or without monolayers differ significantly. Clean silicon oxide surfaces have polar silanol group (Si–OH) at the interface, which makes the surface

hydrophilic (WCA ~20° or less). Surfaces covered with uniform monolayers with alkyl-terminated chain should exhibit hydrophobic surfaces. It is well-known in literature that the WCA values for surfaces covered with alkyl-terminated monolayers should be ~110°.[47-48, 65] The WCA values provide a correlation between the work of adhesion and surface tension of the surfaces using Young's equation (Figure 1.10B):[120-121]

$$\gamma_{lv} \cos \theta_{\gamma} = \gamma_{sv} - \gamma_{sl} \tag{1.10}$$

where γ_{lv}, γ_{sv}, and γ_{sl} represent the liquid-vapor, solid-vapor, and solid-liquid interfacial tensions, respectively. The θ represents the contact angle of the droplet, and sometimes is referred to as Young's contact angle. The contact angle values obtained with non-polar liquid such as hexadecane can provide information about surface oleophobicity. For smooth surfaces coated with uniform fluorinated SAMs, the hexadecane contact angle values range from 75 to 80°.[121]

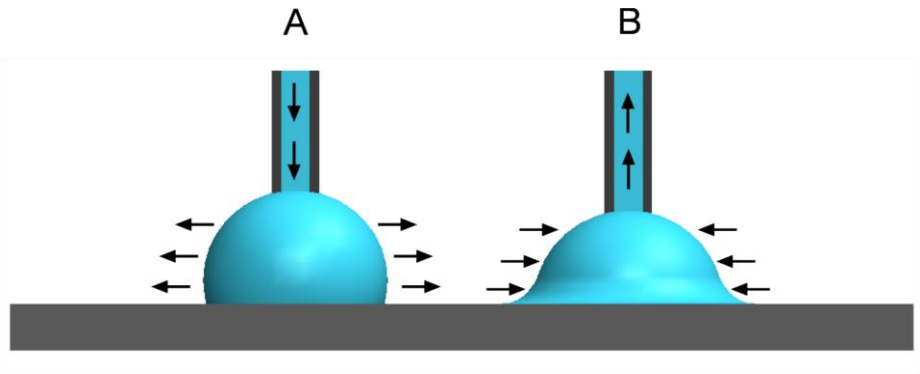

Figure 1.11. Schematic depiction of (A) advancing contact angle and (B) receding contact angle.

According to Young's equation, the values of surface tension parameters should determine a single and unique contact angle value. However, multiple contact angle values can be measured for smooth surfaces that exhibit chemical heterogeneity.[122-124] For example, as fresh liquid advances to wet the fresh surface, different wettability of surfaces could be measured. The contact angles formed by expanding the liquid are referred to as advancing contact angle, θ_a (Figure 1.11A). A difference in wettability can also be observed when the liquid is being contracted from the surfaces. These angles are referred to as receding contact angle, θ_r (Figure 1.11B). The difference between the advancing and receding angle is called the hysteresis (H):[114]

$$H = \theta_a - \theta_r \tag{1.11}$$

Contact angle hysteresis have been extensively investigated with complex physical models.[122-124] In the case of atomically smooth surfaces, chemical heterogeneity would result in a large hysteresis, while homogenous surfaces would exhibit a low hysteresis. Patches of hydrophobic regions will pin the motion of the water front as it advances, causing an increase in the advancing contact angle, while the same region will hold back the contracting motion of liquid front when it recedes, causing a decrease in the receding angle. On an atomically smooth, homogenous surfaces, there should be no contact angle hysteresis. These models suggest that the surfaces covered with uniform organic monolayers should have little or no hysteresis in contact angle values. Large hysteresis is an indication that the monolayers are not uniform, given that the surfaces are smooth.

1.3.2. X-ray Photoelectron Spectroscopy (XPS)

X-ray photoelectron spectroscopy (XPS) can be utilized to evaluate chemical composition of surfaces. It can also be used to evaluate relative surface coverage of organic monolayers formed on smooth surfaces.[125-129] A typical XPS experiment is performed in ultra-high vacuum (~10^{-9} Torr). A monochromatic X-ray (typically Al K_α of 1486.7 eV) with photon energy hv is radiated on the surfaces of a sample. The X-rays eject electrons located in inner electron shells, and these ejected electrons are referred to as photoelectrons. The kinetic energy of these photoelectrons are monitored by an electron energy analyzer. The analysis of the kinetic energy yields the binding energy of the electrons using the following relationship:[130]

$$E_b = hv - E_k - \Phi_s \tag{1.12}$$

where E_b and E_k are the binding energy and kinetic energy of electrons, respectively. The parameters hv and Φ_s represent the energy of incident X-ray and the work function of the spectrometer, respectively. The binding energy is dependent on the element and the orbital from which the photoelectron is ejected from the substrate surfaces. Survey scans of XPS detect electrons for the majority of the elements over a wide range of energy levels (e.g., from nearly 0 eV to 1200 eV binding energies) in a single spectrum. High resolution

scans measure electrons at narrow range of energy levels, typically for a particular orbital of a single element. The high resolution spectrum can reveal differences in the chemical states for the elements. For characterization of organic monolayers on silicon oxide surfaces, the most predominant peaks in the survey scan observed are from oxygen (O_{KLL}, O_{1s}, O_{2s}), carbon (C_{1s}), and silicon (Si_{2s}, Si_{2p}). In case of substrates coated with monolayers containing fluorine or nitrogen, a fluorine signal (F_{KLL}, F_{1s}) or a nitrogen signal (N_{1s}) can also be observed on the XPS spectrum. An example survey scan is shown in Figure 1.12A. High resolution XPS analysis can be utilized to gain in-depth understanding of the chemical composition and surface coverage of thin films. In the case of organic monolayers, high resolution C_{1s} scans are often investigated to determine the chemical structure of the carbons bound to the surfaces. An example high resolution C_{1s} scan for the silicon oxide substrate coated with monolayers derived from 1*H*,1*H*,2*H*,2*H*-perfluoro-1-octanol [$F(CF_2)_6(CH_2)_2OH$] is displayed in Figure 1.12B. The peaks located at binding energies of 294.2, 291.9, 287.6, and 286.2 eV are attributed to **C**F_3, **C**F_2, **C**–O, and **C**–C, respectively. These peaks indicate that the organic monolayers with fluorocarbon backbone are present at silicon oxide surfaces.

Quantitative analysis of high resolution XPS can be performed by comparing the integrated area of the XPS peaks. Such analysis can be used to determine a relative surface coverage of organic monolayers. For instance, Rittikulsittichai *et al.* evaluated relative surface coverage of various thiol-based adsorbates on gold surface by comparing integrated XPS peak areas of Au_{4f} and S_{2p}.[128] A comparison between peak areas at different take-off angles can be quantified to determine the overall organic film thickness and surface coverage. A single molecule thick DNA film immobilized on gold[125] or monolayers derived from 1-alkene and 1-alkyne on hydrogen-terminated silicon[126] have been characterized using this method. Such quantitative XPS analysis enables a more in-depth understanding of surface coverage and film thickness of organic monolayers present on substrate surfaces.

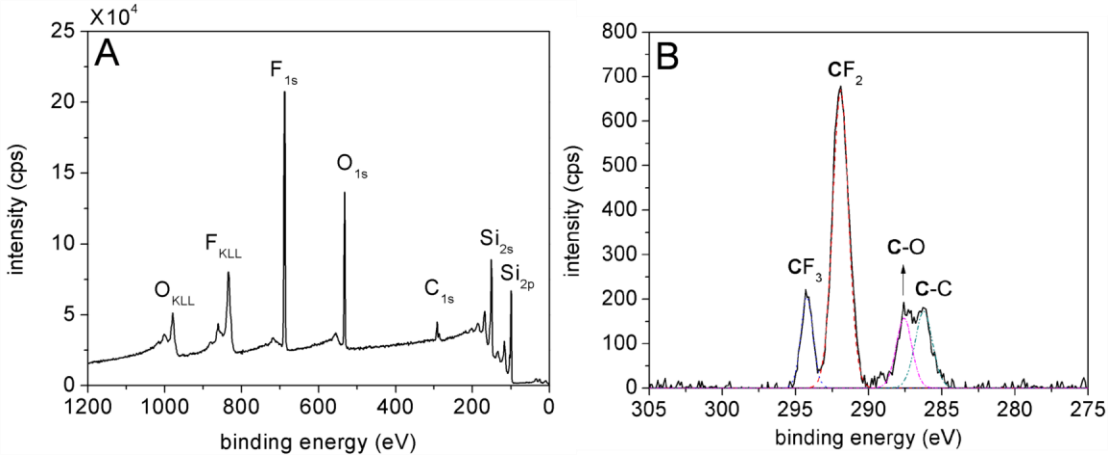

Figure 1.12. Examples of (A) survey and (B) C_{1s} high resolution spectra for a silicon oxide substrate coated with monolayers derived from 1*H*,1*H*,2*H*,2*H*-perfluoro-1-octanol [$F(CF_2)_6(CH_2)_2OH$]. In the survey spectrum, photoelectron and Auger peaks are marked using atomic notations (e.g., O_{1s}) or X-ray notation (e.g., O_{KLL}), respectively. Analysis of high resolution C_{1s} peaks can determine the chemical structure of organic monolayers present at the interface.

The XPS technique can also be utilized to determine thickness of thin films on a flat, chemically homogeneous substrate. This measurement is achieved through the use of angle-resolved XPS (ARXPS). In this technique, the sample stage is rotated to adjust the takeoff angle of the photoelectrons. The XPS spectrum is acquired at a given takeoff angle. The peak intensity of an element within the thin film and that of an element within the underlying substrate is monitored with respect to the takeoff angle. The thickness of the thin film can be calculated using the following equation:[131-133]

$$\ln\left(\frac{I_A}{I_B}\frac{S_B}{S_A}+1\right)=\frac{d}{\lambda}\frac{1}{cos\theta} \tag{1.13}$$

where I_A is the peak intensity of an element A in the thin film, I_B is the peak intensity of an element B in the underlying substrate, d is the thickness of the thin film, λ is the attenuation length of the emitted photoelectrons, and θ is the takeoff angle. As long as the chemical composition of the thin film and the underlying substrate is homogenous, the above equation can be utilized to calculate the thickness of thin films, including organic monolayers.[131-133]

1.3.3. Atomic Force Microscopy (AFM)

Surface topography of materials can be monitored with atomic force microscopy (AFM). The AFM relies on the interaction between an AFM tip and the sample surface. Briefly, as the tip approaches near the surface, it experiences interactions (e.g., van der Waals, magnetic, electrostatic, etc.) with the sample surface. Components of AFM include AFM cantilever, laser source, sample stage, and photodiode (Figure 1.13).[134-140] The AFM cantilever is responsible for probing the sample. The laser beam from the laser source is reflected from the AFM cantilever to the photodiode, where the laser beam is detected. The interaction between the sample and the tip causes the deflection of the tip. This deflection of the AFM cantilever causes the reflection of the laser beam to be displaced on the photodiode. The laser beam on the photodiode is monitored for detecting the interaction between the AFM cantilever and sample. Finally, the distance between the AFM cantilever and the sample is adjusted depending on the result. Vertical resolution of the AFM can range in the subnanometer scale, while horizontal resolution can range between a few nanometers to a several micrometers, depending on the scan rate, scan size, geometry of the AFM tip, and instrumentation.[135, 138-140] The AFM image is constructed from comparative height measured with the tip per each pixel. The AFM can evaluate difference in height between two points, surface roughness from root mean square (RMS) method, or distribution of heights in different regions.

There are two modes of AFM imaging – contact mode and tapping mode. Each mode presents a series of advantages and disadvantages. Contact mode is the imaging technique where the AFM tip is in close contact with the sample surface. Advantages of this technique include a relatively low price of AFM tips available for contact mode, easiness to operate and interpret the result, and less stringent constraints on instrumentation (e.g., feedback controller). Also, other AFM modes such as adhesion force mapping and lateral force microscopy (LFM, sometimes referred to as frictional force microscopy) are based on the contact mode AFM imaging. Key disadvantages of contact mode include limited resolution and noise from interaction of adsorbed species (e.g., water vapor, nitrogen gas) on surface.[134, 141] The contact mode can be affected by the contact areas of the AFM tip and the sample surface, and the result obtained from the contact mode AFM can be convoluted. Tapping mode utilizes an oscillating silicon AFM tip to

probe van der Waals forces between the tip and the sample while the tip hovers slightly above the surface (~5 to 15 nm above). While this technique may need more stringent instrumentation and more expensive AFM tips, it provides higher resolution of AFM images than those obtained from contact mode, allowing characterization of organic monolayers on smooth surfaces.[134-135, 140-141]

Other modes of AFM imaging can be utilized to obtain information about surface properties of a flat substrate. For example, lateral force microscopy (LFM) is a technique derived from contact mode imaging that monitors the friction force between the AFM tip and the sample surfaces. In contact mode AFM, the vertical movement of the AFM tip is measured as it scans across the sample surfaces. In LFM mode, the horizontal movement of the tip is monitored as it scans across the sample surfaces. The deflection of the tip is caused by the changes in the frictional coefficient within the region of the sample surfaces. The LFM is effective in discerning irregularities in surface materials.[135, 137, 140] Kelvin probe force microscopy (KPFM) can be used to determine changes in the work function due to sample inhomogeneity. During KPFM measurements, the AFM tip interacts with the surfaces, but yields information with regards to changes in the work function across these surfaces.[134-135] The AFM probe is coated with a conductive coating to enable a potential to be applied between the tip and the surfaces. It is the flow of electrons to and from the interface (within the sample) as a function of the changes in the capacitance with the tip that lead to an indirect measure of the work function. This method can also effectively discern the chemical irregularities in composition of surface materials if there is difference in work function across the sample surfaces.

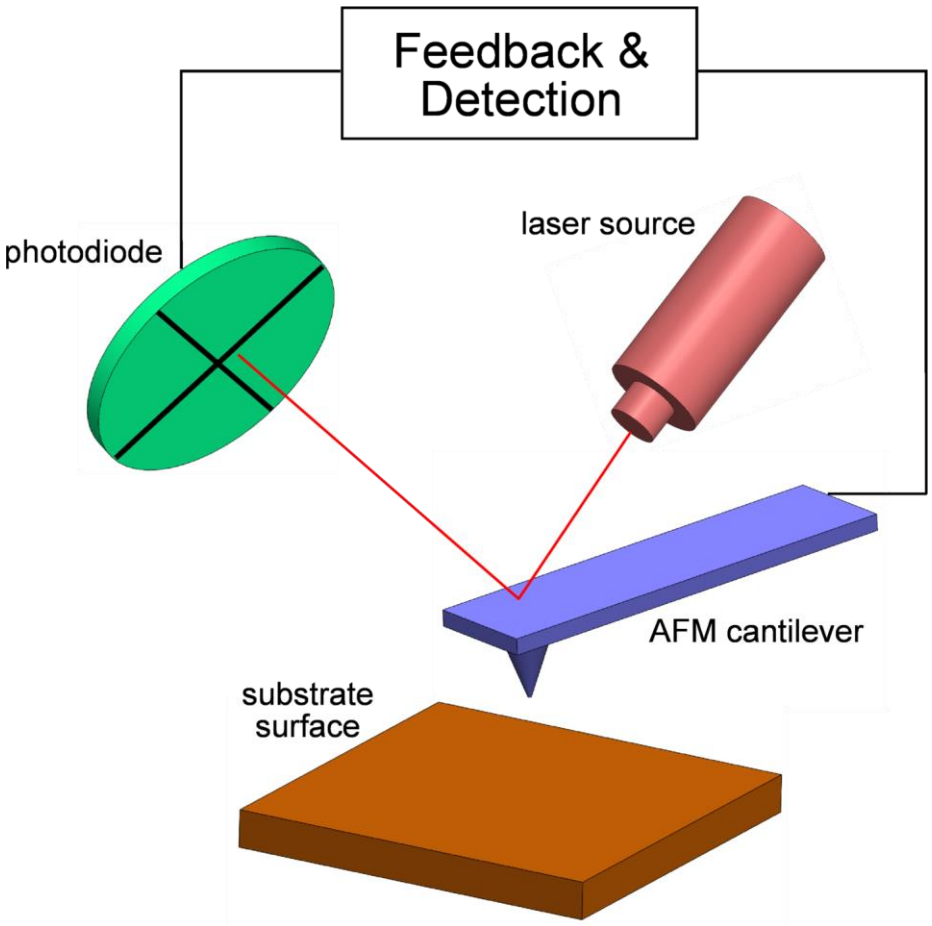

Figure 1.13. Schematic depiction of AFM operation. The AFM cantilever interacts with the surfaces of the substrate. Deflection of the cantilever causes the reflection of the laser beam to be displaced on the photodiode.

1.4. Thesis Overview

Covalent surface modification of silicon oxides with highly uniform organic monolayers is an important topic of study for many research areas. The goal of this thesis work is to provide alternative strategies to form uniform covalently attached organic monolayers on silicon oxides through the use of microwaves. The utilization of microwave heating is particularly effective in the formation of monolayers derived from relatively less reactive species, such as monoreactive silanes and alcohol based reagents. In this dissertation, evaluation of microwave-assisted formation of monolayers on silicon oxide surfaces is discussed in detail. Chapter 1 introduces surface SAMs and different types of

organic precursors used for the formation of SAMs. It also introduces the principle of microwave heating and its application in organic and material chemistry. Chapter 2 introduces microwave-assisted formation of monoreactive alkylsilane based monolayers. The surface coverage and uniformity of monolayers over a different duration of microwave reaction time is assessed using a series of characterization techniques. Chapter 3 focuses on the microwave-assisted formation of alcohol based monolayers on silicon oxide surfaces. Uniformity and stability of monolayers on various silicon oxide substrates are evaluated using various techniques including WCA and AFM over a progressive Soxhlet extraction procedure. Impact of microwave heating of substrates has been evaluated at different microwave powers over quartz and silicon substrates. The technique developed in this chapter is expanded to different types of alcohol containing reagents to tune surface chemistry of silicon oxides. Chapter 4 focuses on tuning surface oleophobicity of silicon oxides through microwave-assisted reaction of mixed fluorinated and aliphatic alcohols. Contact angle measurements with water and non-polar solvents have been utilized as a primary technique to characterize the surface hydrophobicity and oleophobicity. Also, quantitative analyses with XPS and AFM were used to monitor relative surface compositions of each species. Chapter 5 focuses on detailed analyses of aliphatic alcohol based monolayers on silicon oxides surfaces using angle-resolved XPS (ARXPS). The depth profiling of ARXPS determines the molecular thickness of monolayers derived from alcohols with different alkyl chain lengths, and estimates the tilt angles of the monolayers. Chapter 6 will present an overall summary and future directions proposed for further improvements and analyses that can be performed towards covalent surface modification of silicon oxide surfaces.

Chapter 2.

Microwave-Assisted Formation of Monoreactive Perfluoroalkylsilane Monolayers on Silicon Oxide Surfaces

2.1. Notice of Permissions

The following chapter is adapted from Ref. [180] Austin W. H. Lee, Brandy K. Pilapil, Him Wai Ng and Byron D. Gates, "Microwave Assisted Formation of Monoreactive Prefluoroalkylsilane-based Self-Assembled Monolayers", Chemical Communications 2015, 51, 2060-2063 with permission from The Royal Society of Chemistry. Most of the work presented in this paper, including experiments, data acquisition, interpretation and writing has been performed by myself under the guidance of Dr. Byron Gates. Dr. Brandy K. Pilapil assisted in acquiring and interpreting XPS data. Him Wai Ng helped in initial experiments that were utilized as cornerstones of the studies performed herein.

2.2. Introduction

Reactive alkylsilane molecules have been widely used for the formation of self-assembled monolayers (SAMs) since their introduction by Sagiv.[60] These SAMs can be formed on the surfaces of silicon,[60, 142-144] glass,[145] aluminum[146] and copper[147] substrates. The most commonly used alkylsilane molecules in the literature include n-octadecyltrichlorosilane (OTS)[46, 50-51, 142-143, 148-150] and 1*H*,1*H*,2*H*,2*H*-perfluorodecyltrichlorosilane (FDTS).[149, 151-152] The SAMs formed with these molecules have been used to modify the properties of surfaces[50, 144, 153] and to create patterns of varying surface chemistry used in micro and nano-fabrication processes.[55, 143] Many applications require SAMs of a high-quality, since defects in these single-molecule thick films lead to degradation of the surface properties or corrosion of underlying materials.[23, 154] Although trichlorosilane molecules such as OTS or FDTS are effective at modifying the surface properties of a variety of substrates, they can easily cross-link to form an intermolecular polymer.[80] This process often leads to the formation of non-uniform

SAMs.[46, 55] In order to minimize unwanted intermolecular polymerization, trichlorosilane molecules are typically handled in an anhydrous environment. Creating the conditions that regulate hydrolysis and control the rate of condensation of these molecules can be difficult.

To minimize the impact of intermolecular polymerization during the formation of SAMs, monoreactive alkylsilane molecules are used in place of their trireactive counterparts. Monoreactive alkylsilane molecules can either react with the oxide surfaces or with one other molecule in solution. On the other hand, condensation of the monoreactive silane molecules is slow.[153] This can lead to incomplete formation of SAMs, leaving defects in the monolayers. In an effort to minimize defects and to prepare densely packed, uniform SAMs, a number of studies have varied the processing conditions. The simplest way to obtain uniform SAMs is to immerse the substrate into a solvent containing the silane molecules for a sufficiently long duration. However, such a process can take over 10 days to grow densely packed, uniform SAMs.[46] In order to accelerate formation of these SAMs, heat can be applied during their formation,[51, 142, 153] but can still require a relatively long processing time. Silane molecules can also form SAMs on oxide surfaces through multiple iterations of the deposition process to improve their quality,[154-155] but this approach can be cumbersome. Physical adsorption of silane molecules and surface contamination acquired from each deposition process can also decrease the uniformity of the SAMs. An alternative method was sought to more effectively and efficiently form uniform SAMs of monoreactive alkylsilane molecules.

Microwave induced heating has been widely used in molecular synthesis,[83, 99, 156] and the rapid assembly of nanomaterials[86, 99] for its advantages in fast and effective heating.[157] Recently, microwave heating has been utilized in assisting the formation of alkene[158] and thiol[159] based SAMs on silicon carbide and gold surfaces, respectively. Silane based SAMs have been formed with microwave heating of glass slides[157] and cotton fabrics.[160] Although these studies demonstrated the utilization of microwave to the formation of SAMs, they did not provide insight into the impact of microwaves on the quality of SAMs.

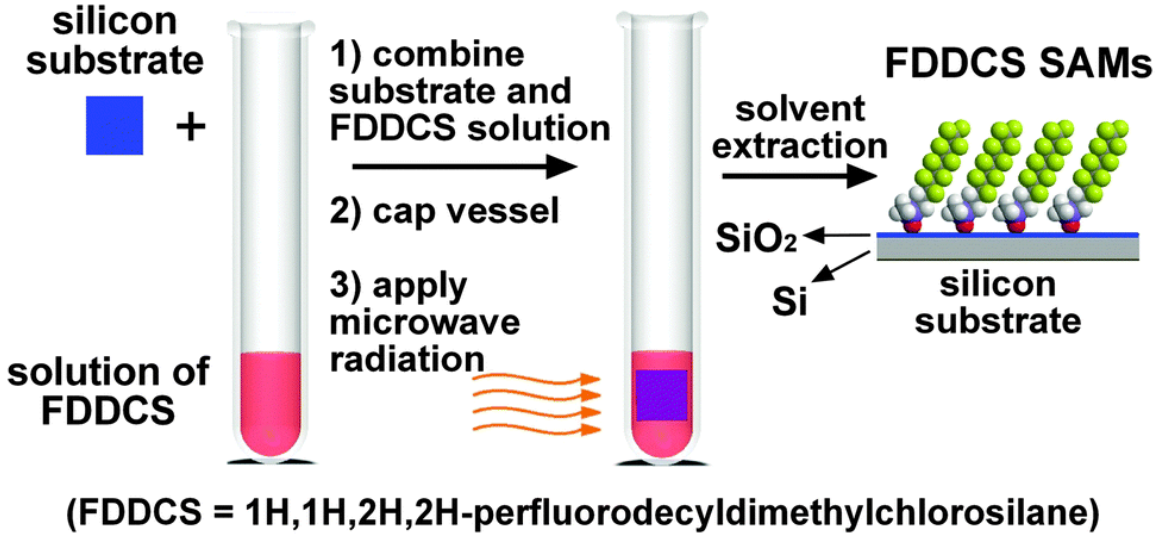

Figure 2.1. Schematic depiction of microwave-assisted formation of silane-based self-assembled monolayers (SAMs) on silicon oxide surfaces. Reprinted with permission from Ref. [180] ©2015 The Royal Society of Chemistry.

The use of microwaves to selectively heat molecules and solids is pursued for accelerating the formation of silane-based SAMs (Figure 2.1) on silicon substrates with 100 nm dry oxide. Microwave reactor (CEM Discover) was used for this study for the advantages of using a closed vessel and for consistency between the experiments.[156] Microwave induced heating is sought to shorten the period of time required to form these monolayers. Microwave heating offers a number of other competitive advantages. Dielectric heating induced by microwave radiation causes a rapid increase in temperature within solids with a high dielectric loss value, such as doped silicon wafers. When the solid is immersed in a liquid, this process releases heat into solution from the surfaces of this solid. Heat can be released at the interface where silane-based SAMs are forming to provide the energy necessary to drive the condensation reaction. The dielectric heating of the polar silane molecules assists with this process, and will also contribute to an increased mass transfer of molecules to and from these interfaces.

The molecule of choice to demonstrate the microwave assisted formation of SAMs was 1*H*,1*H*,2*H*,2*H*-perfluorodecyldimethyl-cholorosilane (FDDCS). A perfluorinated backbone was chosen in part because it is more easily characterized by XPS than a hydrocarbon backbone.[153] Samples were treated with microwave radiation for up to 10 min at 300 W. A subsequent Soxhlet extraction process for 1 h removed adsorbed

molecules and contaminants from the surfaces as per previously described procedures.[153] The impact of microwave radiation on the quality of these SAMs was explored by observing the relative change in hydrophobicity and hysteresis for water contact angle (WCA) measurements, as well as through atomic force microscopy (AFM) and X-ray photoelectron spectroscopy (XPS) analysis of the surface topography and composition, respectively.

2.3. Experimental

Preparation of Silicon Oxide Surfaces. Thermally grown silicon oxide surfaces on a polished silicon wafer were chosen as the substrate for evaluating microwave assisted formation of SAMs. This substrate was chosen in part for the high density and purity of its oxide. Four inch, p-type, single-side polished, <1 0 0> silicon wafers with a 100 nm dry oxide film were purchased from the Nanofabrication Facility in 4D LABS at Simon Fraser University. These oxide coated wafers were cut into 1 cm by 1 cm squares, and cleaned with a piranha solution. Piranha cleaning was performed prior to the formation of SAMs to minimize contamination on the surfaces of the wafer. A 7:2 (v/v) mixture of concentrated sulfuric acid (Anachemia Canada, Inc.) and 30% (v/v) hydrogen peroxide (VWR International) was used to prepare the piranha solution. *CAUTION: Piranha solution is a strong oxidizing agent and reacts violently with organic compounds. This solution should be handled with extreme care.* The wafer pieces were immersed in the piranha solution for ~15 min followed by immersion into 18 MΩ·cm deionized water (Barnsted NANOpure DIamond water filtration system) for 5 min. These substrates were subsequently rinsed under a stream of 18 MΩ·cm deionized water for 1 min with an approximate flow rate of 25 mL per second. These cleaned wafer pieces were dried under a stream of nitrogen gas filtered with a PTFE membrane containing <0.2 micron pores. To further dry these substrates, they were baked in an oven at 120°C for 3 min.

Microwave Assisted Preparation of SAMs. Monolayers of monoreactive perfluoroalkylsilanes were assembled on the clean silicon oxide surfaces by immersing these substrates into a toluene solution. In order to prepare a 30 mM perfluoroalkylsilane solution, 1*H*,1*H*,2*H*,2*H*-perfluorodecyldimethylcholorosilane (FDDCS, product #L16582, 90% purity Alfa Aesar) was added to 25 mL of toluene (ACS Reagent grade, purity >

99.5%; purchased from Fisher Scientific, catalog No. T324-4) in a 25 mL volummetric flask. Solutions containing FDDCS of different concentrations (i.e. 3 mM and 0.3 mM) were prepared from this stock solution by serial dilution. A 3 mL aliquot of the desired perfluoroalkylsilane solution was added to a glass tube (Part no. 908035, CEM Discover) for the microwave reaction.

Silicon substrates were put into the glass tubes containing the desired silane solution. Each silicon substrate was immersed in this solution at room temperature for 5 min before microwave treatment for consistency between experiments (e.g., minimizing variations in the immersion time during preparations for microwave treatment). The solution was exposed to microwaves at a constant power of 300 W in a CEM Discover microwave reactor for increments of 1 min. Because the glass tube potentially reaches high temperatures and high pressures, these glass tubes were kept at room temperature without microwave radiation for at least another 5 min. The silicon substrates were immersed in their silane solution for a total immersion time of 18 min. A consistent immersion time was used to evaluate the influence of microwave radiation on the formation of SAMs while minimizing variations in contact with the solution. The samples were washed with a fresh solution of toluene and placed into a Soxhlet extractor with refluxing toluene for 1 h as per a previously described procedure.[153]

Water Contact Angle (WCA) Measurements. Hydrophobicity and uniformity of the SAMs were evaluated by static water contact angle (WCA) measurements. A 2 μL droplet of 18 MΩ·cm deionized water was dispensed onto the substrate for each measurement. The WCA was measured as the angle between the air-water interface of the droplet and the interface of the water and substrate. Five advancing contact angle measurements were obtained for each sample by adding 2 μL for each subsequent measurement. Four receding WCA measurements were obtained after removing the water in 2 μL increments from the resulting droplet. The average contact angle was determined by taking the average of the advancing contact angle measurements. Hysteresis of these measurements was estimated by comparing the average of the advancing contact angles with the average of the receding contact angles.

Atomic Force Microscopy (AFM) Measurements. In order to characterize the surface topography of the samples, AFM images were acquired using an MFP 3D AFM (Asylum Research) in AC mode using silicon cantilevers from BudgetSensors (Tap150-G, resonant frequency of 150 kHz, force constant 5 N/m). Images were acquired from scan areas of 5 μm by 5 μm with a scan speed of 0.5 Hz and a resolution of 512 by 512. The AFM images were analyzed using Igor Pro 6.22.

X-ray Photoelectron Spectroscopy (XPS) Measurements. Chemical composition and density of the self-assembled monolayers were investigated by XPS. These studies were conducted using a Kratos Analytical Axis ULTRA DLD system with a monochromatic aluminum source (AlKα of 1486.7 eV) operating at 150 W. Survey scans (0 to 1200 eV) were acquired using a pass energy of 160 eV and a dwell time of 200 ms. High resolution scans (0.05 eV spectral resolution) were obtained using a pass energy of 20 eV and a dwell time of 1000 ms. An area of 700 μm by 300 μm was analyzed in three separate regions of each sample to check the uniformity of the surface modification.

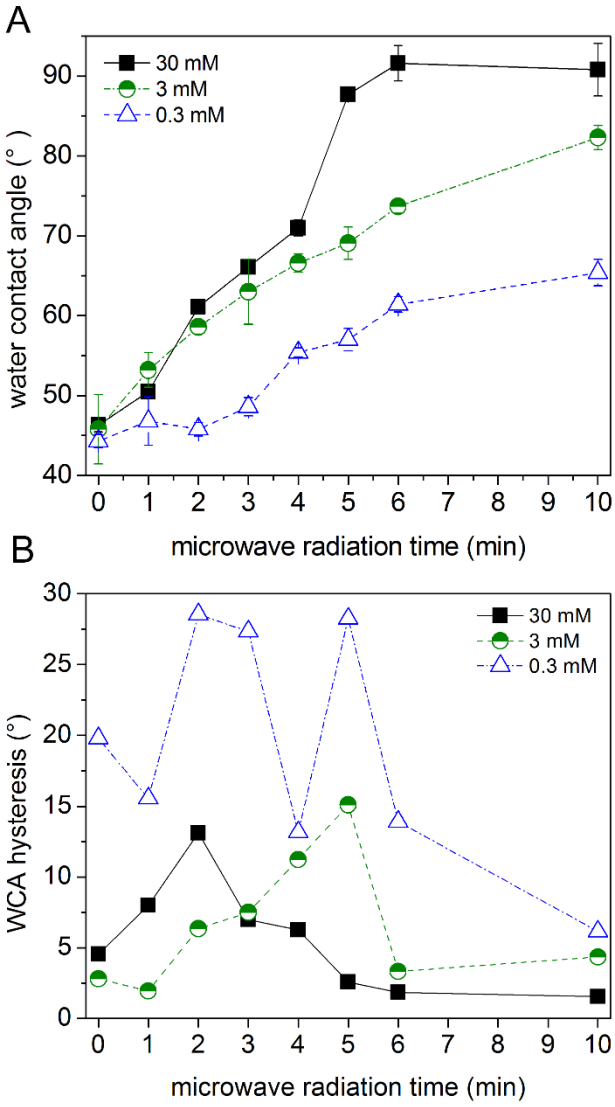

Figure 2.2. **(A) Water contact angle (WCA) measurements of silicon oxide coated silicon substrates after immersion in a toluene solution of monoreactive perfluorinated silanes and treatment with microwave to form self-assembled monolayers (SAMs). Average advancing WCA measurements are plotted with an error bar of one standard deviation from three independent measurements. (B) Hysteresis in the WCA measurements, as determined by taking the difference between the average advancing WCA and the average receding WCA measurements. Reprinted with permission from Ref. [180] ©2015 The Royal Society of Chemistry.**

2.4. Results and Discussion

The hydrophobicity of the perfluoroalkylsilane coated silicon oxide surfaces was probed using water contact angle (WCA) measurements. The hydroxyl terminated silicon oxide surfaces obtained following piranha cleaning of these substrates were hydrophilic. The WCA of these substrates was ~20°. The formation of perfluoroalkylsilane-based SAMs would create surfaces coated with the fluorinated chain of FDDCS, and these surfaces would become hydrophobic. The higher the surface coverage of FDDCS, the more hydrophobic should be these surfaces. In other words, a higher WCA could suggest the formation of higher quality, more densely packed monolayers. As shown in Figure 2.2A, an increase in hydrophobicity was correlated with an increase in the length of time of exposure to microwave radiation. For instance, the substrate that was immersed in 30 mM FDDCS solution without microwave radiation for 15 min exhibited a WCA value of 45°, and the substrate that was immersed in the same solution with 6 min or 10 min microwave radiation for the same immersion time exhibited a WCA value of 90°. These results suggest the surface coverage of the SAMs increased in proportion to the length of time for dielectric heating. For example, the monolayers formed using a 30 mM solution of FDDCS in toluene with 6 min of exposure to microwave radiation reached a WCA of ~90°, which is comparable to previous literature values for Soxhlet extracted surfaces of FDDCS SAMs.[153] The WCA values for this sample remained relatively constant at longer durations (i.e. 10 min) of microwave radiation, which could be attributed to a diminished number of surface reactive sites. The formation of SAMs at lower concentrations of the perfluoroalkylsilane resulted in lower WCA values in comparison to those observed for the 30 mM solutions (Figure 2.2A). The trend associated with the progressive treatment by microwave radiation for each concentration of FDDCS in toluene further demonstrated that the WCA values increased in proportion to the duration of this treatment. These results suggest that microwave radiation can assist in the formation of monolayers with a high surface coverage of perfluoroalkylsilanes on silicon oxide surfaces.

Hysteresis of the WCA measurements was evaluated to gain further insight into the uniformity of the SAMs formed with the assistance of microwave radiation. A large hysteresis in the WCA measurements is indicative of a large variation in uniformity of the monolayers.[161] Hysteresis increased proportionally with an increased duration of

microwave radiation between 0 and 2 min for samples immersed in a 30 mM solution of perfluoroalkylsilane (Figure 2.2B). Uniformity of the WCA initially decreases with longer microwave treatments, but a decrease in hysteresis and corresponding increase in quality of the SAMs was observed with an increase of microwave radiation from 2 to 6 min. The formation of these silane-based monolayers could be initiated by the assembly of FDDCS molecules into islands on the silicon oxide surfaces creating an initially non-uniform surface coverage. As more FDDCS molecules react with the surfaces, these molecules start to form a more uniform coating as indicated by the subsequent decrease in hysteresis with increasing length of exposure to microwave radiation. The sample treated with 10 min microwave radiation had a similar hysteresis to that treated with 6 min microwave radiation, indicating that both samples had SAMs of a comparable uniformity. For a 3 mM solution of FDDCS, the hysteresis progressively increased up to 5 min before decreasing at 6 min of microwave radiation. A longer duration of microwave radiation was required for this solution to form more uniform SAMs. The hysteresis of monolayers prepared from immersion in a 0.3 mM solution of FDDCS was higher than that observed for the other samples. Monolayers were not uniformly formed at this low concentration of perfluoroalkylsilane. The WCA hysteresis measurements suggest there are non-uniformities in the surface density of covalently attached molecules, but this variation could also be attributed to adsorbed species present in each sample. Further analysis was required to discern the potential contributing factors to this variance in the uniformity of the FDDCS SAMs.

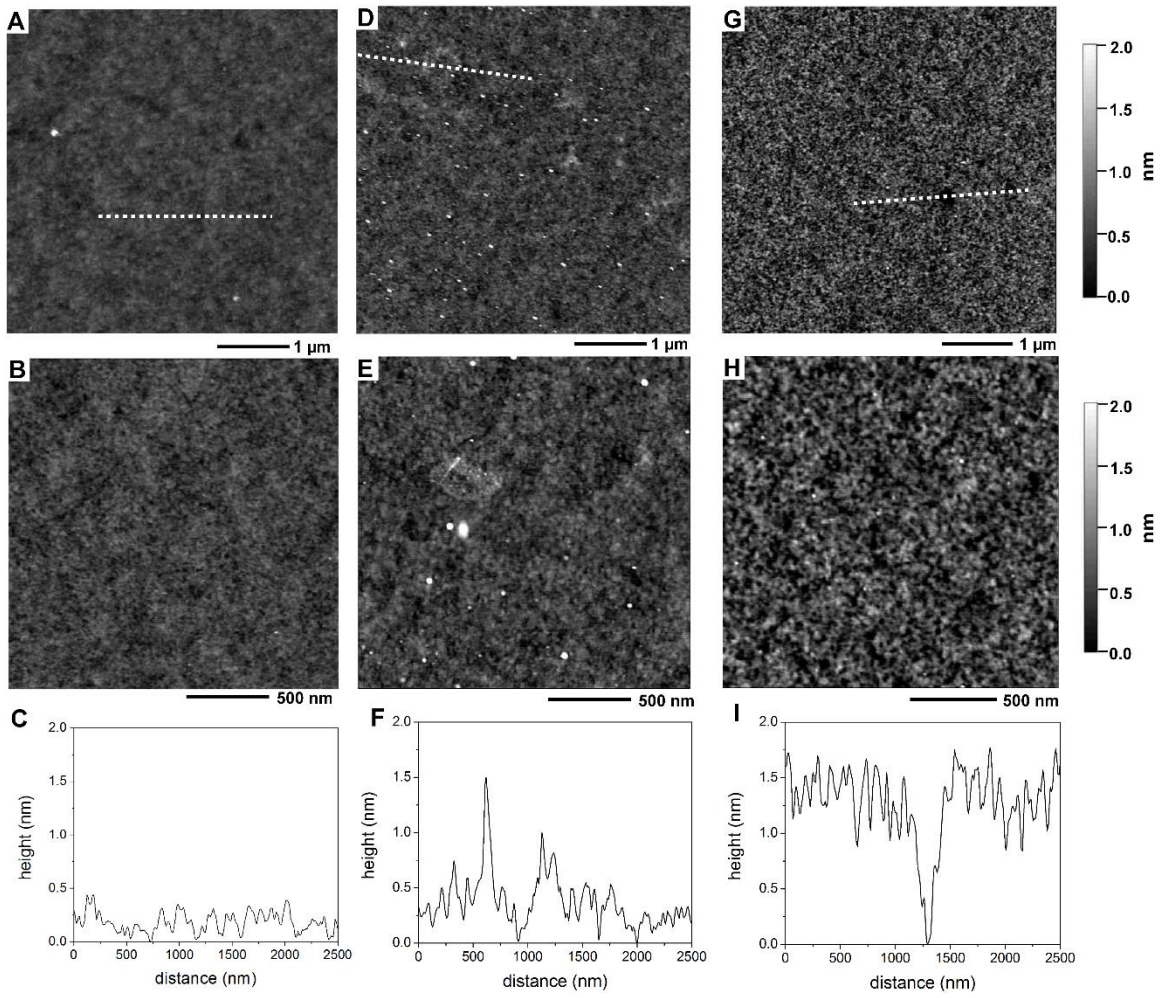

Figure 2.3. Atomic force microscope (AFM) images of (A and B) piranha cleaned silicon oxide surfaces. Cross sectional profile (C) plotted for the region indicated in the image (A) by a white dotted line. This sample had a roughness of 0.15 nm as measured by the root mean square (RMS) method. The AFM images of silicon oxide surfaces coated with SAMs formed by immersion in a toluene solution of 30 mM monoreactive perfluoroalkylsilanes and treated with microwave radiation for either 2 min (D–F) or 6 min (G–I). Cross-sectional profiles (F, I) correspond to the regions indicated by white dotted lines in the images (D, G). Tapping mode AFM imaging was performed with a scan speed of 0.5 Hz for scans of 5 μm by 5 μm (A, D, G) or 2 μm by 2 μm (B, E, H) with 512 by 512 resolution. Adapted with permission from Ref. [180] ©2015 The Royal Society of Chemistry.

Atomic force microscopy measurements were used to analyze changes in the topography of silicon oxide surfaces when modified with SAMs prepared by microwave assisted processing. Although the WCA results indicated an increase in hydrophobicity of

the silicon oxide surfaces when coated with the perfluoroalkylsilane molecules, further investigation was needed to determine the surface coverage of these molecules. The WCA measurements indicated that surface modifications with the highest uniformity and surface coverage of SAMs were achieved with 30 mM FDDCS in toluene and 6 min of treatment by microwave radiation. The solvent extracted samples were imaged by AFM. A comparison was made between monolayers prepared by either 2 or 6 min of microwave radiation while immersed in a 30 mM solution of perfluoroalkylsilane (Figure 2.3). These samples were chosen based on the differences in their WCA and hysteresis. It was anticipated that at 2 min of microwave radiation the sample would have a large variation in surface topography from the formation of islands of FDDCS molecules. Those samples treated with 6 min of microwave radiation should have a higher coverage of SAMs with fewer defects based on its higher WCA and lower hysteresis. The AFM data showed a clear difference between these two types of samples. For the surfaces treated with 2 min of microwave radiation in the presence of 30 mM FDDCS in toluene, islands with heights of 1.1 ± 0.1 nm were attributed to regions of densely packed monolayers. Those samples treated with 6 min of microwave radiation had a higher surface coverage of the FDDCS monolayers. An average height of 1.3 ± 0.2 nm was observed between the tallest features and the lowest recesses within these monolayers. Contributions to the errors in these measurements included tip-sample interactions and surface roughness (Figure 2.3A-C). Small defects observed in these SAMs could be attributed to blocked reactive sites or the existence of nonreactive surface sites. Height of the FDDCS monolayers at 6 min of microwave processing was proportional to the length of these perfluoroalkylsilane molecules (~1.34 nm).

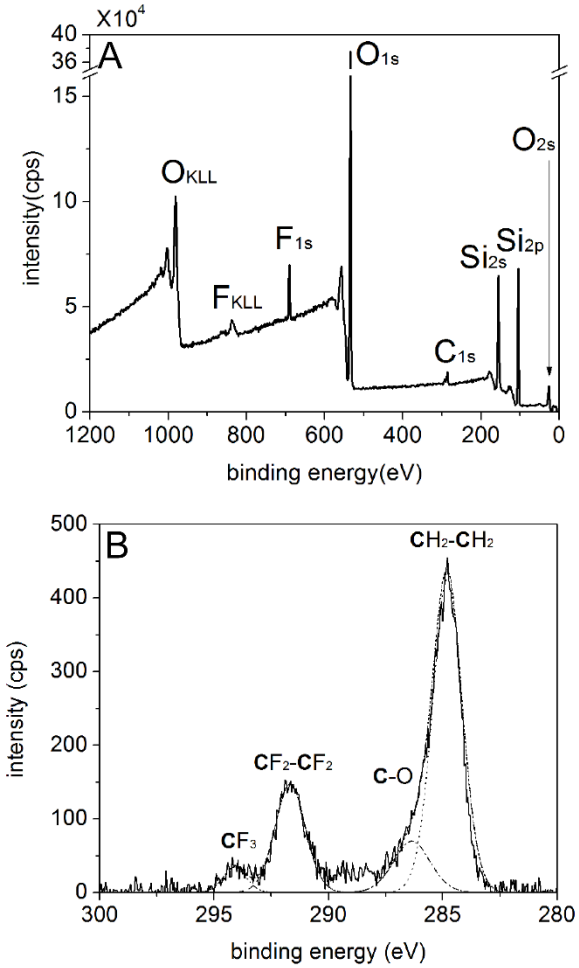

Figure 2.4. (A) Survey and (B) high resolution C1s X-ray photoelectron spectra (XPS) of a silicon oxide coated substrate after 6 min microwave-assisted reaction in 30 mM perfluoroalkylsilane based self-assembled monolayers followed by 1 h of extraction in refluxing toluene. Reprinted with permission from Ref. [180] ©2015 The Royal Society of Chemistry.

An XPS study was performed on the sample treated with 6 min microwave in a 30 mM FDDCS solution in order to verify the elemental composition and the quality of the FDDCS. The XPS analysis detected the presence of F, Si, C, and O in this sample (Figure 2.4A). There were no detectable impurities from other elements. Surface coverage of FDDCS was further assessed by comparing the relative amount of F and Si detected in the sample. A ratio of 0.41 was obtained by integrating the areas for the F_{1s} to Si_{2p} peaks.[153] This value is comparable to previous literature on FDDCS based SAMs prepared from immersion in 1 mM FDDCS in toluene for 1 h at 80 °C followed by Soxhlet

extraction.[153] To gain further insight into the density of the SAMs formed by microwave processing, high resolution XPS analysis was performed on the C_{1s} region to assess the relative signals for **C**F_2–CF_2 and **C**F_3 (Figure 2.4B).[153] A comparison of the ratio of the integrated areas for **C**F_2–CF_2 and **C**F_3, as determined by high resolution XPS analysis, was used to assess the packing density of the perfluoroalkylsilane molecules.[153, 162] Increased density of perfluoroalkylsilane molecules results in an increased **C**F_3 to **C**F_2 signal.[163] Samples treated with microwave radiation for 6 min had a ratio of 0.18 between the **C**F_3 peak area at 295.1 eV (integrated area = 45.1) and the **C**F_2–CF_2 peak area at 292.7 eV (integrated area = 249.2). This ratio is comparable to previous literature that reported values of 0.2 for high-quality SAMs of FDDCS.[153] This result suggests that the monolayers formed from perfluoroalkylsilanes are oriented in a similar orientation as reported previously in the literature.[153] Contributions to the errors in these measurements included surface roughness, peak fitting analysis, and measurement error. The XPS results suggested that FDDCS SAMs of a relatively high density can be formed with the assistance of microwave radiation within approximately one-tenth of the processing time reported in previous literature.[153]

2.5. Conclusions

In summary, microwave radiation was introduced as a technique to facilitate the formation of monoreactive perfluoroalkylsilane based SAMs on a thin film of silicon oxide coated onto a doped and polished silicon wafer. To study the effect of microwave radiation on the quality of the resulting SAMs, the duration of treatment by microwave radiation was varied by up to 10 min during formation of the monolayers. The WCA for surfaces coated with these SAMs demonstrated an increased hydrophobicity with an increase in the duration of microwave treatment. Furthermore, WCA hysteresis measurements revealed non-uniform coatings formed at relatively short durations of treatment with microwave radiation, while more uniform and dense coatings were formed upon treatment with longer durations of microwave radiation. The surface topography of the samples was studied by atomic force microscopy. Single molecule thick islands were observed in the samples treated by a relatively short duration of microwave radiation (2 min). A more uniform surface topography was observed for samples treated with a longer duration of microwave

radiation (6 min). The XPS analysis validated the composition of these SAMs and further verified a relatively high density of molecules within the monolayers prepared by treatment with 6 min of microwave radiation. The use of microwave radiation to assist the formation of silane-based SAMs improved the efficiency of this process in contrast to convective heating methods. The results presented in this study also demonstrate the use of microwave radiation as a simple and quick method to enhance the quality of silane-based SAMs on silicon oxide surfaces.

Chapter 3.

Microwave-Assisted Covalent Surface Modification of Silicon Oxides with Alcohols

3.1. Notice of Permissions

The following chapter is adapted with permission from Ref. [208] Austin W. H. Lee and Byron D. Gates, “Rapid Covalent Modification of Silicon Oxide Surfaces through Microwave-Assisted Reactions with Alcohols”, Langmuir 2016, 32, 7284-7293 ©2016 American Chemical Society. The work presented in this paper, including experiments, data acquisition, interpretation and writing has been performed by myself under the guidance of Dr. Byron Gates.

3.2. Introduction

The formation of SAMs has been widely pursued to tune the surface properties of materials as necessary for a variety of applications that include molecular electronics,[164] microelectromechanical systems (MEMS),[6] microfluidics,[165] optics,[166] catalysis,[167] drug delivery,[168] and biological interfaces.[169-171] Self-assembled monolayers have been successfully formed on silicon oxide surfaces using molecules containing reactive groups such as silanes[3-4, 60] and phosphonic acids.[52, 57-58, 78] Limitations of preparing monolayers from these reactive molecules include the procedures required to prepare these molecules,[2] the robustness of their interactions with silicon oxide surfaces,[52, 78] the susceptibility of these molecules to side reactions and sensitivity to environmental conditions (e.g., humidity),[60, 145, 172-173] and their potential to form multilayer coatings.[57] Alternative approaches to modifying the surfaces of silicon oxides are desirable.

As an alternative class of reactive molecules, alcohols have been utilized to form monolayers on silicon oxides. These monolayers (commonly referred to as self-assembled monolayers or SAMs) are covalently linked to surfaces through the formation of silyl ether (Si–O–C) bonds[62] between the alcohol-functionalized molecules and the surfaces of either

hydrogen-terminated silicon[63-64, 81, 174-176] or silicon oxides.[61, 65, 177] Monolayers prepared from the reaction of aliphatic alcohols with SiO_x surfaces can overcome many of the challenges of using other reagents, such as organosilanes and phosphonic acids. Alcohol-functionalized reagents are abundant, widely available, relatively safe to use, monoreactive, and relatively insensitive to the presence of moisture. The preparation of hydrogen-terminated polished silicon can pose safety concerns because fluoride-ion-containing reagents (e.g., HF, NH_4F) are required to remove any oxide film on the silicon.[81, 174] Moreover, hydrogen-terminated silicon is difficult to form on glass or quartz substrates. The formation of SAMs from the reaction of aliphatic alcohols with SiO_x surfaces has been achieved using convective heating,[65] but this method requires a relatively long reaction time because of the unfavorable energetics of this condensation reaction even at elevated temperatures. These previous studies demonstrated the ability to use aliphatic alcohols as an alternative class of reactive molecules to prepare self-assembled monolayers (SAMs), but it provided limited information on the surface coverage and stability of the resulting SAMs.

To form uniform SAMs of alcohols on the surfaces of silicon oxides in a timely manner, a more effective and efficient strategy is needed to deliver sufficient energy to drive this condensation reaction. Microwave radiation is an attractive alternative means of providing the required thermal energy for the formation SAMs from alcohols. Microwaves can heat a reaction faster and more effectively than convective heating,[178] and microwaves have been widely utilized to initiate reactions in organic synthesis[83-85, 107, 178] and materials science.[86, 179] Recently, processes have been demonstrated that utilize microwave radiation to assist the formation of monolayers of alkanethiolates on gold,[159] alkenes on silicon carbide,[158] and alkylsilanes on glass slides,[157] cotton fabrics,[160] and silicon chips with thermally grown oxides.[180] The use of microwave radiation has been demonstrated for the reaction of alcohols on hydrogen-terminated silicon[181-182] but has not been extended to the condensation reactions between alcohols and silicon oxides.

In this study, we demonstrate a microwave-assisted reaction of aliphatic alcohols and surface-bound silanols as an effective and efficient technique to form monolayers on various types of silicon oxide surfaces. We sought to understand the impact of microwave radiation on the reaction of alcohols with silanol groups on the surfaces of SiO_x-based

substrates having different compositions and structures. The hydrolytic stability of the monolayers formed with this technique was evaluated at different pH values. Finally, we demonstrate the applicability of the technique toward tuning the surface chemistry of silicon oxide surfaces to achieve hydrophobic, oleophobic, and/or charged surfaces.

3.3. Experimental

Reagents and Materials. All reagents were used as received, which included 1-octanol (Sigma-Aldrich, ACS reagent grade, CAS no. 111-87-5), 1*H*,1*H*,2*H*,2*H*-perfluoro-1-octanol (Sigma-Aldrich, 97%, CAS no. 647-42-7), choline chloride (Sigma-Aldrich, BioReagent, CAS no. 67-48-1), glycolic acid (Sigma-Aldrich, ReagentPlus, CAS no. 79-14-1), toluene (J.T. Baker, CMOS grade, CAS no. 108-88-3), sulfuric acid (Anachemia Canada, Inc., ACS reagent grade, CAS no. 7664-93-9), hydrogen peroxide (Fisher Scientific, CAS no. 7722-84-1), hydrochloric acid (ACP Chemicals, ACS reagent grade, CAS no. 7647-01-0), sodium hydroxide (BDH Chemicals, ACS grade, CAS no. 1310-73-2), acetone (Fisher Scientific, reagent grade, CAS no. 67-64-1), and isopropanol (Fisher Scientific, reagent grade, CAS no. 67-63-0). Four inch, p-type, test-grade, single-side-polished ⟨100⟩ silicon wafers with a resistivity of between 1 and 10 Ω·cm and either with or without a 100-nm-thick dry oxide film were purchased from the Nanofabrication Facility in 4D LABS at Simon Fraser University. Soda-lime glass microscope slides were purchased from Leica Microsystems (Surgipath precleaned Micro Slides Snowcoat X-tra), and polished quartz slides were purchased from Chemglass (fused quartz, product no. CGQ0640-01). The polished silicon wafers, soda lime glass microscope slides, and polished quartz slides were diced into 1 cm × 1 cm square pieces that served as substrates for the following experiments.

Preparation of Silicon Oxide Surfaces on Polished Silicon. Piranha cleaning of the diced silicon substrates removed surface contamination, exposing a thin (<2 nm) native silicon oxide layer. To prepare the piranha solution, roughly 4 mL of 30% (v/v) hydrogen peroxide was slowly added to 14 mL of concentrated sulfuric acid to make a 7:2 (v/v) mixture. (*CAUTION! Piranha solution is a strong oxidizing agent and reacts violently with organic compounds. This solution should be handled with extreme care.*) The substrates were immersed in the freshly prepared piranha solution for ~1 h followed by

immersion in 18 MΩ·cm deionized water (Barnstead Nanopure Diamond water filtration system) for 5 min. These substrates were subsequently rinsed under a stream of 18 MΩ·cm deionized (DI) water for 1 min with an approximate flow rate of 25 mL/s. These cleaned wafer pieces were dried under a stream of nitrogen gas filtered with a PTFE membrane containing <200 nm pores.

Preparation of Soda Lime Glass and Polished Quartz Substrates. The diced soda lime glass substrates were initially cleaned with hot water and glassware detergent (Sparkleen), followed by washing sequentially with acetone and isopropanol. The diced quartz substrates were washed with acetone and isopropanol without the use of glassware detergent. Each of the cleaned substrates was immersed for 24 h in a sodium hydroxide (NaOH) solution, prepared from a mixture of 6.5 g of sodium hydroxide, 100 mL of isopropanol, and 100 mL of DI water. The substrates were subsequently rinsed under a stream of DI water for 1 min. These steps were necessary to ensure minimal organic contamination prior to the standard piranha cleaning process. After the substrates were dried under a stream of nitrogen (N_2) gas filtered with a PTFE membrane containing <0.2 μm pores, they were treated with piranha solution, similar to the procedure described in the section above. The cleaned substrates were further rinsed under a stream of DI water and dried under a stream of N_2 gas.

Procedure for the Formation of Alcohol-Based SAMs Using a Microwave Reactor. Each cleaned substrate was placed in a separate 10 mL test tube (part no. 908035, CEM Discover) containing a ~2 mL solution of 1-octanol. The test tube was exposed to microwave radiation using a CEM Discover microwave reactor for the desired duration (up to 30 min) and with specified limits (as noted in the following discussion) for microwave power and/or reaction temperature. Each sample was cooled for 5 min after the microwave-assisted reaction before further handling. Upon completion of this microwave process, the test tube was removed from the microwave reactor. The treated substrates were removed from their cooled test tube and washed sequentially under a stream of acetone and isopropanol. Each washed substrate was dried under a stream of filtered N_2 gas.

Formation of SAMs at 180 °C Using Convective Heating. Cleaned substrates were placed into separate 10 mL glass test tubes (part no. 908035, CEM) each containing 2 mL of 1-octanol. Each test tube was held in a silicone oil bath maintained at 180 °C for periods of time from 30 min to 24 h. Each sample was cooled for 5 min before handling the substrate. The substrates were removed from the cooled test tubes and washed sequentially under streams of acetone and isopropanol. The washed substrates were dried under a stream of filtered N_2 gas.

Soxhlet Extraction Procedure. The rinsed and dried substrates were loaded into a customized glass substrate holder. This holder, loaded with the substrates, was carefully placed in a Soxhlet extractor containing CMOS-grade toluene in the still pot. The still pot was heated to boil the toluene and to start the extraction procedure, and a condenser above the sample chamber was chilled with recirculating water. The extraction process was performed for up to 24 h. Once this extraction procedure was complete, the substrate holder was carefully unloaded from the Soxhlet extractor, and each substrate was dried under a stream of filtered N_2 gas.

Characterization Procedures. The solvent-extracted substrates were each characterized by a series of analytical techniques to assess their surface topography, hydrophobicity, and chemical composition. Multiple measurements were obtained to determine the surface coverage of the SAMs on each substrate as well as the consistency between substrates. The parameters for each of the analytical techniques are outlined in detail below.

Water Contact Angle (WCA). WCA measurements were performed with a contact angle goniometer (Dataphysics, model OCA 15) in the Nanofabrication Facility of 4D LABS at Simon Fraser University. A 2 µL droplet of 18 MΩ·cm deionized water was dispensed onto the substrate for each measurement. The WCA was measured as the angle between the air− water interface of the droplet and the interface between the water and the substrate. Where applicable, the error bars for the WCA measurements are reported as one standard deviation of at least five independent measurements.

Atomic Force Microscopy (AFM). AFM images were acquired using an MFP 3D AFM (Asylum Research) operating in AC mode using silicon cantilevers from BudgetSensors (Tap 150-G, resonance frequency of 150 kHz, force constant of 5 N/m). Images were acquired from scan areas of 5 μm × 5 μm with a scan speed of 0.4 Hz and a resolution of 512 × 512. The AFM images were analyzed using Igor Pro 6.22.

X-ray Photoelectron Spectroscopy (XPS). XPS measurements were performed to investigate the chemical composition and relative surface coverage of the SAMs. These studies were conducted using a Kratos Analytical Axis ULTRA DLD system with a monochromatic aluminum source (Al Kα of 1486.7 eV) operating at 150 W with a 90° takeoff angle. Survey spectra (0 to 1200 eV) were acquired using a pass energy of 160 eV, a dwell time of 100 ms, and 1 sweep. High-resolution spectra were obtained using a pass energy of 20 eV, a dwell time of 500 ms, and 10 sweeps. For insulating substrates such as soda lime glass and quartz substrates, the XPS analysis had to be performed with the assistance of a charge neutralizer because of charging effects of both substrates. An area of 700 μm × 300 μm was analyzed in three separate regions of each sample to check the uniformity of each surface modification. XPS peak analysis was performed using Vision Processing.

3.4. Results and Discussion

Varying Duration of Microwave Radiation at a Set Reaction Temperature. A detailed investigation was performed using a microwave reactor to pursue the formation of monolayers from aliphatic alcohols with precise control of the reaction temperature and duration. This study also investigated the impact of microwave heating on the composition of different SiO_x substrates. The CEM microwave reactor is used because of its ability to safely and reliably control and monitor the reaction temperature and pressure while minimizing the evaporation of the solvent.[84-85] All of the microwave reactions included a ramp-up time of 30 s before the radiation cycle and a 5 min cool-down period (in the absence of microwave radiation) to ensure repeatability and a safe experimental design. After the completion of each reaction, the coated substrates were treated with continuous Soxhlet extraction in hot toluene for up to 24 h. The toluene extraction process was also systematically investigated by varying the duration of extraction (e.g., 1, 5, or 24 h). The

results of these processes were assessed primarily by WCA measurements to determine the relative extent to which covalent bonds were formed between 1-octanol and the silanol groups as a result of microwave radiation. The surface topography was investigated with AFM for selected substrates covered with 1-octanol to assess the uniformity.

The duration of exposure to microwave radiation was systematically varied to evaluate the influence of the total dose of microwave radiation on the quality of the monolayers. The duration of this reaction was varied from 1 to 30 min. This study was conducted using four different types of substrates containing surface-bound silanols – polished silicon substrates with either a native oxide or a 100-nm-thick layer of thermally grown silicon oxide, soda lime glass (i.e. glass microscope slides), and polished quartz. The target temperature of the reaction vessel was set to 180 °C to avoid overpressurizing the vessel due to substantial evaporation of 1-octanol (b.p. of 1-octanol is ~195 °C). The microwave power was adjusted throughout each reaction to maintain the set-point temperature.

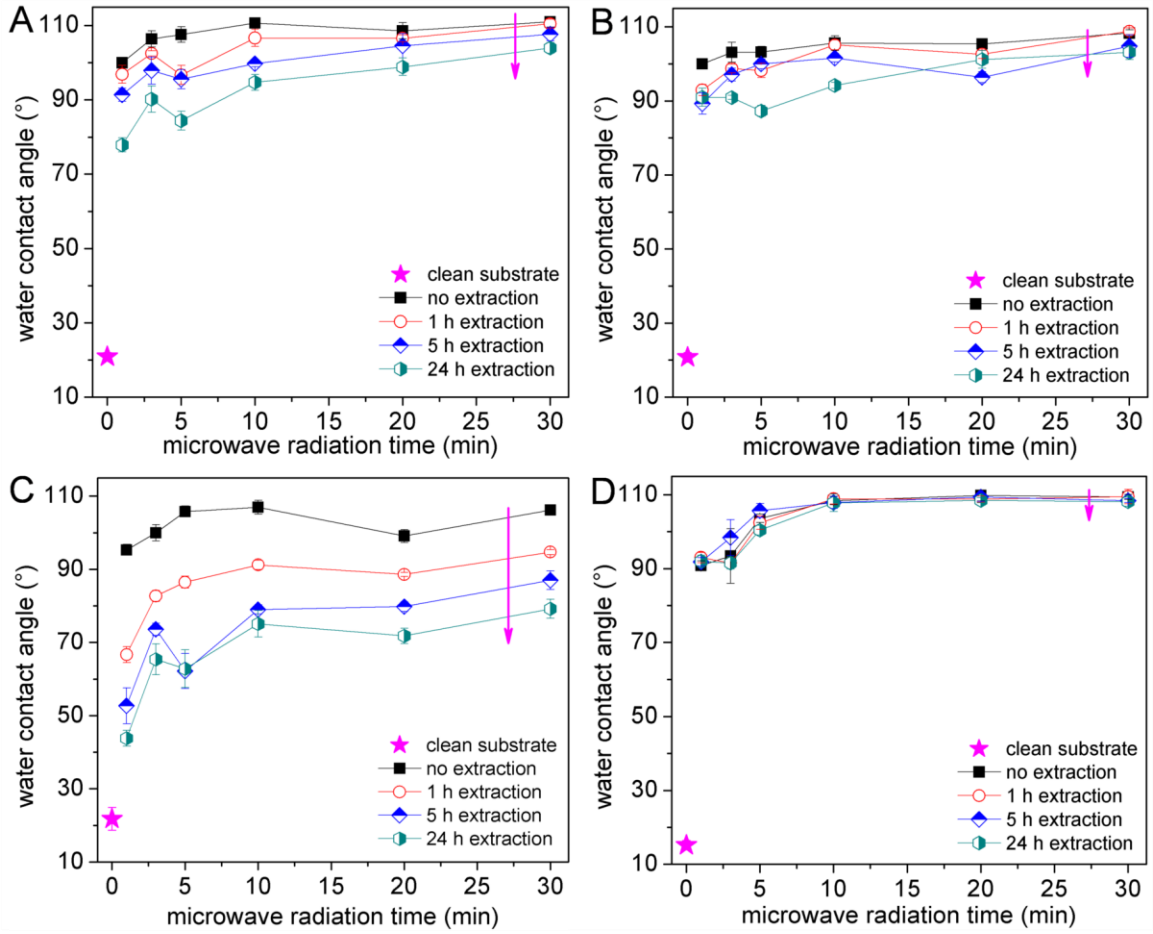

Figure 3.1. **Water contact angle (WCA) measurements for (A, B) polished silicon substrates coated with a native oxide or 100-nm-thick thermal oxide, respectively, (C) soda lime glass, and (D) polished quartz substrates as a function of the duration of treatment with microwave radiation while immersed in 1-octanol. Corresponding WCA measurements are included for these substrates after 1, 5, and 24 h of continuous Soxhlet extraction. The pink star on each plot indicates the WCA values after piranha cleaning but before the microwave-assisted reaction with 1-octanol. Reprinted with permission from Ref. [208] ©2016 American Chemical Society.**

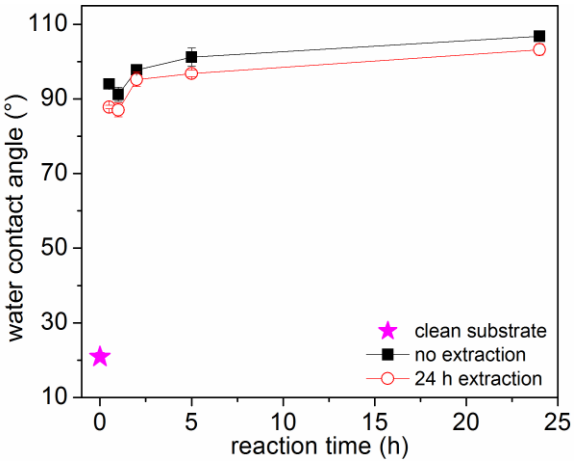

Figure 3.2. The WCA measurements for piranha cleaned polished silicon substrates after immersion in a neat solution of 1-octanol at 180 °C using an oil bath for the duration indicated in a closed vessel. Reprinted with permission from Ref. [205] ©2016 American Chemical Society.

Water contact angle measurements of the modified silicon oxide surfaces were obtained after specific durations of exposure to microwave radiation. The substrates were initially hydrophilic with WCA values of ~20° for all substrates. Microwave processing in the presence of 1-octanol with a set point of 180 °C resulted in a rapid increase in WCA to ~100° within 1 min of treatment (Figure 3.1A). This result suggests that the microwave radiation enabled a more rapid reaction of aliphatic alcohols with the surfaces of silicon oxides to form hydrocarbon monolayers, compared with an oil bath reaction at the same temperature (Figure 3.2). The findings of our study also present an improvement in reaction time in comparison to the results previously reported for the modification of either hydrogen-terminated silicon or silanol-terminated SiO_x using other methods that include UV illumination (2.5 h),[174] assistance from metal catalysis (1 to 72 h),[177] or convective heating (2.5 h).[65] The WCA values continued to increase with an increasing duration of exposure to microwave radiation until reaching a value of 110°. This high WCA was obtained after only 10 min of exposure to microwave radiation for the native oxide-coated substrates. The WCA plateaued at 110°, in agreement with values reported in the literature on hydrocarbon-terminated surfaces.[48] These results suggested that the surfaces were covered with aliphatic alcohols after only 10 min of treatment with microwave radiation. This rapid reaction rate could be attributed in part to the effective removal of the surface adsorbed water layer by means of dielectric heating.[84] It was previously reported that an

efficient removal of water adsorbed on the surfaces of silica could lead to the preparation of monolayers with a high surface coverage.[61] Water molecules effectively absorb microwave radiation because of their dielectric properties, which could result in the thermally induced removal of these molecules from the surfaces of the substrate. This simple, effective mechanism for microwave-assisted water removal from the reactive interfaces of the SiO_x substrates could facilitate the condensation reaction.

Soxhlet extraction of the monolayer-modified SiO_x surfaces was performed to evaluate the extent to which these surfaces were covalently modified with the aliphatic alcohols. The extraction process should remove 1-octanol that is only weakly interacting with the substrates.[153, 180] The relative change in WCA following extraction continued to decrease with an increasing duration of microwave radiation (Figure 3.1). In other words, the hydrophobicity of the monolayer-covered surfaces remained consistent after prolonged extraction with hot toluene when the monolayers were prepared with a longer (e.g., 30 min) duration of microwave treatment. The measured hysteresis for these WCA measurements also improved after a prolonged Soxhlet extraction, decreasing from an average value of ~4° to ~1° (Appendix A1). These results indicated that the uniformity of the measured hydrophobicity of the native SiO_x surfaces after reaction with 1-octanol was proportional to the length of exposure to microwave radiation for periods of up to 30 min. Monolayers formed on either the native oxide and 100-nm-thick SiO_x surfaces exhibited similar results to those observed for the native oxide substrates. (Figure 3.1A and B). The microwave-assisted reaction of 1-octanol with silanol groups to form hydrophobic monolayers was effective for both types of substrates.

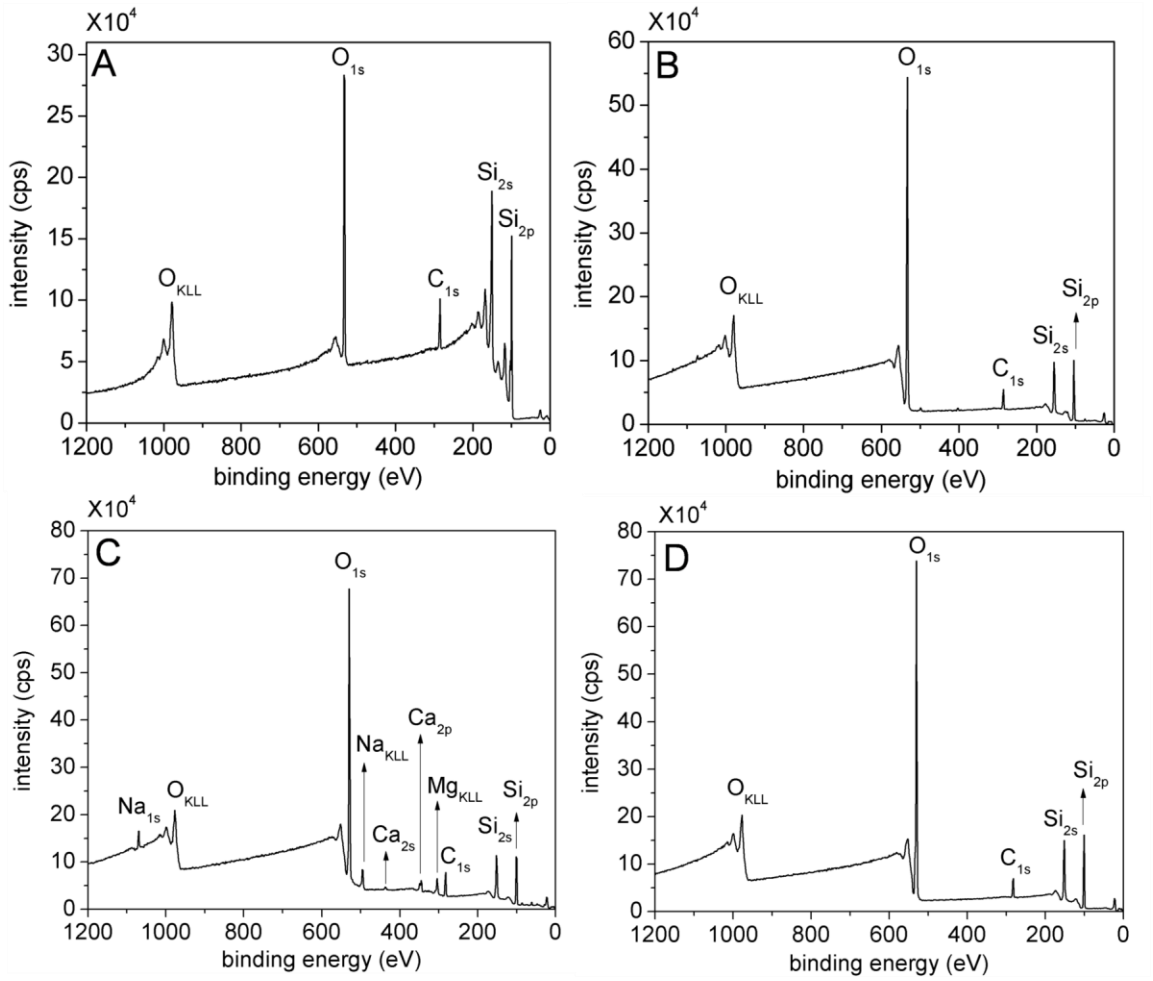

Figure 3.3. Survey XPS spectra of a piranha cleaned silicon substrate (A) without or (B) with a 100-nm thick thermally grown oxide film, (C) a soda-lime glass, and (D) quartz substrate after microwave-assisted reaction with 1-octanol and 24 h continuous Soxhlet extraction with hot toluene. Reprinted with permission from Ref. [208] ©2016 American Chemical Society.

One of the most noteworthy advantages of forming monolayers on surface-bound silanols through condensation with alcohols is its applicability in the wide variety of substrates that can be modified using the technique. To demonstrate this versatility, monolayers of aliphatic alcohols were also prepared by treatment with microwave radiation in the presence of soda lime glass and polished quartz substrates. This study provided further insight into the impact of the composition of the SiO_x substrates on the quality of the resulting monolayers. The WCA measurements for soda lime glass and quartz substrates after microwave reaction with 1-octanol are plotted in Figure 3.1C and

D. The WCA increased from ~20° to 110° for both substrates as a function of increased duration of exposure to microwave radiation. The rates of reaction and degree of change in WCA for these systems were comparable to the results obtained for the thin films of SiO_x on polished silicon (Figure 3.1A and B). As mentioned for the study using a silicon substrate, the formation of monolayers on SiO_x substrates is likely influenced by the dielectric heating of the adsorbed water layer. The relatively rapid formation of SAMs on both soda lime glass and polished quartz substrates could also be attributed to the removal of this surface water layer. Differences were, however, observed following the hot toluene extraction. The WCA values decreased with the extraction of the soda lime substrates (Figure 3.1C). This result suggested that a substantial amount of 1-octanol was physically adsorbed onto these surfaces, which was subsequently removed during the toluene extraction process. In contrast, the WCA values remained consistent throughout the extraction process for the quartz substrates with an average WCA value of 108° and a hysteresis of 0° after 24 h of Soxhlet extraction (Appendix A1). The larger decrease in WCA values for the treated soda lime substrates could be attributed to the impurities (e.g., Na, Mg, Ca) present in these substrates (Figure 3.3C). Unlike multireactive silanes (e.g., alkyltrichlorosilanes) that can form multilayers via intermolecular polymerization,[46] the aliphatic alcohols do not cross-link to form an extended polymer because each aliphatic alcohol will react with only one surface-bound silanol group. Molecules adsorbed onto the soda lime surfaces without covalent bonding are easily removed during the Soxhlet extraction procedure. The monolayers could also be compromised by the breakage of covalent bonds induced by the diffusion of impurities within these surfaces during the Soxhlet extraction process. The quality of the monolayers on soda lime glass substrates can be improved by the deposition of an additional layer of silica, such as by sol–gel processing,[183] prior to the formation of monolayers (See Appendix B). In contrast, the quartz substrates had relatively fewer surface impurities (Figure 3.3D). Monolayers prepared from 1-octanol on the polished quartz substrates exhibited the highest surface coverage and the highest quality following Soxhlet extraction.

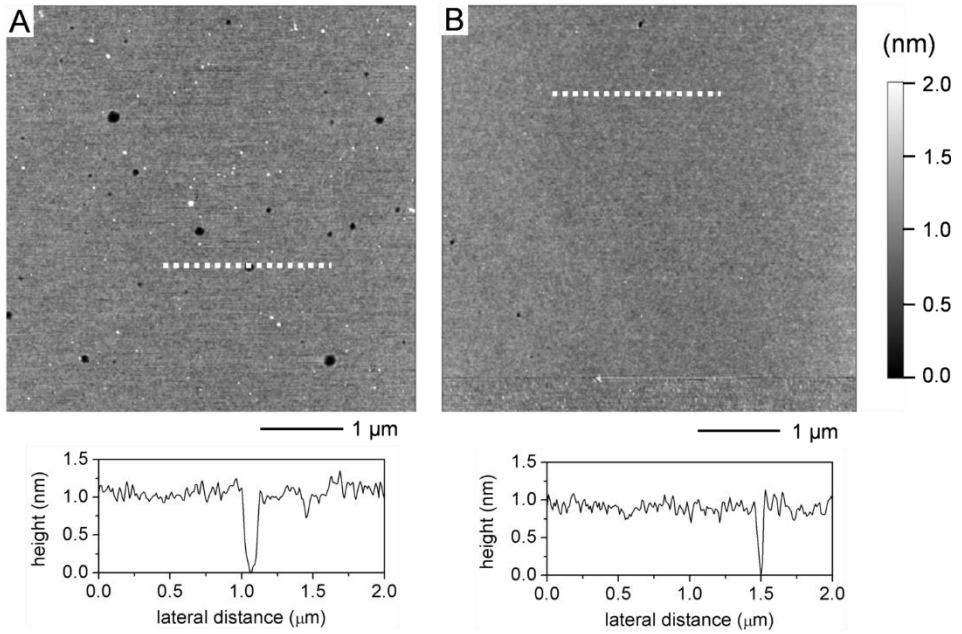

Figure 3.4. **Atomic force microscope (AFM) images and cross-sectional profiles (corresponding to the white dashed lines) for piranha-cleaned polished silicon substrates after microwave-induced reaction with 1-octanol for (A) 1 min and (B) 30 min. Substrates were treated with 24 h continuous Soxhlet extraction in hot toluene before analysis by AFM. Reprinted with permission from Ref. [208] ©2016 American Chemical Society.**

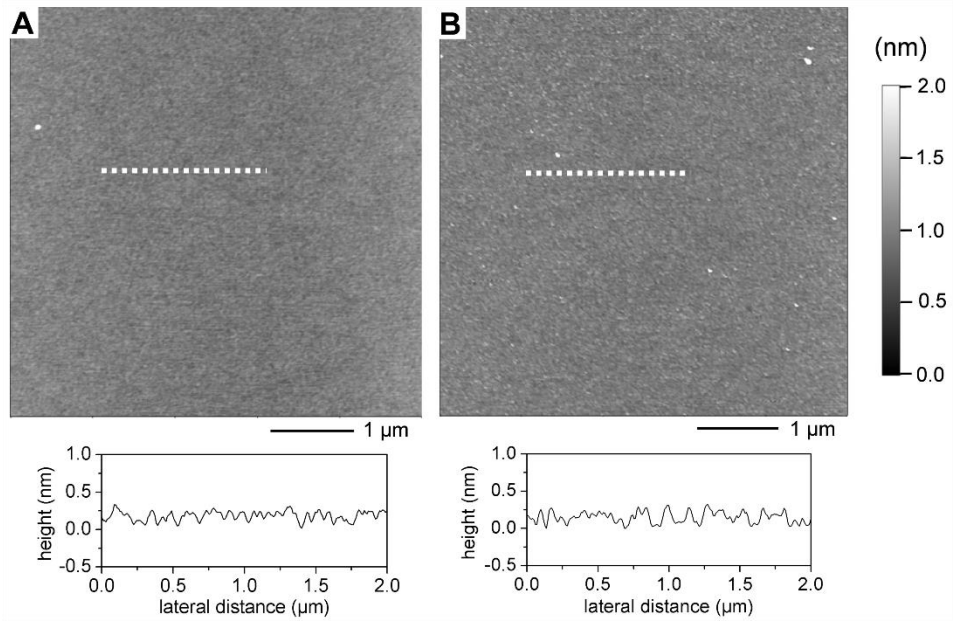

Figure 3.5. Atomic force microscopy (AFM) images and cross-sectional profiles (corresponding to the dashed white lines) of polished silicon substrates with either (A) a native oxide or (B) a 100-nm thick thermal oxide after piranha cleaning. Root mean square (RMS) roughness values of these cleaned substrates were 0.11 and 0.17 nm, respectively. Reprinted with permission from Ref. [208] ©2016 American Chemical Society.

The surface topography of the monolayer-modified SiO_x substrates was analyzed by AFM. Specifically, piranha-cleaned silicon substrates treated with microwave radiation while immersed in 1-octanol for either 1 or 30 min were analyzed after 24 h of Soxhlet extraction to correlate observations made by WCA analyses to surface features. The surfaces depicted relatively smooth topography with RMS roughnesses of 0.23 and 0.10 nm after 1 and 30 min of treatment with microwave radiation, respectively (Figure 3.4A and B). The higher roughness factor for samples treated for 1 min was attributed to the defects observed in the monolayers. The samples treated for 30 min with microwave radiation had a similar roughness to that of the piranha-cleaned silicon substrate (i.e., 0.11 nm, Figure 3.5). These AFM analyses suggested that the SAMs on the native oxide are relatively uniform with a few distinguishable defects after 1 min of microwave radiation. These defects were ~1 nm in height, corresponding to the approximate molecular length of 1-octanol. Fewer defects were observed in the SAMs after 30 min of microwave treatment. These results further supported the assessment that a higher surface coverage of 1-octanol is achieved with a longer exposure to microwave radiation.

In summary, a systematic study into the microwave-assisted reaction of 1-octanol with various silicon oxide substrates was performed using the CEM microwave reactor. Increases in the duration of exposure to microwave radiation of up to 30 min increased the hydrophobicity of these substrates, quickly achieving a WCA value of 110°. This value is in agreement with the accepted literature value for uniform SAMs prepared from linear, methyl-terminated species.[48] Furthermore, consistent WCA values with an average hysteresis of <2° after an extensive Soxhlet extraction further demonstrated the uniformity of these monolayers. The quality of monolayers was largely dependent on the composition of the underlying silicon oxide surfaces.

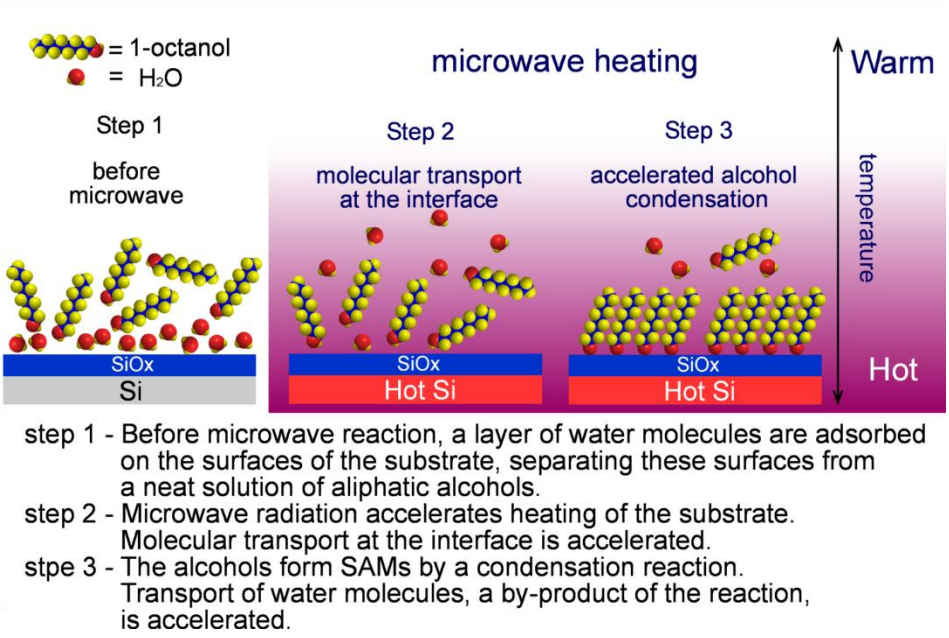

Figure 3.6. Schematic depiction of the Formation of Self-Assembled Monolayers (SAMs) by Microwave-Assisted Reaction of Aliphatic Alcohols with Silicon Oxide Surfaces. Reprinted with permission from Ref. [208] ©2016 American Chemical Society.

Influence of Microwave-Induced Substrate Heating on Monolayer Formation. A kinetic study into the microwave-assisted formation of SAMs on SiO_x substrates was pursued for both polished silicon and quartz substrates to investigate the impact of microwave-induced substrate heating. Microwave radiation can induce the heating of materials by ionic or electronic conduction losses.[98, 109] This process can induce the selective heating of conductive materials, such as metals[109, 184] and other conductive thin films.[113] Microwave heating of p-type doped silicon substrates could influence the kinetics

of the reactions of 1-octanol with the SiO_x surfaces. Microwave heating of the doped silicon substrates could yield high temperatures at the SiO_x surfaces, where the condensation of 1-octanol takes place (Figure 3.6). For the reaction to occur, the alcohol molecules need to interact with surface-bound silanol groups. Molecular transport of the adsorbed water layer away from the surfaces and of the aliphatic alcohol toward these surfaces is accelerated by the dielectric heating of water molecules and the conduction loss of the substrate.[84, 109] Aliphatic alcohols form covalent silyl ether (Si–O–C) bonds through a condensation reaction, analogous to a Williamson ether synthesis.[65] This condensation reaction is activated through the thermal energy provided by microwave heating. Microwave radiation will further assist the reaction by also enhancing the mass transport of water molecules produced as a byproduct of this reaction. In summary, microwave radiation can effectively induce the rapid covalent surface modification of SiO_x surfaces.

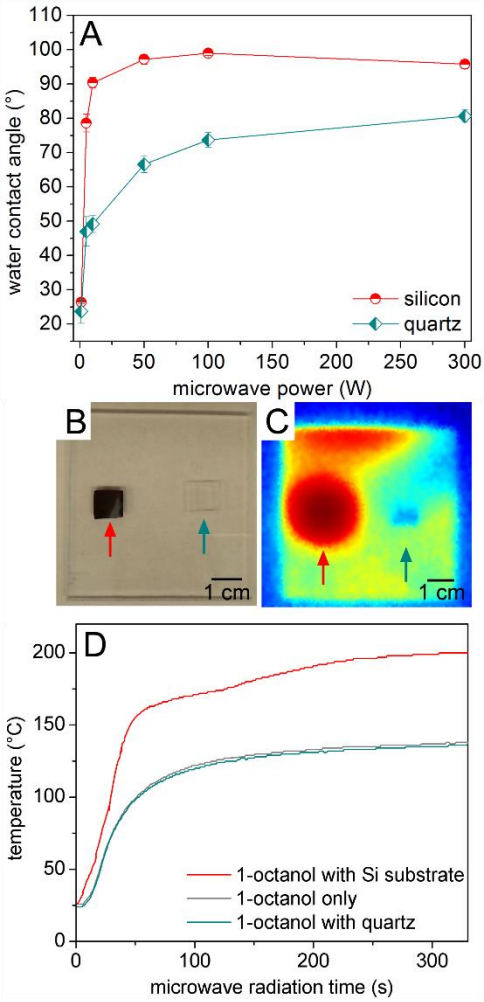

Figure 3.7. **(A) Water contact angle trends for polished silicon and polished quartz substrates as characterized after a 5 min exposure to various levels of microwave power. (B) Visible light and (C) infrared images of the silicon and quartz substrates supported on an acrylic plate obtained after direct exposure to microwave radiation for 15 s. (D) Temperature profiles recorded in a 1-octanol solution during exposure to microwave radiation at 300 W for up to 5 min in the presence of either a silicon or quartz substrate as well as in the absence of either substrate. Reprinted with permission from Ref. [208] ©2016 American Chemical Society.**

To further investigate the impact of microwave-induced substrate heating, the native-oxide-coated silicon and the quartz substrates were separately treated with microwave radiation at predetermined levels of microwave power for a constant duration (i.e. 5 min) without temperature constraints. After microwave processing, Soxhlet extraction was performed for 24 h before obtaining WCA measurements (Figure 3.7A).

This analysis indicated a clear discrepancy in reaction rates between these two types of substrates. As the microwave power increased, an increase in WCA was observed for both substrates. The WCA values for the monolayers on the polished silicon quickly reached a plateau at ~100°, and the WCA values for the monolayers on polished quartz more steadily approached 80°. This result indicated that the rate of formation of the monolayers was faster on the polished silicon than on the polished quartz substrates. The discrepancy between these reaction rates is attributed to the differences in the rate of substrate heating induced by microwave radiation. To better assess the microwave-induced heating of the substrates, the silicon and quartz substrates were treated with microwave radiation in the absence of aliphatic alcohols for 15 s while being supported on an acrylic plate (Figures 3.7B). The thermal image in Figure 3.7C portrays a difference in temperature between the substrates after exposure to microwave radiation. Differences in substrate heating could be attributed to dielectric and electronic loss of these materials.[109] These differences in substrate heating were also observed when monitoring changes in solution temperature induced by microwave radiation at 300 W over 5 min (Figure 3.7D). Although the amount of microwave energy delivered to the reaction vessels was kept consistent between these experiments, the temperature of the solution was higher for the reaction vessel containing the polished silicon substrates than for the polished quartz substrates. The increased reaction rate observed for the polished silicon could be attributed to differences in the temperature of the reaction, likely induced by substrate heating. In summary, the properties of the substrate materials could alter the rate of the microwave-assisted reaction. In particular, the doped silicon substrates coated with a native oxide film were more efficient at absorbing microwave energy than the quartz substrates. Although high-quality monolayers can be achieved for both types of substrates (Figure 3.1A and D) at a prolonged duration of exposure to microwave radiation, the rates of reaction can be substantially different. In conclusion, differences in electronic and dielectric characteristics of the substrates can play a role in the efficiency of microwave-induced heating, influencing the overall rates of reaction for the condensation of 1-octanol on surface-bound silanols.

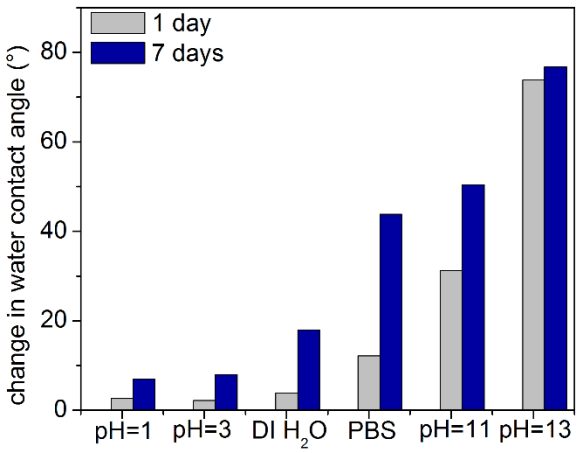

Figure 3.8. Hydrolytic stability of monolayers formed on piranha-cleaned silicon substrates through a microwave-induced reaction with 1-octanol as evaluated by WCA measurements. Reprinted with permission from Ref. [208] ©2016 American Chemical Society.

Hydrolytic Stability of Monolayers Derived from Microwave-Assisted Reactions with Alcohols. The stability of covalently attached monolayers are of great interest.[72] Monolayers derived through the condensation reaction of alcohols with surface-bound silanols would contain silyl ether (Si–O–C) bonds, which could hydrolyze upon immersion in either acidic or basic aqueous solutions.[185] The hydrolytic stability of monolayers of 1-octanol on SiO_x substrates prepared by microwave-assisted reactions was evaluated by published procedures.[72] In particular, the hydrolytic stability of the monolayers was evaluated at room temperature while immersed in aqueous solutions at different pH values for different periods of time (e.g., 1 day and 7 days). The stability of the monolayers was assessed by monitoring changes in WCA values. As depicted in Figure 3.8, the monolayers exhibited differences in their hydrophobicity when immersed in aqueous solutions of different pH values. The hydrolytic stability of the monolayers demonstrated a comparable result to monolayers derived from 1-octadecene on silicon oxide surfaces when immersed in acidic solutions, but the hydrolytic stability of the 1-octanol monolayers was worse in both DI water and PBS buffer.[72] This discrepancy could be attributed to the difference in the length of the alkyl chains used in these studies. Monolayers derived from 1-octanol contain a backbone of 8 carbons, whereas the monolayers derived from 1-octadecene possess a backbone of 18 carbons. The longer carbon chain would improve the passivation of the surfaces to the hydrolysis of the silyl ether bond, providing further stability to the SAMs. The substrates coated with 1-octanol

undergo catastrophic failure when immersed in an aqueous solution at pH 13. These substrates also had opaque white spots, suggesting that the underlying silicon oxide film had been etched. This result could be attributed to the hydrolysis of the silyl ether bond (Si–O–C) under basic conditions, which would compromise the integrity of the monolayers. A high concentration of hydroxide ions can also promote the degradation of the silicon oxide films, which would accelerate the degradation of the monolayers. This instability of the monolayers is attributed to water and hydroxide ion penetration into the monolayers at high pH values, which can hydrolyze the Si–O–C bonds that anchor the 1-octanol to the SiO_x substrates.[186] The monolayers of 1-octanol were more stable under acidic conditions in comparison to deionized water or more basic solutions. The quality of the monolayers in acidic conditions was retained possibly because there were fewer hydroxide ions available in solution to drive the cleavage of the silyl ether bonds. In conclusion, monolayers formed by the microwave-assisted condensation of aliphatic alcohols are more stable under acidic conditions and less stable under basic conditions.

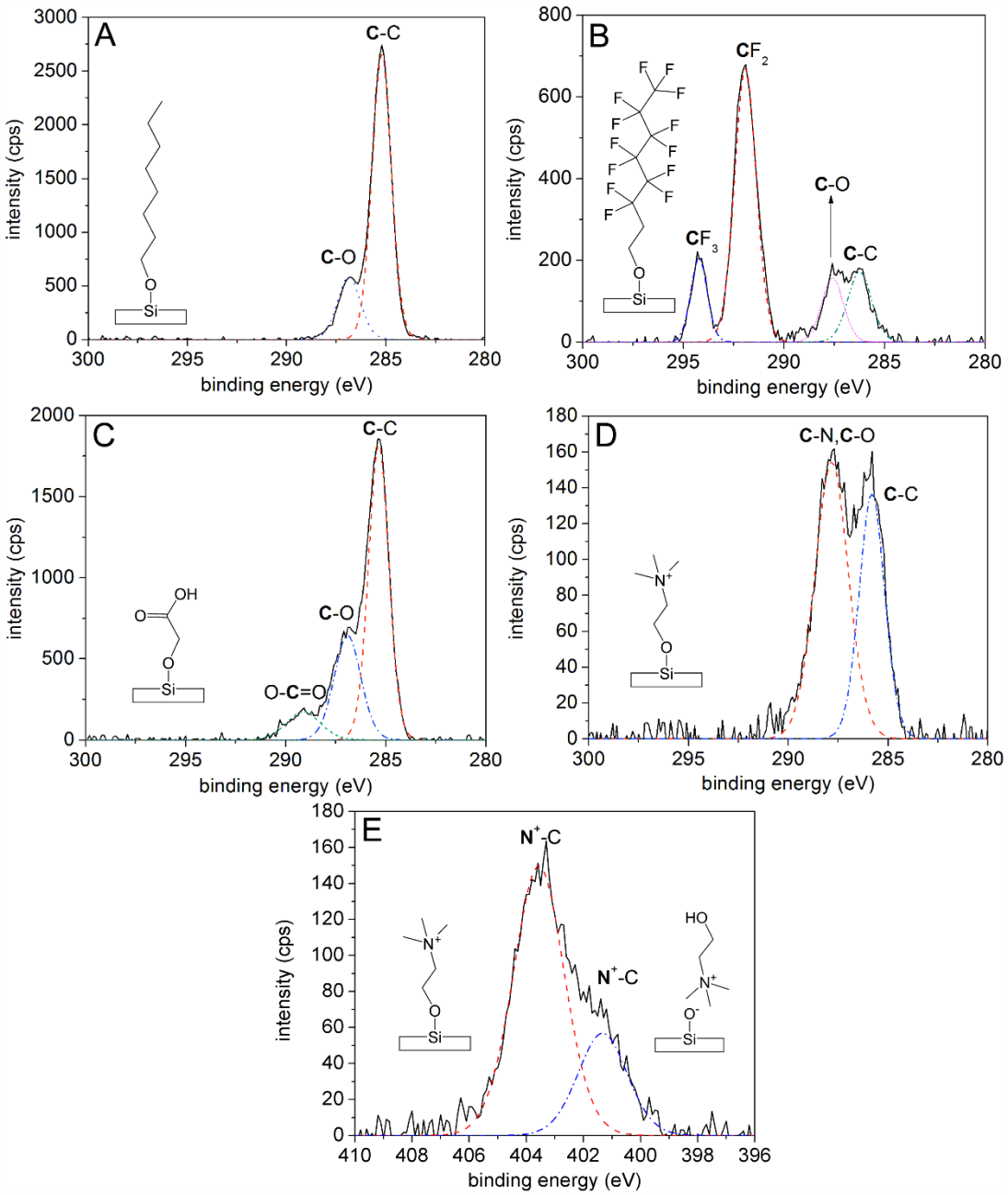

Figure 3.9. **High-resolution XPS spectra of silicon substrates after microwave-assisted reactions with different functional alcohols. Carbon spectra (C_{1s}) after microwave reactions of (A) 1-octanol, (B) 1H,1H,2H,2H-perfluoro-1-octanol, (C) 1 M glycolic acid, and (D) 1 M choline chloride. (E) Nitrogen (N_{1s}) spectrum for the substrate reacted with 1 M choline chloride. Reprinted with permission from Ref. [208] ©2016 American Chemical Society.**

Controlling Surface Chemistry Using Microwave-Assisted Reactions with Alcohol Compounds. Tuning the functionality of SiO_x surfaces is often desired for their use in fields of study that include microelectronics[6] and biological interfaces.[157, 169-171] The techniques introduced in this chapter can be expanded to further modify the surface chemistry of SiO_x surfaces. For instance, these surfaces can be functionalized with fluorocarbons, a quaternary ammonium, or carboxylic acids. Piranha-cleaned silicon substrates were treated with microwave radiation while being immersed in a neat solution of 1*H*,1*H*,2*H*,2*H*-perfluoro-1-octanol, 1 M choline chloride, or 1 M glycolic acid at 120 °C for 30 min. We have chosen a lower reaction temperature for these processes to prevent potential thermal degradation of these reagents. The modified substrates were thoroughly washed and sonicated with a series of solvents including acetone, isopropanol, ethanol, and water upon completion of the microwave reaction. The substrates were characterized with X-ray photoelectron spectroscopy (XPS). High-resolution carbon spectra (C_{1s}) of these substrates after the microwave-induced reaction exhibited a clear difference in the chemical composition of their surfaces (Figure 3.9). Two carbon peaks were observed for surfaces reacted with 1-octanol, which were attributed to C–C and C–O peaks at binding energies of 285.2 and 286.9 eV, respectively. The substrates reacted with 1*H*,1*H*,2*H*,2*H*-perfluoro-1-octanol exhibited four carbon peaks with a contribution of fluorocarbons (**C**F_3 and **C**F_2) at binding energies of 294.2 and 291.9 eV. The ratio between the peak areas of **C**F_3 and **C**F_2 was 0.22. This fluorocarbon reactant contains five **C**F_2 and one **C**F_3 per molecule, respectively. The peak area ratio matches the ratio of **C**F_3 to **C**F_2 anticipated from the molecular structure, suggesting that the composition of these monolayers agrees with the chemical structure of the reactant. Additional peaks associated with **C**–O and **C**–C were identified at binding energies of 287.5 and 286.3 eV, respectively. The higher binding energies observed for the **C**–O and **C**–C peak positions relative to those observed for 1-octanol could be attributed to the more electronegative backbone of the fluorocarbon.

The SiO_x substrates can also be coated with monolayers that exhibit a polar functional group. For instance, glycolic acid can be grafted onto silicon oxide to exhibit a carboxylic acid-functionalized surface. The glycolic acid was dissolved in deionized water prior to the microwave-assisted reaction. Three peaks were observed in the high-resolution C_{1s} XPS spectrum of these modified substrates, corresponding to **C**–C, **C**–O, and O–**C**=O peaks at binding energies of 285.4, 286.9, and 289.1 eV, respectively (Figure

3.9C). Choline chloride can also be covalently attached if it is desired to derive SiO_x substrates with surfaces exhibiting quaternary ammonium functional groups. Similar to glycolic acid, choline chloride was dissolved in deionized water prior to the microwave-assisted reaction. The presence of choline chloride was confirmed by high-resolution XPS C_{1s} and N_{1s} spectra (Figure 3.9D and E). Doublets of the carbon peaks were assigned as overlapping **C**–O and **C**–N peaks (287.8 eV) and a **C**–C peak (285.8 eV).[187] The high-resolution N_{1s} spectrum had a relatively high intensity in comparison to the intensities in the C_{1s} spectrum. The N_{1s} spectrum exhibited two peaks (403.4 and 401.3 eV) assigned to charged nitrogen in two different states.

3.5. Conclusions

We have successfully demonstrated a microwave-assisted reaction of silicon oxide surfaces with alcohol-containing compounds. These prevalent laboratory reagents can be utilized for the covalent surface modification of silicon oxide surfaces without any specific considerations needed to control exposure to ambient moisture in the laboratory. Systematic studies demonstrated the formation of monolayers with 1-octanol on various SiO_x surfaces using a microwave reactor. For these studies with 1-octanol, a reaction time of as little as 1 min could render each of the surfaces sufficiently hydrophobic to achieve WCA values of up to 100°. The WCA values for these substrates plateaued at ~110° after further treatment with microwave radiation. The quality of the 1-octanol monolayers, as measured by the extent to which these monolayers covalently modify the SiO_x surfaces, was evaluated using a Soxhlet extraction process with hot toluene. The WCA and hysteresis values remained relatively consistent, demonstrating the formation of high-quality monolayers. The rates of reaction were also studied for polished silicon and quartz substrates at constant microwave power and durations of exposure to microwave radiation to investigate the impact of substrate heating when exposed to microwave radiation. It was determined that the rate of the reaction was faster for polished silicon substrates than for polished quartz substrates as observed from trends in their resulting WCA values. The hydrolytic stability was also assessed for monolayers of 1-octanol. It was determined that these monolayers were relatively stable under acidic conditions but exhibited only moderate stability in deionized water or PBS buffer. The monolayers degraded under

basic conditions. The microwave-assisted reactions introduced in this chapter can be utilized to control the surface chemistry of a variety of silicon oxide surfaces. The techniques demonstrated in this study can be utilized to covalently modify silicon oxide surfaces using a variety of molecules containing alcohols.

Chapter 4.

Formation of Mixed Monolayers of Aliphatic and Fluorinated Alcohols to Tune Oleophobicity of Silicon Oxide Surfaces

4.1. Notice of Permissions

The following chapter is adapted with permission from Ref. [227] Austin W. H. Lee and Byron D. Gates, "Tuning Oleophobicity of Silicon Oxide Surfaces with Mixed Monolayers of Aliphatic and Fluorinated Alcohols", Langmuir 2016, 32, 13030-13039 ©2016 American Chemical Society. The work presented in this paper, including experiments, data acquisition, interpretation and writing has been performed by myself under the guidance of Dr. Byron Gates.

4.2. Introduction

Silicon oxide surfaces with a fine-tuned oleophobicity were prepared using microwave-assisted reactions with mixtures of fluorinated and aliphatic alcohols. Fluorinated or partially fluorinated surfaces have been previously investigated for their ability to tailor the physical properties of surfaces, such as friction and wettability, electronic properties, or resistance to biomolecules,[2, 188-189] for usage in applications that include antiwetting,[120] oil-water separation,[118] electronic devices,[5-6, 190-191] and biomaterials.[36, 192-193] In particular, silicon oxide surfaces modified with fluorocarbon or hydrocarbon chains have been widely pursued in fields requiring a fine control over interface wetting,[194-196] electronics,[5-6, 190-191] and separation science.[26, 197-201] In order to functionalize silicon oxides with fluorocarbons or hydrocarbons, silane-based compounds have been widely utilized to modify the properties of these surfaces through the formation of molecular-scale coatings, commonly referred to as SAMs.[2, 4, 60, 180] Challenges in the formation of silane-based monolayers include the reactivity of silanes with water, their sensitivity to intermolecular polymerization, and tendency to form multilayers.[46, 172, 202] These challenges ultimately limit the control over composition of the monolayers,

especially when mixed monolayers are required for tailoring the properties of surfaces. In contrast, alcohol based reagents forego many of these challenges due to their minimal reactivity with water. Such advantages enable a simple experimental setup under ambient laboratory conditions while also tuning the oleophobicity and hydrophobicity of silicon oxides through precisely controlling the composition of the reactants.

Previously, the surface modification of silicon oxide surfaces with various alcohol compounds has been achieved through a microwave-assisted condensation reaction.[180] Microwaves can effectively deliver thermal energy to drive the condensation reaction of alcohols with surface bound silanol groups. Formation of monolayers can be accelerated through microwave-induced heating of doped silicon substrates as well as heating via surface-adsorbed water molecules. High temperatures created at the interface accelerate the condensation of alcohol and desorption of water molecules at the silicon oxide surfaces.[180] Microwave radiation techniques can also provide good control over the temperatures of solutions in pressurized reaction vessels.[84] Here, we utilize these heating techniques to tune the oleophobicity and hydrophobicity of silicon oxide surfaces. These properties were controlled by tuning the molar ratio of fluorinated and aliphatic alcohols used as reagents in these reactions. First, we investigated the reactivity, surface properties, and elemental composition of monolayers formed with three different fluorinated alcohol compounds. Their characterization was performed using contact angle measurements and XPS analyses. Monolayers with a fluorocarbon backbone should be easily discernible using these techniques due to their ability to alter the surface wetting properties of the silicon oxide surfaces,[2, 189] while also possessing a unique spectroscopic signature.[153] We evaluated each of these three compounds for their ability to effectively modify the surface properties of silicon oxide substrates. Next, surface oleophobicity was tuned by systematically controlling the molar ratio of fluorinated and aliphatic alcohols within the reaction medium. This approach enabled us to tune the composition of monolayers on silicon oxide surfaces (e.g., fluorinated backbones relative to their hydrocarbon content) in order to finely adjust their resulting surface properties.

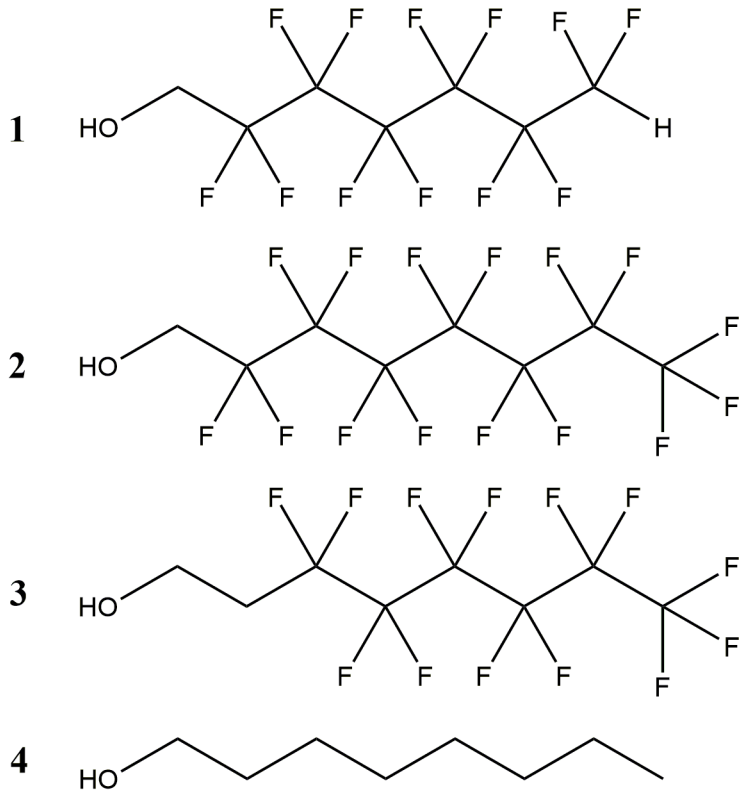

Figure 4.1. Structures of Alcohol-Containing Compounds Evaluated for Their Ability To React with and Modify the Properties of Silicon Oxide Surfaces. Reprinted with permission from Ref. [227] ©2016 American Chemical Society.

A series of three compounds, each with a unique fluorinated, linear backbone and an alcohol head group, were chosen for evaluating their ability to modify silicon oxide surfaces through microwave-assisted reactions. The compounds chosen for this study were 1H,1H,7H-perfluoro-1-heptanol ($H(CF_2)_6(CH_2)OH$, compound 1), 1H,1H-perfluoro-1-octanol ($CF_3(CF_2)_6(CH_2)OH$, compound 2), and 1*H*,1*H*,2*H*,2*H*-perfluoro-1-octanol ($CF_3(CF_2)_5(CH_2)_2OH$, compound 3). A fourth compound used for comparison was 1-octanol ($CH_3(CH_2)_7OH$, compound 4). The molecular structures of these four compounds are shown in Figure 4.1. Each compound has distinguishable traits. Compound 1 possesses a terminal CHF_2 moiety, unlike compounds 2 and 3 that each possess a terminal CF_3. Differences in the terminal group could affect the overall surface properties of the resulting monolayers due to deviations in their packing density and chemical properties, which is analogous to monolayers of linear chain thiols on gold surfaces.[203-205] Another difference in the molecular structure of compounds 1–3 is in the length of

hydrocarbon spacer in between the fluorocarbon chain and the hydroxyl group. Both compounds 1 and 2 have a methylene group between the hydroxyl head group and the fluorocarbon chain, while compound 3 has a bridging ethylene group. The length of bridging hydrocarbon chain between hydroxyl group and fluorocarbon chain may influence the overall packing density of the resulting monolayers, which could ultimately impact their ability to control the wettability of the modified surfaces.[206-207] In this study, we sought to find a fluorinated alcohol compound capable of forming monolayers with a high packing density and a maximum hydrophobicity and oleophobicity. The compounds of interest for this study (compounds 1–3) were chosen because of the similarities in their molecular chain lengths and fluorocarbon contents. Compound 4 was also studied as a reference compound containing only a hydrocarbon backbone with a similar molecular chain length to the other reagents. All four compounds also possess low melting points and are liquids at room temperature with the exception of compound 2, which was heated to ~50 °C prior to further use. Reactions were initially carried out using only neat solutions of each reactant; no solvents were used to dilute any of these reactants. Variation in the composition of each reactant was the primary variable in the initial study. This study sought to determine the effectiveness of each reactant to tune the surface properties of silicon oxides. Other parameters, such as microwave reaction time and temperature, were kept constant for this study. In the second part of the study, formation of mixed monolayers was sought in order to tune the oleophobicity of silicon oxide surfaces. This reaction was achieved through microwave processing of the substrates while immersed in a mixture of fluorocarbon alcohols and aliphatic alcohols. Oleophobicity, hydrophobicity, surface composition, and surface adhesion properties of the modified substrates were evaluated using contact angle measurements, X-ray photoelectron spectroscopy (XPS), and atomic force microscopy (AFM).

4.3. Experimental

Reagents and Materials. All reagents were used as received, which included 1*H*,1*H*,7*H*-dodecafluoro-1-heptanol [$H(CF_2)_6(CH_2)OH$, Alfa Aesar, 97%, CAS no. 335-99-9], 1*H*,1*H*-perfluoro-1-octanol [$CF_3(CF_2)_6(CH_2)OH$, Alfa Aesar, 97%, CAS no. 307-30-2], 1*H*,1*H*,2*H*,2*H*-perfluoro-1-octanol [$CF_3(CF_2)_5(CH_2)_2OH$, Sigma-Aldrich, 97%, CAS no.

647-42-7], 1-octanol [$CH_3(CH_2)_7OH$, Sigma-Aldrich, ACS reagent grade, 99%, CAS no. 111-87-5], octyldimethylchlorosilane (Sigma-Aldrich, 97%, CAS no. 18162-84-0), toluene (Fisher Scientific, Laboratory grade, 99.5%, CAS no. 108-88-3), hexadecane (Sigma-Aldrich, 99%, CAS no. 544-76-3), sulfuric acid (Caledon, ACS reagent grade, CAS no. 7664-93-9), hydrogen peroxide (ACP, ACS reagent grade, CAS no. 7722-84-1), anhydrous ethyl alcohol (Commercial Alcohols, P016EAAN, CAS no. 64-17-5), acetone (Fisher Scientific, reagent grade, CAS no. 67-64-1), and isopropanol (Fisher Scientific, reagent grade, CAS no. 67-63-0). Four inch, p-type, test grade, single-side polished, ⟨100⟩ silicon wafers were purchased from the Nanofabrication Facility in 4D LABS at Simon Fraser University.

Preparation of Silicon Substrates. Preparation of the silicon substrates is described in the previous chapter and in the previous literature.[208]

Microwave-Assisted Reactions. The procedure for the microwave-assisted surface modification of silicon oxides with 1-octanol was described previously.[208] Briefly, 2 mL of a reactant or a mixture of reactants was placed with a cleaned substrate into a 10 mL glass test tube (part no. 908035, CEM). Separate tubes were used for each distinct reaction. Each sample was exposed to microwave radiation using a CEM Discover microwave reactor for 30 min at a set point temperature of 130 °C. All samples were cooled after the reaction for 5 min before handling. After removing each substrate from its glass reaction vessel, the substrates were individually washed with a series of solvents, such as acetone and isopropanol. Each washed substrate was dried under a stream of filtered N_2 gas. To remove physically adsorbed molecules and contaminants, the substrates were sonicated in anhydrous ethyl alcohol for ~2 min, rinsed with DI water, and dried under a stream of filtered N_2 gas.

Preparation of Mixed Monolayers. Mixtures containing different ratios of 1*H*,1*H*,2*H*,2*H*-perfluoro-1-octanol and 1-octanol were prepared with specific mole ratios of each reagent. The amount of each reactant required to create these mixtures were calculated from the molar masses of each compound. These solutions were vortexed using a vortex mixer (Vortex-Genie 2, Scientific Industries Inc.) vigorously to ensure homogeneous mixing. Approximately 2 mL of each mixture was loaded into separate 10

mL glass test tubes along with clean silicon substrates for microwave processing as described above.

Contact Angle (CA) Measurements. Contact angle measurements were performed to evaluate surface coverage of the monolayers and the effectiveness of tailoring the wettability of the modified surfaces. In particular, hydrophobicity and oleophobicity of the substrates were evaluated by CA measurements using droplets of DI water, toluene, or hexadecane. These measurements were obtained for 2 μL droplets of each solvent dispensed onto distinct regions of each substrate. The CA was measured as the angle between the air–liquid interface of each droplet and the interface of each liquid and the substrates. Five advancing contact angle measurements were obtained for each sample by adding 2 μL per consecutive measurement. Four receding contact angle measurements were subsequently obtained by retracting 2 μL per consecutive measurement. The average and standard deviation were determined by calculating the average and the standard deviation of these five advancing contact angle measurements.

X-ray Photoelectron Spectroscopy (XPS). Chemical composition of modified silicon oxide surfaces were investigated by XPS. These studies were conducted using a Kratos Analytical Axis ULTRA DLD system with a monochromatic aluminum source (Al Kα of 1486.7 eV) operating at 150 W at a 90° take-off angle. Survey scans (0–1200 eV) were acquired using a pass energy of 160 eV, a dwell time of 100 ms, and 1 sweep. High-resolution scans were obtained using a pass energy of 20 eV, a dwell time of 500 ms, and 15 sweeps. An area of 700 μm by 300 μm was analyzed for each measurement. The XPS peak analyses and quantification of the peak areas were performed using Vision Processing.

Adhesion Force Measurements. In order to characterize the adhesion force of the samples, force spectroscopy measurements were acquired using an MFP 3D AFM (Asylum Research) using silicon nitride (Si_3N_4) cantilevers from BudgetSensors (Contact-G, tip radius of 10 nm, resonant frequency of 13 kHz, force constant 0.2 N/m). Some cantilevers were coated with octyldimethylchlorosilane by vapor deposition at room temperature in a vacuum desiccator over a period of 17 h. The AFM force measurements were calibrated using the software algorithm provided by the supplier using Igor Pro 6.22

to verify the spring constant of the cantilever. The force measurements were acquired using force-distance measurement technique (see Appendix C, Figure C2 for details) from scan areas of 5 μm by 5 μm with 1024 measurements. The adhesion forces were obtained using Igor Pro 6.22.

4.4. Results and Discussion

The goals of this work include demonstrating the utility of microwave reactions for attaching monolayers of fluorinated alcohols to the surfaces of silicon oxides and further tuning their oleophobicity. Before systematically tuning their oleophobicity, it was essential to first assess the surface properties of the silicon oxide surfaces reacted with different types of fluorinated alcohols. A series of fluorinated alcohols were selected for these microwave-assisted reactions, and the modified surfaces were investigated for changes in their hydrophobicity and oleophobicity. The structures of the fluorinated alcohols chosen for this study are depicted in Figure 4.1. Compound 4, 1-octanol, was chosen as a reference compound for its similar chain length to these reactants and for its known properties when reacting with silicon oxides through microwave-assisted reactions.[208] Piranha-cleaned silicon substrates were immersed in neat solutions of each compound (1 to 4) and subsequently heated in a microwave reactor (i.e. performing separate reactions between the silicon oxide surfaces and each of the compounds).

Experimental conditions were tuned as required for the formation of monolayers from each compound. The reaction temperature was set to 130 °C, and the reaction time was set to 30 min. In previous work, 1-octanol was exposed to microwave radiation at 180 °C, as this temperature yielded the most uniform monolayers with relatively high water contact angle (WCA) values.[208] In the studies described herein, thermal degradation of the fluorinated alcohols was an important limiting factor for the reaction temperature (see Appendix C). It was determined that thermal degradation of compounds 1 to 3 was minimal at a reaction temperature of 130 °C. The duration of each microwave reaction was set to 30 min to ensure the reactions reached completion. Polished silicon substrates covered with a native silicon oxide layer were chosen as the test substrates, which were diced into smaller sections (~1 cm^2) and cleaned in a piranha solution prior to use in these studies.

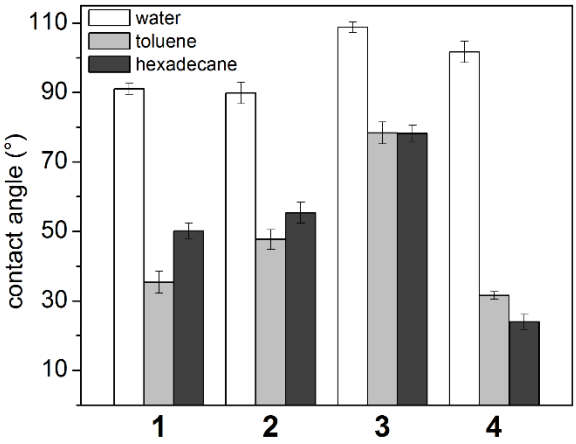

Figure 4.2. Contact angle measurements for silicon substrates modified using a microwave-assisted reaction with compound 1, 2, 3, or 4. These measurements were performed with water (white), toluene (light gray), and hexadecane (dark gray). The average of five advancing contact angle measurements are plotted along with error bars indicating one standard deviation. Reprinted with permission from Ref. [227] ©2016 American Chemical Society.

Correlation between Molecular Structure of Reactants and Quality of Monolayers. The hydrophobicity of the silicon oxide surfaces after each microwave triggered reaction was investigated through water contact angle (WCA) measurements (Figure 4.2). The WCA values provided insight into the uniformity and surface coverage of the monolayers formed on the silicon oxide surfaces. Clean silicon substrates with a native oxide film have WCA values of ~20°, which is attributed to the hydrophilic silanol groups on these surfaces. The WCA values for surfaces reacted with either compound 1 or 2 were 91° and 90°, respectively (Figure 4.2). These results indicated that the silicon oxide surfaces were rendered hydrophobic when reacted with compound 1 or 2. However, the WCA values for these modified surfaces were not as high as those reported in the literature for various types monolayers prepared from alkyl chains on oxide surfaces[2] or alkanethiols on gold surfaces,[48] with the reported WCA values ranging from 105° to 110°. Average water contact angles of 109° and 102° were achieved for the silicon oxide substrates following their microwave-assisted reaction with compound 3 or 4, respectively (Figure 4.2). These results indicated that hydrophobic surfaces were achieved using either compound 3 or 4. The results also suggest that surface coverage and uniformity of the monolayers derived from reactions with compound 3 were the best among the fluorinated compounds evaluated in this study. This outcome could be attributed to differences in the

degree of steric hindrance at the reaction site while the monolayers are being formed from compounds 1 to 3. Compounds 1 and 2 both have a methylene spacer between the hydroxyl head group and their fluorocarbon chain. The closer proximity of the bulkier fluorocarbon chain to the reacting silanol groups on the surfaces could compromise the reaction by steric hindrance. On the other hand, the ethylene linker in compound 3 could provide a higher degree of freedom of motion for the alcohol head group relative to the other two compounds. It was anticipated that compound 3 would also be better able to reorient itself when immobilized at the interface to minimize steric hindrance within the monolayers.

To further characterize the properties of surfaces modified with compounds 1 to 4, contact angle measurements were also performed using toluene and hexadecane. There was a clear difference in the oleophobicity of the substrates when reacted with fluorinated compounds (1 to 3) and a non-fluorinated compound (4) (Figure 4.2). The contact angles of toluene and hexadecane were 31° and 23°, respectively, for substrates reacted with compound 4. These results indicated that the modified surfaces were oleophilic. These values were lower than those obtained from monolayers of undecanethiol on gold surfaces, which yielded a contact angle value of ~50° with hexadecane.[120] The discrepancy between the results for the monolayers of alkanethiols and those reported herein could be attributed to limited van der Waals interactions within monolayers prepared from compound 4 due its shorter hydrocarbon chain length. The average contact angle values were 35°, 48°, and 78° for toluene, and 50°, 55°, and 78° for hexadecane, for substrates reacted with compound 1, 2, or 3, respectively. These results suggest an increase in the oleophobicity of those surfaces reacted with each of the fluorinated alcohols in comparison to those modified with compound 4. These values also indicate that the oleophobicity of these surfaces could vary depending on the molecular structure of the fluorinated alcohol. The substrates that exhibited the highest degree of oleophobicity were those that were reacted with compound 3. Furthermore, this wettability result agrees well with the properties observed for thiol-containing fluorocarbon analogues on gold surfaces reported in the literature, with reported contact angles for hexadecane plateauing at a slightly lower value than 80°.[120, 206] The substrates reacted with compound 2 yielded lower toluene and hexadecane contact angles than those reacted with compound 3. Discrepancies between the monolayers formed using either compound 2 or 3 could be

attributed to differences in their overall surface coverage. Hydrocarbon chains between the fluorocarbon and hydroxyl group could aid in packing of monolayers by adjusting the molecular tilt to maximize the intermolecular van der Waals interactions.[206] A short hydrocarbon chain spacer could compromise these intermolecular interactions and result in a lower surface coverage within the monolayers. Substrates reacted with compound 1 exhibited the lowest degree of oleophobicity. This result could be attributed, in part, to a decrease in the overall surface coverage of these monolayers. This surface coverage could be compromised by the molecular structure of compound 1, including its relatively short alkyl spacer between the alcohol head group and the fluorocarbon chain. These results are consistent with reports indicating the formation of disordered monolayers for thiol analogues to compound 1 on gold surfaces.[189, 204] In addition, the partially fluorinated character or hydrogen content of the terminal carbon (CHF_2) for compound 1 could also alter the overall oleophobicity of the resulting monolayers.[203] Further analyses were required to verify the chemical composition of each of the monolayers when coated onto the silicon oxide surfaces.

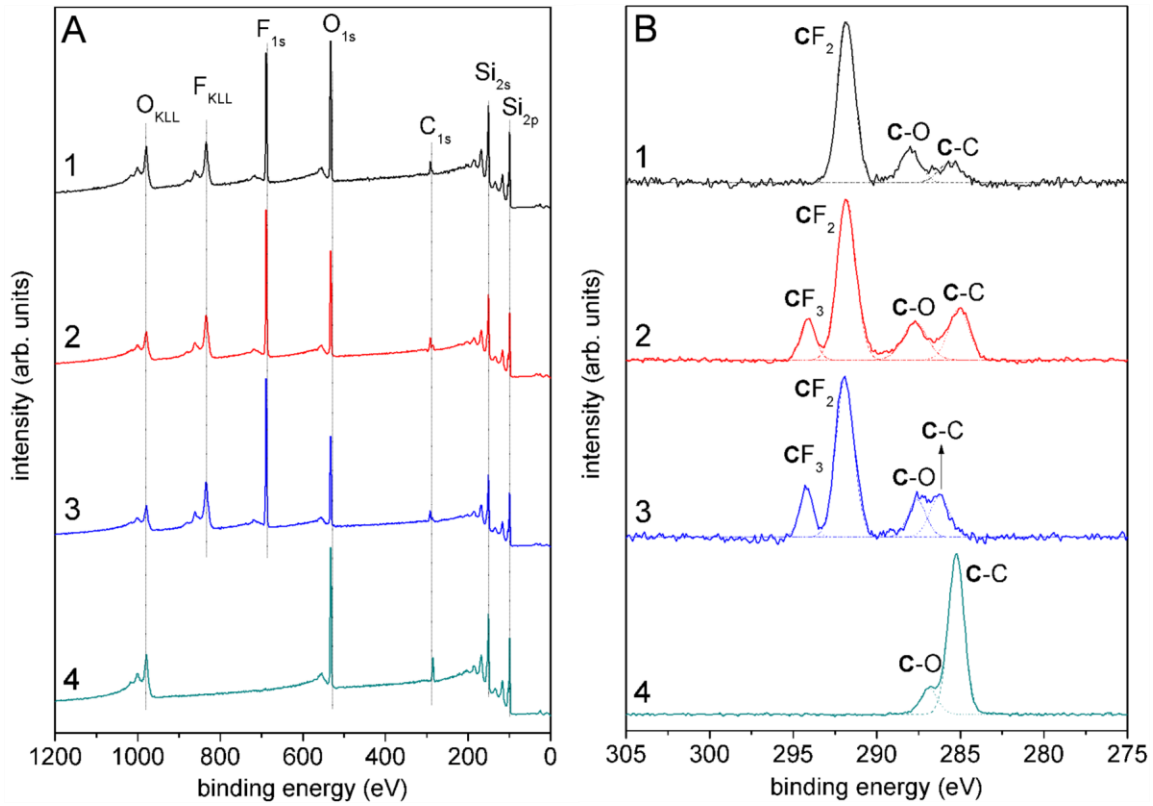

Figure 4.3. X-ray photoelectron spectroscopy (XPS) of silicon substrates after a microwave-assisted reaction with compound 1, 2, 3, or 4. Data for each reaction include (A) survey scans and (B) high-resolution C1s scans. Reprinted with permission from Ref. [227] ©2016 American Chemical Society.

Composition of the modified silicon oxide surfaces was analyzed by XPS. All surfaces exhibited a strong fluorine signal (F_{1s}), with the exception of compound 4, due to the high number of fluorine atoms in the fluorocarbon chains of compounds 1 to 3 (Figure 4.3A). These results further confirmed that the surfaces were modified with the fluorocarbon-containing reactants. Analysis of the high-resolution C_{1s} spectra for substrates modified by each compound provided further confirmation of the molecular structure within the resulting monolayers. For instance, surfaces reacted with compound 1 exhibited a single fluorocarbon peak (**C**F_2) and two additional peaks associated with **C**–O and **C**–C. Substrates modified with compound 2 or 3 exhibited two fluorocarbon peaks (**C**F_2 and **C**F_3), the **C**–O peak, and the **C**–C peak. The lack of the trifluorocarbon (**C**F_3) peak for the substrates reacted with compound 1 confirmed the molecular structure of compound 1 within the resulting monolayers, which did not possess a terminal CF_3. The

CF_3 to **C**F_2 peak ratio was slightly higher for the substrates reacted with compound 3 because compound 2 contained a chain of seven difluorocarbons (**C**F_2) and a terminal **C**F_3, while compound 3 had a chain of only six CF_2 and one CF_3 per molecule.

An interesting observation is made in the shift in the relative positions of the hydrocarbon peaks in association with the fluorinated alcohols as observed by XPS relative to the peak position for compound 4. Monolayers formed with compound 4 (aliphatic alcohol) exhibited peak positions for **C**–C at 285.2 eV. The **C**–C peak position reported herein is shifted slightly in comparison to literature reported values.[203, 207] This shift in peak position is attributed to discrepancies in the ability to distribute surface charges for the monolayers on thin silicon oxides in comparison to monolayers on gold films.[209-210] The **C**–C peak position for monolayers prepared from compound 3 was 286.2 eV, indicating a higher relative binding energy for the **C**–C bond. Contributions from differences in chain lengths between each of the fluorocarbon and hydrocarbon chains should be minimal because all four compounds have a similar molecular length, and furthermore, attenuation lengths of photoelectrons in the fluorocarbon films have been reported to be similar to those in hydrocarbon films.[127] This argument is further supported by the observation that the **C**F_2 peak position remained centered at 291.8 eV for substrates coated with compounds 1 to 3. The shift in binding energy of the **C**–C peak for compound 3 could be attributed to contributions from the terminal fluorocarbon chain that possess stronger electronegativity in comparison to the hydrocarbon spacer. The **C**–C peaks observed for monolayers formed with compound 1 or 2 showed minimal shift as these peaks are attributed to miscellaneous contamination present on their surfaces. These monolayers, however, displayed a shift in the peaks attributed to the **C**–O peaks. The **C**–O peak positions for monolayers formed with compound 1, 2, 3 or 4 were 288.0, 287.8, 287.6, and 286.9 eV, respectively. This shift in **C**-O peak position is attributed to the stronger electronegativity of the fluorocarbon chain in comparison to the hydrocarbon chain. The magnitude of the shift observed for the **C**-O peak position of monolayers prepared from compound 3 is less significant than that observed for the substrates reacted with compound 1 or 2. This difference in the observed shift in binding energy of the **C**–O species is attributed to the location in the fluorocarbon chain in compound 3 being further away from the **C**–O bond within the head group of the monolayers.

Table 4.1. Quantitative Analysis of the XPS Survey Scans Obtained from Substrates Reacted with Compound 1, 2, or 3. Reprinted with permission from Ref. [227] ©2016 American Chemical Society.

samples	F_{1s} XPS area	Si_{2p} XPS area	peak area ratio	no. of F atoms	Peak area ratio / no. of F	% Relative packing density
compound **1**	397315	230208	1.73	12	0.144	67
compound **2**	902928	427618	2.11	15	0.141	66
compound **3**	597861	215782	2.77	13	0.213	100

Quantitative XPS analysis was performed to evaluate the relative packing density of the monolayers formed using the fluorinated alcohols. In particular, peak area ratios of the F_{1s} signal relative to the Si_{2p} signal were analyzed for each of the monolayers prepared from the respective fluorinated alcohols (Table 4.1). A comparison was sought to provide insight into the relative surface composition of each of these monolayers.[204] Relative packing densities were estimated by comparing these XPS peak area ratios to the predicted fluorine content for each of these monolayers using the stoichiometric ratio of fluorine atoms within the respective compounds. The highest relative packing density was obtained for substrates coated with compound 3. The relative packing density of compounds 1 and 2, normalized to the density achieved with compound 3, was 67% and 66%, respectively. These results suggest that the overall packing density of monolayers formed with compounds 1 and 2 were lower than those formed using compound 3. Furthermore, the results between the XPS analyses and those of the wettability studies indicated that the degree of hydrophobicity and oleophobicity of monolayers is correlated with their packing density on the silicon oxide films. Similar correlations have been drawn between wetting properties and the packing densities of monolayers on gold surfaces prepared from thiols with fluorocarbon or hydrocarbon backbones as evaluated by XPS.[205, 211] In summary, quantitative XPS analyses suggests that the monolayers formed using compound 3 have a substantially higher relative packing density than those prepared with compound 1 or 2.

Overall, the contact angle and XPS analyses matched well to the anticipated properties and compositions of monolayers prepared from compounds 1 to 4 on silicon

oxide surfaces. Among the three fluorinated alcohol compounds, monolayers formed with compound 3 exhibited the best ability to create surfaces that were both hydrophobic and oleophobic. Compound 3 was chosen to perform a detailed investigation into monolayers on silicon oxide surfaces containing a mixture of fluorocarbon and hydrocarbon chains to maintain a hydrophobic state while also being able to control and tune their oleophobicity.

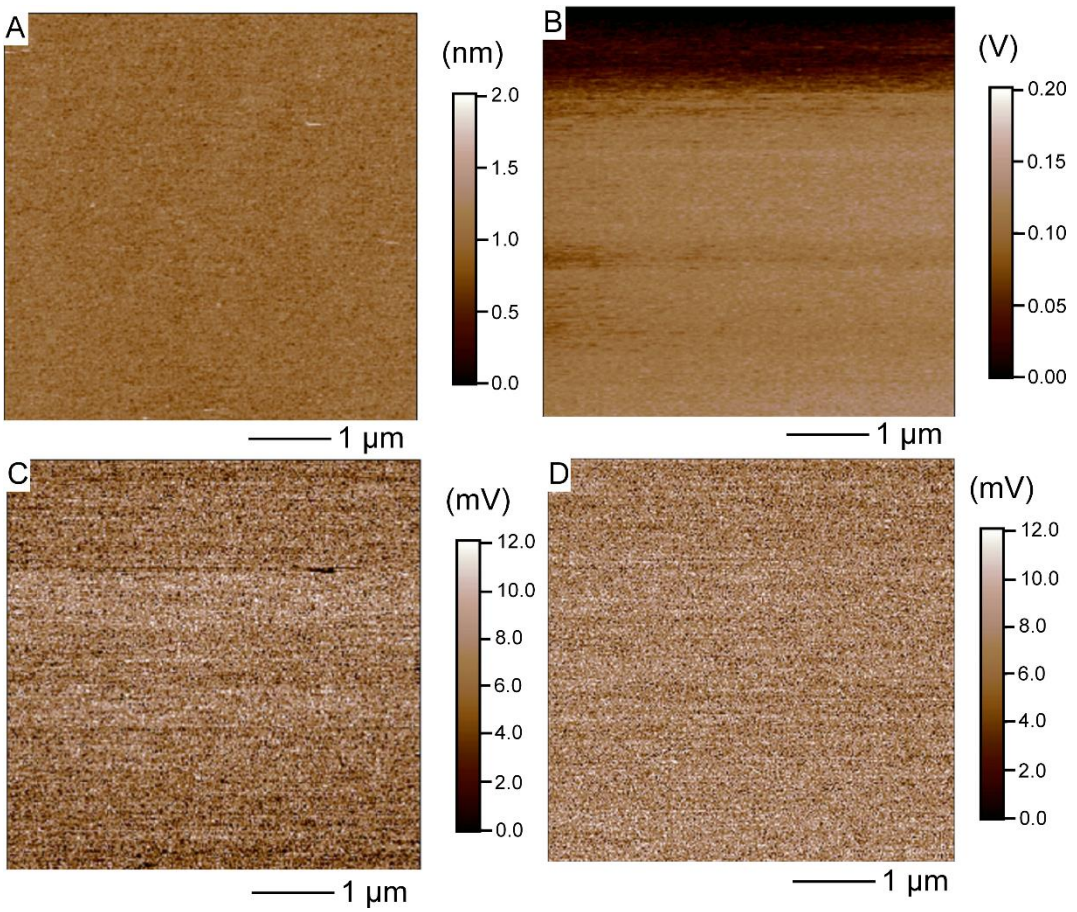

Figure 4.4. (A) Contact mode atomic force microscopy (AFM), (B) Kelvin probe force microscopy (KPFM), (C) lateral force microscopy (LFM) with a Si_3N_4 tip, and (D) LFM with an octyldimethylchlorosilane modified Si_3N_4 tip for a silicon substrate coated with mixed monolayers of compound 3 and compound 4 prepared from a 1:1 molar ratio of these reactants. Reprinted with permission from Ref. [227] ©2016 American Chemical Society.

Tuning Oleophobicity through Formation of Mixed Monolayers Prepared from Alcohol-Based Reagents. We have successfully prepared a series of silicon oxide surfaces modified with either fluorinated or hydrocarbon based alcohols to alter the properties of these surfaces. Compound 3 was identified as an effective reactant to form

uniform, fluorinated monolayers on silicon oxide surfaces. We sought to further tune the properties of these monolayers by controlling the molar ratio of compounds 3 and 4 within the reaction mixture. The oleophobicity of the resulting surfaces were evaluated after reacting with mixtures of compounds 3 and 4. These reaction mixtures were prepared as a molar ratio of compound 3 to compound 4 with specific ratios of 4:1, 3:1, 2:1, 1:1, and 1:2. Previous studies have demonstrated that phase separation can be observed in mixed monolayers prepared from different chemical constituents.[212-217] It was necessary to determine whether this phenomenon was also observed in the monolayers prepared from a mixture of compounds 3 and 4. Atomic force microscopy (AFM), lateral force microscopy (LFM), and Kelvin probe force microscopy (KPFM) measurements were obtained from substrates coated with the mixed monolayers, but no distinct phase separation was observed from these measurements (Figure 4.4). Phase separation observed in previous reports for mixed monolayers was driven by the intermolecular interactions between the adsorbed molecular species. The degree of intermolecular interaction and phase separation observed for monolayers prepared from mixtures of distinct chemical species can be influenced by a number of factors, which include the processing techniques, polarity of solvent(s), reaction mechanism, degrees of freedom (e.g., tilt) of the molecular species within the monolayers, concentrations of each reagent, and temperature of the system.[212, 216-218] The absence of phase separation observed in our system of study was attributed to relatively high processing temperatures, the degrees of freedom of the molecular species within the monolayers, and the polarity of solutions used to prepare the monolayers. High temperatures can disrupt molecular structures formed as the result of the separation of distinct chemical species, such as micelles or emulsions formed as a suspension, that are otherwise held together by relatively weak intermolecular interactions. In addition, the alcohol-based reagents become immobilized on the surfaces through the formation of covalent bonds, which hinders their rearrangement on these surfaces. In contrast, thiol analogues on gold form semi-covalent bonds and can exhibit desorption and lateral migration of species within the monolayers at elevated temperatures.[218-219] The solvents used in the preparation of monolayers from alcohol-based reagents were the reagents themselves. This approach is distinct from the methods commonly used to prepare monolayers from thiol-based species on gold surfaces, which are typically performed using polar solvents such as ethanol. These factors could play a role in the adsorption kinetics during the formation of monolayers. No phase separation

was observed within the monolayers prepared from the mixtures of alcohol-based reagents, indicating that the fluorocarbon and hydrocarbon species (compounds 3 and 4, respectively) formed intermixed coatings over the surfaces of the substrates.

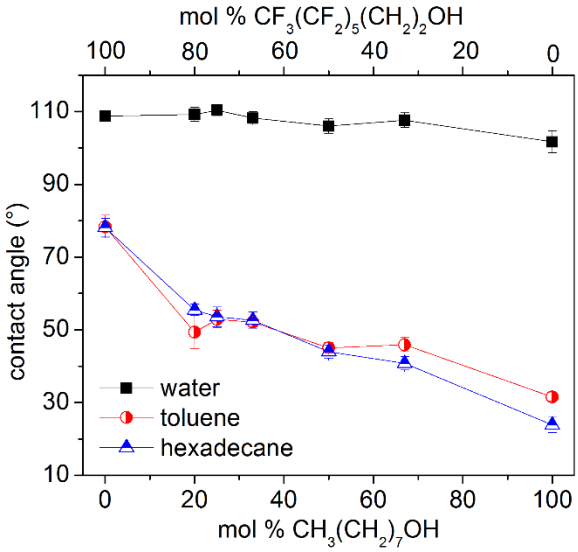

Figure 4.5. Contact angle measurements (water, toluene, and hexadecane) for silicon substrates after microwave-assisted reactions in the presence of mixtures of reactants 3 [$CF_3(CF_2)_5(CH_2)_2OH$] and 4 [$CH_3(CH_2)_7OH$] at the specified molar ratios. Reprinted with permission from Ref. [227] ©2016 American Chemical Society.

Silicon oxide surfaces coated with a series of distinct mixtures of compounds 3 and 4 were evaluated by contact angle measurements. Hydrophobicity of these surfaces was evaluated through WCA measurements (Figure 4.5). Their hydrophobicity remained consistent across the series of samples with a WCA of ~110° regardless of the composition of the reaction mixture. This observation suggests that the uniformity of each of these monolayers was relatively consistent regardless of the molar ratio of the fluorinated and hydrocarbon-based alcohols in solution. Contact angle measurements were also performed using toluene and hexadecane to assess the oleophobicity of these surfaces (Figure 4.5). Their oleophobicity progressively decreased as the molar ratio of fluorinated alcohols within the reaction mixture decreased. The relatively small hysteresis values from each of these contact angle measurements (see Supporting Information) further demonstrated the uniform composition of these monolayers prepared from a mixture of fluorocarbon and hydrocarbon reagents. The smaller quantity of fluorinated alcohols within the reaction mixture would, ideally, correspond to the formation of

monolayers containing less fluorocarbons and more hydrocarbons. As the proportion of hydrocarbon based alcohols within the mixed monolayers increases, the surfaces should become increasingly oleophilic. The oleophobicity of silicon oxide surfaces was tuned by controlling the molar ratio of fluorinated and hydrocarbon based alcohols in the reaction mixture, suggesting that the composition within the monolayers closely followed the composition of the mixture in solution. Further studies were, however, required to assess the surface properties and composition of the modified substrates.

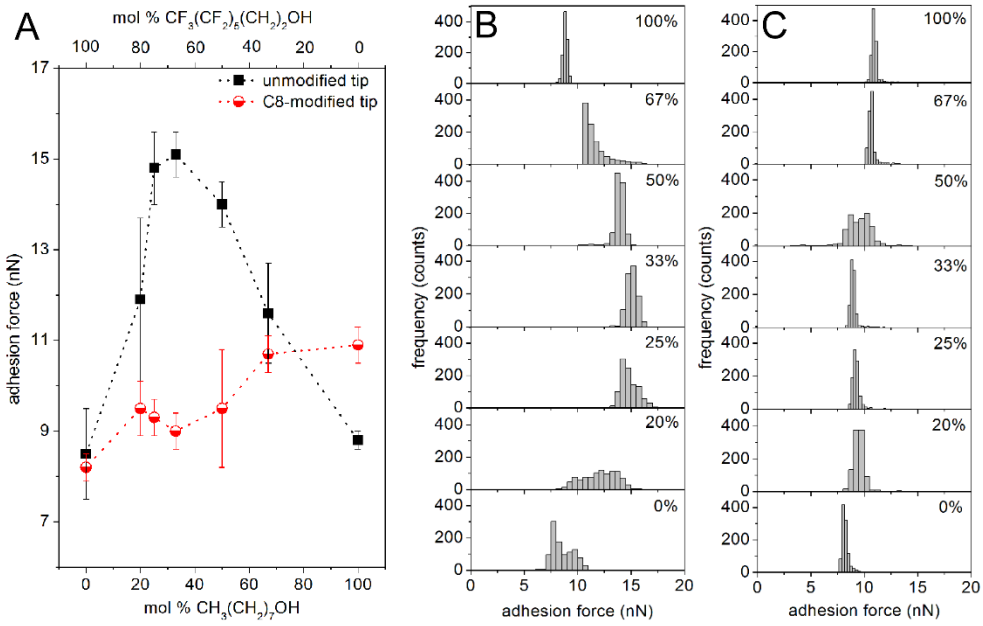

Figure 4.6. **(A) Average adhesion force measurements for substrates coated with different molar ratios of 1*H*,1*H*,2*H*,2*H*-perfluoro-1-octanol and 1-octanol. Histograms depict the results of the force spectroscopy measurements performed using either (B) an unmodified silicon nitride (Si_3N_4) tip or (C) a Si_3N_4 tip modified with octyldimethylchlorosilane (C8-silane). The corresponding mole fraction of 1-octanol in the reaction mixture is displayed in the upper right corner of each histogram. Reprinted with permission from Ref. [227] ©2016 American Chemical Society.**

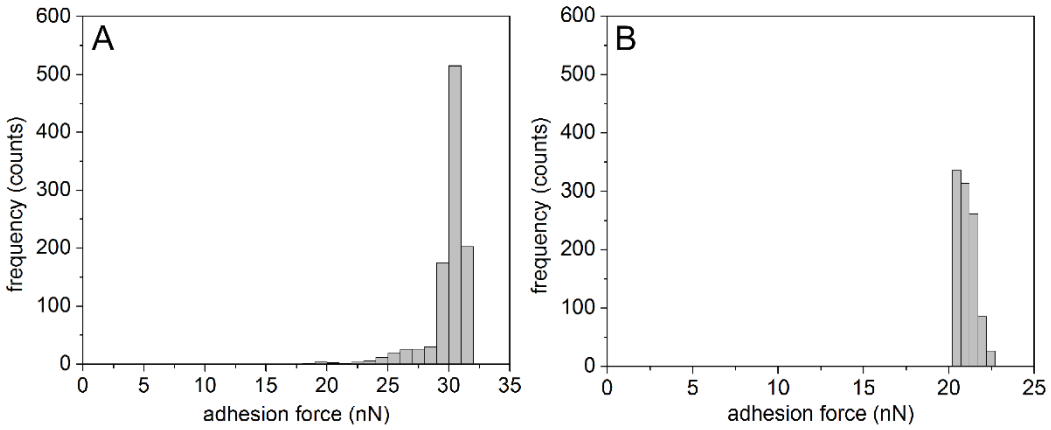

Figure 4.7. Histograms of adhesion force measurements on a piranha cleaned silicon substrate with (A) a Si_3N_4 tip or (B) a C8-silane modified Si_3N_4 tip. Reprinted with permission from Ref. [227] ©2016 American Chemical Society.

Adhesion properties for substrates covered with these mixed monolayers were assessed by AFM (Figure 4.6). Two types of AFM tips were used in this study, which were silicon nitride (Si_3N_4) tips either with or without a coating of octyldimethylchlorosilane (C8-silane). The interactions between the monolayers on the silicon oxide surfaces and the native Si_3N_4 tips exhibited an interesting correlation between the magnitude of the measured adhesion forces and the composition of the monolayers. Monolayers of either 1-octanol or 1*H*,1*H*,2*H*,2*H*-perfluoro-1-octanol exhibited relatively low adhesion forces with average values of 8.5 and 8.8 nN, respectively, in comparison to the monolayers prepared from both components. The substrates with mixed monolayers exhibited adhesion forces up to 15.1 nN. The trends observed in this study suggest that a change in the composition of the monolayers is closely associated with changes to the molecular-scale interactions between the contacting surfaces. This result suggests that the diverse contributions to adhesion are benefiting from the molecular-scale changes in steric strain and nearest-neighbor interactions within the mixed monolayers, which is in agreement with previous studies on mixed monolayers prepared from thiols on gold.[204-205] The adhesion forces measured with the C8-silane coated tips, however, progressively increased with an increasing content of 1-octanol in the monolayers. This interaction is likely dominated by the stronger van der Waals interactions between the hydrocarbon chains on the tip and those within the monolayers on the silicon oxide, which is in contrast to the weaker interactions between the fluorocarbons and hydrocarbons. This observed

trend corresponds with observations from the studies on the wetting properties of the mixed monolayers; contact angles for the nonpolar solvents increased as the fluorocarbon content increased within the mixed monolayers. In conclusion, the adhesion forces between a Si_3N_4 tip and the single-component monolayers were lower than those observed for the mixed monolayers. Furthermore, the adhesion forces between the mixed monolayers and an alkylsilane-modified AFM tip progressively decreased with an increase in the fluorocarbon content of the monolayers. Quantitative spectroscopic information on these mixed monolayers was necessary to gain further insights into how the observed properties correlated with specific changes in the surface composition.

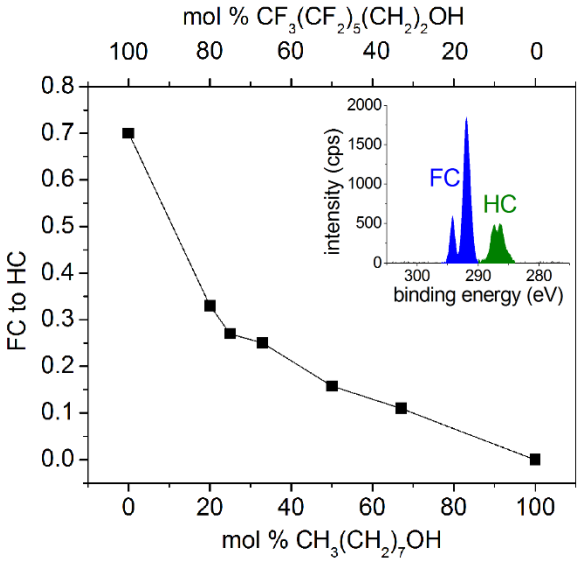

Figure 4.8. X-ray photoelectron spectroscopy (XPS) analyses of peak area ratios of fluorocarbon (FC) to hydrocarbon (HC) content for silicon substrates after a series of microwave-assisted reactions with mixtures of compounds 3 [$CF_3(CF_2)_5(CH_2)_2OH$] and 4 [$CH_3(CH_2)_7OH$] at the specified molar ratios. Inset plots indicate the peaks analyzed in each of these studies. Reprinted with permission from Ref. [227] ©2016 American Chemical Society.

The compositions of surfaces capped with mixed monolayers were analyzed by XPS. In particular, high-resolution C_{1s} scans were quantitatively analyzed by comparing the peak areas associated with the hydrocarbon and fluorocarbon content of the modified surfaces. These peaks were well separated in the high-resolution C_{1s} spectra. Relative hydrocarbon and fluorocarbon contents of the mixed monolayers were estimated by analyzing the ratio of the respective XPS peak areas. Composition observed for these

monolayers on silicon oxide surfaces deviated from the linear changes in molecular composition of the reaction mixtures (Figure 4.8). There are two distinct trends observed in the composition of the mixed monolayers. Both trends are approximately linear, but with a distinct change in slope or a rate of change in composition between the two regions. The first region corresponds to reaction mixtures containing 0–25 mol % of 1-octanol-containing reaction mixture, and the second region is for reaction mixtures containing 33–60 mol % of 1-octanol. Similar trends were observed in the adhesion force measurements, where the average adhesion forces reached a maximum value for monolayers prepared from a reaction mixture containing either 25 or 33 mol % of 1-octanol (Figures 4.7A and B). Deviation between the composition within a solution and that within the resulting monolayers has been reported for mixtures of fluorinated and aliphatic thiol-based monolayers on gold surfaces.[129, 189, 220] Additional literature previously reported that the composition of mixed monolayers prepared from fluorocarbon and hydrocarbon based thiols exhibited a linear correlation to the composition of the solution. These studies include mixtures of linear chain, monoreactive species, such as n-decanethiol and 10-heptadecafluoro-1-decanethiol used to prepare monolayers on silver,[221] and mixtures of bidentate adsorbates, such as (5-(9,9,10,10,11,11,12,12,13,13,14,14,15,15,16,16,16-heptadecafluorohexadecyloxy)-1,3-phenylene)dimethanethiol (PFPDT) and (5-(hexadecyloxy)-1,3-phenylene)-dimethanethiol (HDPDT) used to prepare monolayers on gold surfaces.[129] The deviation observed in the surface composition of the mixed fluorocarbon and hydrocarbon monolayers derived from alcohol compounds can be attributed to distinct differences between these reagents. One aspect is the discrepancy in the van der Waals diameter of the fluorocarbons and hydrocarbons in the monolayers. The molecular volume of fluorinated species is larger than that of the corresponding hydrocarbon species.[49, 220, 222-223] This difference in molecular volume can decrease the overall packing density of fluorinated species in monolayers, in contrast to hydrocarbon species. The result is a lower fluorocarbon content than anticipated in the resulting mixed monolayers assuming a relative surface area for each species that is proportional to their molar ratio in the reaction mixture. Experimental studies have shown that although such differences in molecular volume should drive a preferential increase in hydrocarbon content over that of fluorocarbons in monolayers, the surface composition of fluorocarbon species is often higher than theoretically predicted.[220-221] The lower fluorocarbon content could also be attributed to another important factor, which is the increase in polarity of

solvents used to prepare many monolayers and their influence on the entropy of mixing.[47] Surface composition of mixed monolayers can deviate from the solution composition due to interactions of the reactants with the polar solvents.[47, 214] In contrast, our mixed monolayers utilized solutions prepared from mixtures of relatively nonpolar alcohol-based reactants. The interactions of these reactants with a polar solvent were minimized in our studies by using mixtures of two nonpolar alcohols with similar chain lengths. The preferential adsorption of hydrocarbon based alcohols in contrast to the fluorinated alcohols could be attributed to stronger intermolecular interactions (e.g., van der Waals) between the aliphatic alcohols than between the fluorinated alcohols.[189] These stronger intermolecular interactions between the aliphatic alcohols could accelerate their transport to and therefore reaction with the surfaces. Steric hindrance arising from differences in the molecular tilt angle between the fluorocarbon and hydrocarbon species could, in contrast, suppress the reaction between the fluorinated alcohols and the silicon oxide surfaces. The condensation of the alcohol-based reagents with the silanol groups on the oxide surfaces results in the immobilization of these reagents. The preferential immobilization of aliphatic alcohols could lead to a further deviation of the surface composition from that in solution as a result of the intermolecular interactions between the species in solution and that bound to the silicon oxide surfaces. To summarize, the oleophobicity of the silicon oxide surfaces progressively decreased with a decrease in the molar ratio of fluorinated alcohol in the reaction mixture, but the fluorocarbon content of the resulting mixed monolayers deviated from the molar ratio of reagents in solution. Monolayers on silicon oxides containing a mixture of fluorocarbon- and hydrocarbon-based alcohols were derived from a one-pot microwave-assisted reaction, which demonstrates the utility of this process to prepare monolayers with a customized composition.

4.5. Conclusions

In summary, we systematically investigated the microwave reaction of fluorinated alcohols with silicon oxide surfaces to control surface hydrophobicity and oleophobicity. These modifications were accomplished under ambient laboratory conditions (e.g., without the need of a drybox or vacuum conditions). These processes utilized microwave-assisted reactions of neat solutions of fluorinated or aliphatic alcohols as well as mixtures

of these reagents. Monolayers were initially prepared from a series of different fluorinated alcohols, which were evaluated by contact angle measurements. It was determined that the highest quality monolayers of the fluorinated alcohols were those prepared using compound 3 (1*H*,1*H*,2*H*,2*H*-perfluoro-1-octanol). The contact angle values for monolayers prepared from compound 3 were 109°, 78°, and 78° with hysteresis values of 1° or less for water, toluene, and hexadecane, respectively. X-ray photoelectron spectroscopy (XPS) results confirmed the presence of fluorinated species within these monolayers as evidenced by the strong F_{1s} signal and the fluorocarbon content observed in the high-resolution C_{1s} scans. These results demonstrated that a microwave-assisted condensation reaction with a neat solution of fluorinated alcohols could yield fluorinated monolayers on silicon oxide surfaces. The process demonstrated in this chapter is a simple method to form monolayers of a fluorinated species but can also be extended to preparing mixed monolayers. The compositions of mixed monolayers can be controlled by altering the molar ratio of fluorocarbon- and hydrocarbon-based alcohols in the reaction mixture to tune the fluorocarbon content of these surface modifications. The oleophobicity of the surfaces progressively decreased as the molar ratio of fluorinated alcohols in the reaction mixture also decreased, while the monolayers maintained their hydrophobic properties, as demonstrated by contact angle measurements. Adhesion force measurements of this series of mixed monolayers were assessed using either native Si_3N_4 AFM tips or the same tips after modification with octyldimethylchlorosilane. The observed trends in the adhesion forces correlated with the wetting properties of the mixed monolayers. The fluorinated composition of these mixed monolayers was analyzed by high-resolution XPS C_{1s} scans. These results indicate a distinct difference from mixed monolayers prepared in a relatively polar solvent. Overall, the results of these studies indicate that the ratio of fluorocarbon- and hydrocarbon-based alcohols within mixed monolayers on silicon oxide surfaces can be tuned using a one-pot reaction.

Chapter 5.

Determination of Film Thickness of Alcohol Based Monolayers

5.1. Notice of Permissions

A manuscript based on the work presented in this chapter is currently in preparation. The work presented in this paper, including experiments, data acquisition, interpretation and writing has been performed by myself under the guidance of Dr. Byron Gates. Mr. Dongho Kim assisted in data interpretation with literature values for the film thickness and tilt angle of the alcohol based monolayers measured from angle-resolved XPS.

5.2. Introduction

In this chapter, the thickness of monolayers derived from a microwave-assisted reaction of aliphatic alcohols with silicon oxide surfaces were determined using angle-resolved X-ray photoelectron spectroscopy (ARXPS). The covalent modification of surfaces through the formation of monolayers is being widely pursued for applications that include molecular electronics,[5, 143, 164, 224-225] microelectromechanical systems (MEMS),[6, 152, 226] and microfluidics.[1, 11, 13, 15, 165] The modification of silicon oxide surfaces specifically has been achieved with molecules containing reactive groups, such as silanes[3, 37, 60] and phosphonic acids.[52, 57-58, 78] One of the major challenges in forming these monolayers is the potential to achieve multilayer films, intermolecular polymers, and other undesirable side reactions.[57, 60, 145, 172-173] These challenges can result in unpredictable electronic characteristics of the monolayers, as well as non-uniform chemical or physical surface properties. Ultimately, these defects can lead to a detrimental failure of miniaturized devices. Other limitations of using silanes and phosphonic acids as molecular coatings include their limited accessibility, and the relatively high cost to prepare these reagents at the required purity.[2]

Alcohol containing compounds have been proposed as an alternative reagent to modify silicon oxide surfaces via the formation of silyl ether (Si–O–C) bonds. The alcohol molecules can form silyl ether bonds with either hydrogen terminated silicon[63-64, 81, 174-176] or silicon oxides (i.e. silanol terminated surfaces).[65, 177, 208, 227] Minimal side reactions for these processes enable a convenient approach to prepare uniform monolayers, which includes the use of ambient environmental conditions. Our recent work demonstrated the formation of uniform monolayers derived from 1-octanol on various silicon oxide surfaces.[208] This technique is utilized here to form uniform monolayers of a well-defined and tunable thickness as these films can be derived from a series of aliphatic alcohols of different alkyl chain lengths. Detailed analyses for a series of monolayers formed using aliphatic alcohols of different alkyl chain length were performed by ARXPS.[131, 133, 228] The results of these analyses were used to determine the overall thickness of each of the monolayers derived from distinct aliphatic alcohol species. The results obtained from these analyses provide insight into the uniformity of the monolayers derived from aliphatic alcohols, and demonstrate a precise control over the thickness of these monolayers on silicon oxide surfaces.

5.3. Experimental

Reagents and Materials. Reagents were used as received, which included 30% (v/v) hydrogen peroxide (Fisher Scientific, CAS no. 7722-84-1), sulfuric acid (Anachemia Canada, Inc. ACS reagent grade, CAS no. 7664-93-9), 1-butanol (Caldedon, reagent grade, CAS no. 71-36-3), 1-hexanol (Sigma Aldrich, reagent grade, CAS no. 111-27-3),1-octanol (Sigma Aldrich, ACS reagent, CAS no. 111-87-5), 1-decanol (Sigma Aldrich, 99%, CAS no. 112-30-1), and 1-dodecanol (Sigma Aldrich, reagent grade 98%, CAS no. 112-53-8). Test grade, four inch, <100>, p-type silicon wafers with a resistivity between 1 to 10 Ohms·cm with and without a 100-nm thick thermally grown silicon oxide film were purchased from the Nanofabrication Facility in 4D LABS at Simon Fraser University. The wafers were diced into 1 cm by 1 cm square pieces that served as the substrates for the following experiments.

Preparation of Silicon Oxide Surfaces. Piranha cleaning of the diced substrates was performed to remove surface contamination as described previously.[33] *CAUTION:*

Piranha solution is a strong oxidizing agent and reacts violently with organic compounds. This solution should be handled with extreme care. Briefly, the piranha solution was freshly prepared, in which the silicon substrates were immersed for ~1 h. Then, the substrates were washed in 18 MΩ·cm deionized water (Barnstead Nanopure DIamond water filtration system). A stream of nitrogen (N_2) gas filtered with a PTFE membrane containing <200 nm pores was used for drying the substrates.

Procedure for the Formation of Monolayers with Aliphatic Alcohols. A cleaned silicon substrate was placed into a separate quartz tube (Part no. 34042, ATS Scientific Inc.) containing an ~10 mL solution of alcohol (i.e. 1-butanol, 1-hexanol, 1-octanol, 1-decanol, or 1-dodecanol), and placed into a microwave vessel (Part no. 33806, ATS Scientific Inc.). The vessels were radiated with microwave using a microwave reactor (Ethos Plus Microwave Labstation) for the desired time in a closed vessel at a set temperature of 150 °C for 2 h with a ramp time of 5 min. The test tubes were subsequently cooled to room temperature over at least 20 min. The substrates were removed from the test tubes, washed sequentially under a stream of acetone and isopropanol, and dried under a stream of filtered N_2 gas.

Angle Resolved X-ray Photoelectron Spectroscopy (ARXPS) measurements were conducted using a Kratos Analytical Axis ULTRA DLD system with a monochromatic aluminum source (Al Kα of 1486.7 eV) operating at 150 W. Survey scans were acquired using a pass energy of 160 eV, a dwell time of 100 ms, and 1 sweep. High resolution scans were obtained using a pass energy of 20 eV, a dwell time of 500 ms, and averaging of 5 scans. An area of 700 µm by 300 µm was analyzed for each sample.

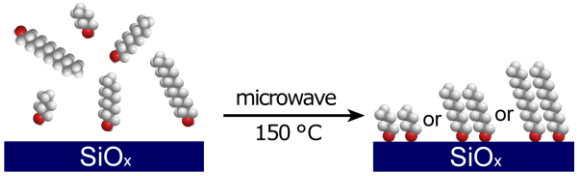

Figure 5.1. Schematic depiction of the formation of self-assembled monolayers (SAMs) from the microwave assisted reaction of aliphatic alcohols with silicon oxide surfaces.

5.4. Results and Discussion

The primary goal of this study was to utilize ARXPS for assessing the thickness of monolayers on silicon oxides derived from aliphatic alcohols. Monolayers were prepared from a series of aliphatic alcohols of increasing chain length (Scheme 1). Specifically, we formed monolayers on silicon oxide surfaces from 1-butanol, 1-hexanol, 1-octanol, 1-decanol, and 1-dodecanol. These alcohols were used neat during microwave assisted reactions held at a temperature of 150 °C. After these reactions, the substrates were rinsed and sonicated in ethanol to ensure minimal physical adsorption of unreacted aliphatic alcohols or other contaminants. Angle-resolved XPS was utilized to assess the continuity and thickness of the monolayers for its ability to analyze the properties of films that have a thickness less than 10 nm.[131, 133, 229] The thickness of the monolayers can be determined from a series of ARXPS measurements. The relative XPS intensity of the carbon in the aliphatic alcohols derived monolayers to the silicon in the silicon oxide surfaces are correlated to the angle of these measurements and thickness of the monolayers through the following equation:[132-133, 229]

$$\ln\left(\frac{I_{C1s}}{I_{Si2p}}\frac{S_{Si}}{S_C}+1\right)=\frac{d}{\lambda}\frac{1}{\cos\theta} \tag{5.1}$$

where λ is the escape depth of the emitted photoelectrons, and I_{C1s} and I_{Si2p} are the intensities of the C_{1s} and Si_{2p} XPS signals, respectively. The value of λ can be obtained either experimentally, with a value of 25 Å for carbon based thin films.[132] The values S_{Si} and S_C are the relative sensitivity factors for silicon and carbon, respectively. The term θ is the takeoff angle, and d is the thickness of the monolayers (Figure 5.2A). This calculation assumes that the underlying substrate has a homogeneous chemical composition (i.e. no chemical variation or contamination throughout the substrate). To assess if a homogeneous chemical composition would be measured for the underlying material, ARXPS studies were performed on silicon substrates without monolayers. A 100-nm thick thermally grown silicon oxide film was anticipated to be a suitable material for the substrates in these ARXPS experiments because its chemical composition (i.e. SiO_2) would be homogenous throughout the anticipated penetration depth (typically less than 10 nm) of the photoelectrons obtained during the XPS measurements.[131] A piranha cleaned silicon substrate, on the other hand, would not be a suitable substrate as the

thickness of its native oxide layer would be ~2 nm,[153] which is less than the penetration depth of photoelectrons. The composition of this thinner silicon oxide substrate would, therefore, change significantly over a series of XPS measurements collected at various takeoff angles. To demonstrate this variability, a series of ARXPS measurements was collected for piranha cleaned silicon substrates either with or without the 100-nm thermally grown silicon oxide. The peak intensities for the Si_{2p} and O_{1s} species were compared to assess the changes in chemical composition observed over θ values from 0° to 80°. Each of these datasets were collected by varying the angle θ in increments of 10° (Appendix D). The ARXPS measurements for the 100-nm thick thermally grown silicon oxide film exhibited a homogenous composition of the Si_{2p} and O_{1s} species over tilt angles from 0 to 60°. In contrast, the piranha cleaned silicon substrate exhibited a varying relative composition of the Si_{2p} and O_{1s} species over the same tilt angles. The silicon substrates with the 100-nm thermally grown silicon oxide film were utilized to prepare the series of monolayers for the subsequent ARXPS studies, and the determination of the thickness of each of these monolayers.

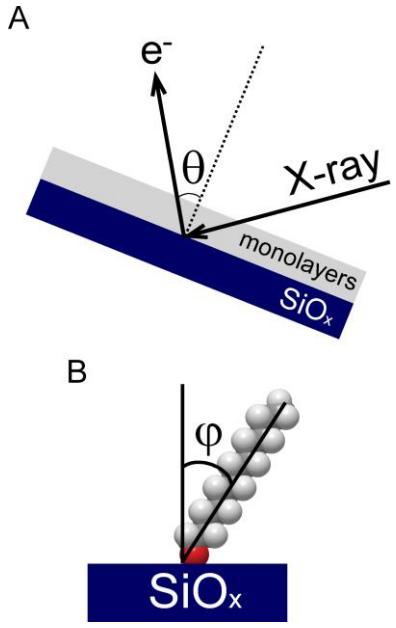

Figure 5.2. **(A) A schematic of the setup for the angle-resolved X-ray photoelectron spectroscopy (ARXPS) measurements and (B) a schematic of typical aliphatic alcohol depicting its configuration for covalent attachment to the silicon oxide surfaces. The θ value is the takeoff angle between photoelectron ejected at the surface and the surface normal. The φ value is the tilt angle of the molecules within the monolayers away from the surface normal.**

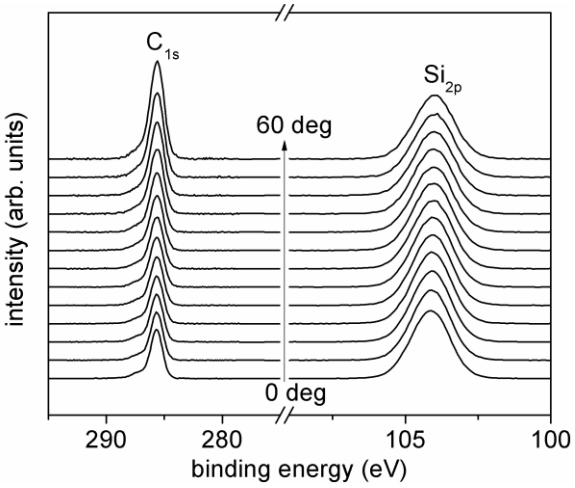

Figure 5.3. Angle-resolved X-ray photoelectron spectroscopy measurements of 1-dodecanol obtained from θ values of 0 to 60°.

An extensive set of ARXPS measurements were obtained for each of the substrates modified with the monolayers derived from the aliphatic alcohols. These experiments were used to determine the thickness d, and the average tilt angle, φ, of the bound molecules within the monolayers (Figure 5.2B). The high resolution XPS peaks of carbon (C_{1s}) and silicon (Si_{2p}) were acquired for θ values between 0 and 60° at increments of 5°. The θ values beyond 60° were not considered for this analysis because these datasets could yield inaccurate results due to contributions from elastic scattering and surface roughness.[133] A series of XPS measurements were obtained for each of the substrates, such as the spectra plotted in Figure 5.3 for a substrate coated with 1-dodecanol. The C_{1s} and Si_{2p} peaks were normalized against the high resolution oxygen (O_{1s}) peaks obtained under the same conditions to enable a direct comparison between each spectrum. While the silicon peak intensities maintained a consistent intensity over the series of θ values, carbon peak intensities gradually increased with an increase in θ. This result was expected as the relative elemental composition of the substrate (i.e. the ratio of silicon to oxygen) should be similar regardless of θ. On the other hand, the relative increase in the carbon peak intensity with increasing values for θ is attributed to the more significant contributions from the organic monolayers in comparison to that of the bulk material (i.e. Si or O). In summary, an increase in the takeoff angle of ARXPS measurements increased the C_{1s} signal relative to the Si_{2p} signal, which was expected for the substrates coated with monolayers.

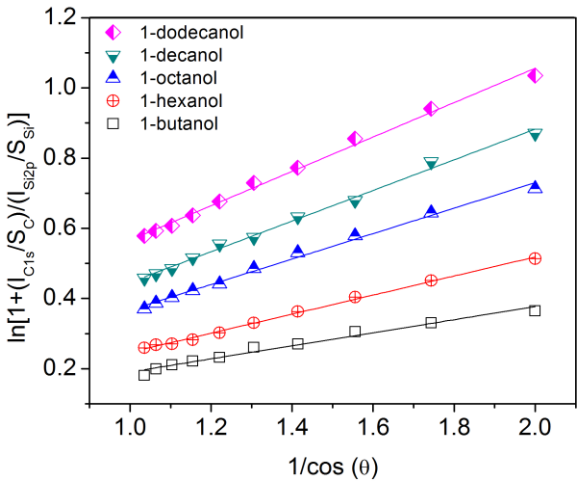

Figure 5.4. The plot of $\ln[1+(I_{C1s}/S_C)/(I_{Si2p}/S_{Si})]$ vs. $1/\cos(\theta)$ for a series monolayers on silicon oxide surfaces prepared from aliphatic alcohols of increasing chain length. Each data set was obtained from a series of ARXPS measurements.

The ARXPS measurements were analyzed in further detail to derive the thickness of each of the monolayers. This analysis was performed by comparing the relative peak intensities for carbon and silicon as a function of the tilt angle. Specifically, the term $\ln[1+(I_{C1s}/S_C)/(I_{Si2p}/S_{Si})]$ was plotted as a function of $1/\cos(\theta)$. The plots displayed a linear trend over the datasets associated with each of the substrates. These results suggest that the monolayers were continuous and uniform, regardless of the alkyl chain length (Figure 5.4). On the other hand, the same type of plot obtained from a piranha cleaned silicon substrate supporting only a 100-nm thermally grown oxide film did not show a linear trend for the same analysis of the relative intensities of C_{1s} and Si_{2p}. The lack of a regular trend observed for the piranha cleaned silicon substrate was attributed to the non-uniform adsorption of volatile carbon based species or miscellaneous contamination (Appendix D, Figure D2). The thickness of each of the monolayers were calculated from each set of ARXPS data using a λ value of 25 Å.[132] The estimated thicknesses of the monolayers and tilts of the molecules within the series of monolayers prepared from aliphatic alcohols are summarized in Table 5.1. The calculated average thicknesses were 0.46, 0.68, 0.91, 1.09, and 1.22 nm for the monolayers derived from 1-butanol, 1-hexanol, 1-octanol, 1-decanol, and 1-dodecanol, respectively. The increase in the thickness of the monolayers was proportional to an increase in the chain lengths of the aliphatic alcohols. This result

indicated that the physical properties of the monolayers were consistent with those of the aliphatic alcohol used to prepare these monolayers.

Table 5.1. Estimated film thickness and molecular tilt angles for monolayers derived from aliphatic alcohols on silicon oxide.

	# of carbons	slope	y-intercept	R^2	film thickness (nm)	molecular length (nm)	tilt angle φ (°)
1-butanol	4	0.1859	0.0052	0.9740	0.46 ± 0.03	0.49	33 ± 3
1-hexanol	6	0.2714	0.0244	0.9969	0.68 ± 0.01	0.74	35 ± 1
1-octanol	8	0.3623	0.0053	0.9926	0.91 ± 0.03	0.99	35 ± 1
1-decanol	10	0.4362	0.0102	0.9945	1.09 ± 0.03	1.2	35 ± 1
1-dodecanol	12	0.4893	0.0773	0.9937	1.22 ± 0.03	1.5	39 ± 1

An average tilt angle (φ) of the monolayers can be estimated based on the monolayer thickness as determined from the ARXPS measurements. The molecular chain length of each aliphatic alcohol was estimated from their molecular models projected in ChemDraw 3D (Appendix D, Figure D1). The Cartesian coordinates were determined for the oxygen atom and carbon atom at either end of these linear molecules. The distance between these terminal atoms was calculated using the Pythagorean Theorem (Appendix D, Equation D.1). The measured thickness of the monolayers were slightly less than the molecular lengths calculated from this model. This observation was anticipated because the monolayers were expected to adopt a tilted position at the silicon oxide surfaces.[1,230] The molecular tilt angle, φ, was an estimate of the angle at which the molecules within the monolayers tilted away from the surface normal (Figure 1B). The calculated values for φ ranged from 33° to 39°, with an average φ of 35°. Tilt angles reported for n-alkanethiol SAMs on gold surfaces range from 20 to 35.3°, which were determined using various techniques including ARXPS, ellipsometry, and infrared spectroscopy.[1, 66, 231-233] The tilt angles of molecules within organosilane based monolayers on silicon oxide surfaces are reported to be ~35°. The tilt angles for the species in the alcohol based monolayers are within the ranges of tilt angles reported for these other types of monolayers. This result suggests that the physical properties and the uniformity of the alcohol based monolayers are consistent with monolayers derived from other organic precursors, such as alkanethiols or alkylsilanes. The discrepancy in the tilt angles calculated for the series of monolayers derived from the alcohol based reagents could be attributed to experimental errors resulting from ARXPS analyses and/or variations in the structure of the bond

between the silicon oxide and the anchoring groups of the monolayers at this interface.[1, 66] The trends observed in the previous studies also indicated that the average increase in thickness of the monolayers per each addition of a methylene (CH_2) group to the molecular chain was approximately 1.0 to 1.5 Å.[234-235] The average increase in film thickness of alcohol based monolayers associated with the same addition of a CH_2 group was determined to be ~1.0 Å. Thickness of the alcohol based monolayers derived from microwave-assisted reactions agreed with the measurements from previously studied monolayers, such as thiolates on gold or silane based monolayers on silicon oxide surfaces. The relationship between the chain lengths of organic based monolayers and their overall film thickness is consistent between different types of monolayers.

5.5. Conclusions

In summary, we have determined the thickness of monolayers derived from the microwave assisted condensation of aliphatic alcohols of different chain lengths on silicon oxide surfaces. Monolayers of 1-butanol, 1-hexanol, 1-octanol, 1-decanol, and 1-dodecanol formed on silicon oxide surfaces were characterized by angle-resolved X-ray photoelectron spectroscopy (ARXPS), and the peak intensities of C_{1s} and Si_{2p} were analyzed as a function of changes in the takeoff angle. The average thickness of each of these monolayers were determined to be 0.46, 0.68, 0.91, 1.09, and 1.22 nm corresponding to monolayers derived from 1-butanol, 1-hexanol, 1-octanol, 1-decanol, and 1-dodecanol, respectively. Thickness of the monolayers increased with increases in the length of the hydrocarbon chain of the aliphatic alcohol reagents with an average molecular tilt angle of 35°. The alcohol based monolayers possess a similar film thickness and tilt angle as thiol based monolayers on gold surfaces or silane based monolayers on silicon oxide surfaces, further suggesting a consistency in the physical characteristics of these monolayers.

Chapter 6.

Covalent Surface Modification of Silicon Oxides with Alcohols in Polar Aprotic Solvents

6.1. Notice of Permissions

The following chapter is adapted with permission from Austin W. H. Lee and Byron D. Gates, “Covalent Surface Modification of Silicon Oxides with Alcohols in Polar Aprotic Solvents”, *Langmuir* **2017**, *33*, 8707-8715 ©2017 American Chemical Society. The work presented in this paper, including experiments, data acquisition, interpretation and writing has been performed by myself under the guidance of Dr. Byron Gates.

6.2. Introduction

In this chapter, the formation of alcohol-based monolayers on silicon oxide surfaces were prepared using polar aprotic solvents. The modification of surfaces with organic monolayers has been of great importance in the fields of electronics,[1, 5-7] microfluidics,[11-14, 236] separation sciences,[26-29] electrochemical sensing,[30-32] and biological interfaces.[2, 4, 36-40] Precursors based on silanes and phosphonic acids[3-4, 37, 52, 58] have been widely utilized to form organic monolayers on silicon oxide surfaces. The use of these monolayers (SAMs) has been limited in part by the challenges of working with these precursors, such as a susceptibility to competing reactions (e.g., hydrolysis) and intermolecular polymerization, their commercial accessibility, and toxicity.[2]

Alternative covalent surface modification strategies have been pursued to address these concerns.[2] For instance, the use of precursors such as alkenes,[158, 237-239] alkynes,[240-243] and alkyl halides[241] have been pursued to form organic monolayers on various substrates. In addition to these alternatives, alcohols have been proposed as alternative building blocks to prepare organic monolayers on silicon oxide (SiO_x) surfaces.[61-62, 65, 81, 208] Alcohols are attractive alternatives for their widespread availability, low toxicity, and minimal susceptibility to side reactions with moisture.[65, 81, 208, 244] Both hydrogen-terminated

silicon and hydroxyl-terminated silicon oxide surfaces have been functionalized with alcohol reagents using reactions initiated by convective heating,[65] UV radiation,[81] or microwave heating.[208, 227] These reports relied on reactions carried out at relatively high temperatures in mostly neat solutions. These approaches provide a simple reaction strategy for the formation of monolayers. However, some methods, such as microwave heating, can limit the choice of alcohols available for the reaction due to possible thermal degradation or other side reactions at high temperatures. Moreover, neat solutions will have fundamental implications on the reaction kinetics and the formation of multicomponent monolayers.[47, 53, 189, 227] It is desirable to identify a solvent to facilitate the formation of alcohol-based monolayers for a versatile tuning of the surface chemistry of silicon oxides.

Here, we investigated the formation of alcohol-based monolayers in polar aprotic solvents to modify the surface properties of silicon oxides. We selected a number of polar aprotic solvents based on their physical properties (e.g., melting and boiling points), solubility of both alcohols and water, as well as their relatively low toxicity and reactivity.[245] We screened these solvents and selected the best performing polar aprotic solvent for further investigation. This investigation included assessing changes in composition of the silicon oxide surfaces after reacting with various solutions containing alcohol-based reagents. The alcohol-based reagents included 1*H*,1*H*,2*H*,2*H*-perfluoro-1-octanol, Zonyl FSN fluorosurfactant, 5-hydroxypentanal, glycolic acid, adenosine 5'-monophosphate, thiamine, choline chloride, and 2-dimethylaminoethanol. We also sought to understand the impact of changes in the reaction temperature, as well as concentration and composition (e.g., alkyl chain lengths) of the alcohol reagents on the rate of formation and overall uniformity of the resulting monolayers. The properties of the monolayer-coated silicon oxide surfaces were assessed by water contact angle (WCA) measurements, atomic force microscopy (AFM), and X-ray photoelectron spectroscopy (XPS).

6.3. Experimental

Reagents and Materials. All reagents were used as received, which included dimethyl sulfoxide (DMSO, Sigma-Aldrich, 99.9%, CAS no. 67-68-5), dimethylformamide (DMF, EM Science, CAS no. 68-12-2), propylene carbonate (Sigma-Aldrich, 99%, CAS

no. 108-32-7), ethylene carbonate (Sigma Aldrich, 98%, CAS no. 94-49-1), diethylene glycol diethyl ether (Sigma Aldrich, 98%, CAS no. 112-36-7), dibasic ester (DBE, Sigma Aldrich, dibasic ester mixture), 1-octanol (Sigma-Aldrich, ACS reagent grade, CAS no. 111-87-5), 1H,1H,2H,2H-perfluoro-1-octanol (Alfa Aesar, 97%, CAS no. 647-42-7), choline chloride (Sigma-Aldrich, BioReagent, CAS no. 67-48-1), glycolic acid (Sigma-Aldrich, 99%, CAS no. 79-14-1), thiamine hydrochloride (Sigma-Aldrich, 99%, CAS no. 67-03-8), adenosine 5'-monophosphate monohydrate (Sigma-Aldrich, 97%, CAS no. 18422-05-4), 2-dimethylaminoethanol (Sigma-Aldrich, 99.5%, CAS no. 108-01-0), 5-hydroxypentanal (Sigma-Aldrich, CAS no. 4221-03-8), Zonyl FSN fluorosurfactant (Sigma-Aldrich, 40%, CAS no. 65545-80-4), 1-dodecanol (Sigma-Aldrich, 98%, CAS no. 112-53-8), 1-tetradecanol (Sigma-Aldrich, 97%, CAS no. 112-72-1), 1-hexadecanol (Sigma-Aldrich, 99%, CAS no. 36653-82-4), 1-octadecanol (Sigma-Aldrich, 99%, CAS no. 112-92-5), sulfuric acid (Caledon, ACS reagent grade, CAS no. 7664-93-9), hydrogen peroxide (ACP, ACS reagent grade, CAS no. 7722-84-1), acetone (Fisher Scientific, reagent grade, CAS no. 67-64-1), isopropanol (Fisher Scientific, reagent grade, CAS no. 67-63-0), and anhydrous ethyl alcohol (Commercial Alcohols, P016EAAN, CAS no. 64-17-5). Four inch, p-type, prime grade, single-side polished, ⟨100⟩ silicon wafers were purchased from the Nanofabrication Facility in 4D LABS at Simon Fraser University.

Preparation of Silicon Substrates. The silicon substrates were diced into ~1 cm^2 pieces and washed with acetone and isopropanol. These substrates were dried under a stream of nitrogen gas filtered with a PTFE membrane containing <200 nm pores. The silicon substrates were further cleaned by immersion into a piranha solution followed by rinsing with water prior to the formation of the monolayers as described in previous literature.[208] CAUTION: Piranha solution is a strong oxidizing agent and reacts violently with organic compounds. This solution should be handled with extreme care. The silicon substrates were immersed in the freshly prepared piranha solution for at least 1 h followed by placement for 5 min into 18 MΩ·cm deionized (DI) water (Barnstead Nanopure DIamond water filtration system). After further washing with DI water, these cleaned substrates were dried under a stream of filtered nitrogen gas.

Formation of Monolayers. The formation of monolayers was performed on substrates placed in a glass round-bottom flask that was placed in a silicone oil bath at

the desired reaction temperatures (e.g., 50 or 100 °C). The flask contained 50 mL of the reaction mixture containing a reagent (e.g., 1-octanol) dissolved in a polar aprotic solvent (e.g., propylene carbonate). The silicon substrates were loaded onto a customized glass holder. This holder loaded with multiple substrates was placed into the round-bottom flask containing the reaction mixture. After heating for the desired period of time, each substrate was taken out individually and immersed into separate solutions of ethanol. Each substrate was sonicated for at least 3 min in ethanol, rinsed further with ethanol, and finally rinsed with DI water. The rinsed substrates were dried under a stream of the filtered nitrogen gas.

Water Contact Angle (WCA) Measurements. Water contact angle measurements evaluated the hydrophobicity of the substrates. Each measurement was obtained from 2 μL droplets of solvent dispensed onto the substrates. The WCA was measured as the angle between the air−water interface of the droplet and the interface of the water and the substrate. Five advancing contact angle measurements were obtained for each sample by adding 2 μL for each subsequent measurement. The mean of the WCA values was determined by taking the average of the advancing contact angle measurements. One standard deviation (1σ) from the mean was evaluated for each sample and taken as the error associated with the WCA values.

Atomic Force Microscopy (AFM). The surface topography of the samples was characterized by AFM. The AFM images were acquired using an MFP 3D AFM (Asylum Research and Oxford Instruments) operating in alternating current (AC) mode using silicon cantilevers from BudgetSensors (Tap150-G, resonant frequency of 150 kHz, force constant 5 N/m). Images were acquired from scan areas of 5 μm × 5 μm with a scan speed of 0.4 Hz and a resolution of 512 × 512. The AFM image analysis and the determination of the root-mean-square (RMS) roughness were performed using Igor Pro 6.22.

X-ray Photoelectron Spectroscopy (XPS). Chemical composition of the surfaces of the substrates were investigated by XPS. These studies were conducted using a Kratos Analytical Axis ULTRA DLD system with a monochromatic aluminum source (Al Kα of 1486.7 eV) operating at 150 W with a 90° takeoff angle. Survey scans (0−1200 eV) were acquired using a pass energy of 160 eV, a dwell time of 100 ms, and 1 sweep. High-

resolution scans were obtained using a pass energy of 20 eV, a dwell time of 500 ms, and integrating the results of 10 sweeps. An area of 700 μm by 300 μm was analyzed in three separate regions of each sample to check the uniformity of each surface modification. The XPS peak analysis and quantification of atomic composition of the elements (e.g., carbon) was performed using Vision Processing.

6.4. Results and Discussion

Covalent Immobilization of 1-Octanol on Silicon Oxide Surfaces in Polar Aprotic Solvents. The goal of this study was to form alcohol-based monolayers in polar aprotic solvents for tailoring the surface properties of silicon oxides. An appropriate solvent was sought to facilitate the formation of alcohol-based monolayers. Covalent attachment of alcohols to silicon oxide surfaces is achieved through a condensation reaction between the hydroxyl groups of the alcohol reagents and surface bound silanols, forming silyl ether (Si−O−C) bonds with water as a byproduct.[65] The solvent must be able to dissolve both the alcohol containing reactants and water while avoiding side reactions or other unfavorable interactions with the reactants. It is also desirable for the solvent to possess a low melting point and a high boiling point to carry out reactions over a wide ranges of temperatures. Nonpolar solvents were eliminated for their relatively poor solubility of polar reagents, while polar protic solvents were eliminated for their ability to undergo unwanted side reactions with the silanol groups. A series of polar aprotic solvents were selected for their minimal reactivity toward the silanol groups and their ability to dissolve a wide range of polar compounds. The choice of solvent was important as it would facilitate solvation and transport of both alcohol molecules and water to and from the silicon oxide surfaces. Hydrophobicity of the substrates after the reaction with 1-octanol in a series of solvents was evaluated using WCA measurements to screen the solvents for their ability to form alkyl terminated monolayers on silicon oxide surfaces.

Polar aprotic solvents with boiling points >150 °C were initially selected for the reaction. In particular, dimethyl sulfoxide (DMSO), dimethylformamide (DMF), and propylene carbonate were initially chosen as potential solvents. Piranha cleaned silicon substrates were immersed into each solvent containing 600 mM 1-octanol and heated at 100 °C for 24 h. The substrates reacted with 1-octanol dissolved in DMSO or DMF yielded

water contact angle (WCA) values of 17° ± 5° and 4° ± 3°, respectively. The hydrophilicity of these substrates suggested a negligible amount of 1-octanol reacted with these substrates. These results deviate from previous literature that successfully demonstrated the formation of silyl ether (Si−O−C) bonds in DMF during the synthesis of organic compounds.[185, 246] This discrepancy is attributed to differences in the steric hindrance of the silanol groups at the silicon oxide surfaces. Adsorption of DMF molecules could interact with the silicon oxide surfaces, further hindering the reaction with 1-octanol.[185, 246] It is possible that DMSO hinders the reaction in a similar manner to DMF. On the other hand, the substrates reacted with 1-octanol in propylene carbonate yielded a WCA of 108° ± 3°, indicating a substantial change in hydrophobicity. This result suggested that monolayers were formed on silicon oxide surfaces from alcohol-based reagents dissolved in propylene carbonate. The successful formation of monolayers was attributed to the advantages of propylene carbonate. For example, propylene carbonate effectively dissolves both polar and nonpolar compounds, including water and the alcohol-based reagents. Effective molecular transport of water and alcohol-based reagents at the interface can facilitate the covalent modification of the silicon oxides with the alcohol-based compounds. In addition to its relatively high boiling point, propylene carbonate possesses a number of other desirable properties, such as its relatively low price, high solubility of polar reactants and byproducts, as well as relatively low toxicity.[245] Although monolayers derived from 1-octanol were not achieved using DMF or DMSO as a solvent, propylene carbonate was demonstrated to be a suitable solvent. The reactions were carried out in other polar aprotic solvents (e.g., ethylene carbonate, diethylene glycol diethyl ether, dibasic ester) to compare the ability to form monolayers in different polar aprotic media. Hydrophobicity of the substrate was evaluated at different time points of the reaction (e.g., 1, 3, 5, 24, 48, or 72 h) using a series of water contact angle (WCA) measurements (Figure 6.1). While the WCA values plateaued at 110° for the substrates reacted in propylene carbonate, the other contact angle values plateaued at low values in other solvents. Propylene carbonate was selected for a detailed investigation into the formation of monolayers on SiO_x surfaces using a variety of alcohol containing reagents.

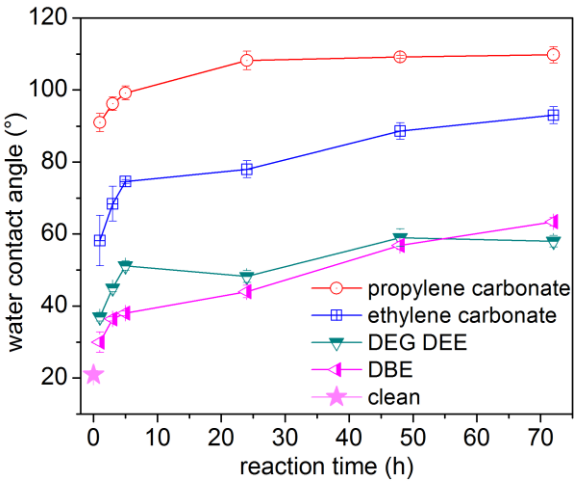

Figure 6.1. **Water contact angle measurements for silicon substrates after reacting these at 100 °C in 600 mM solutions of 1-octanol in various solvents as indicated [i.e. propylene carbonate, ethylene carbonate, diethylene glycol diethyl ether (DEG DEE), and dibasic ester (DBE)]. Reprinted with permission from Lee A. W. H. and Gates. B. D. *Langmuir* 2017 DOI: 10.1021/acs.langmuir.7b00820 ©2017 American Chemical Society.**

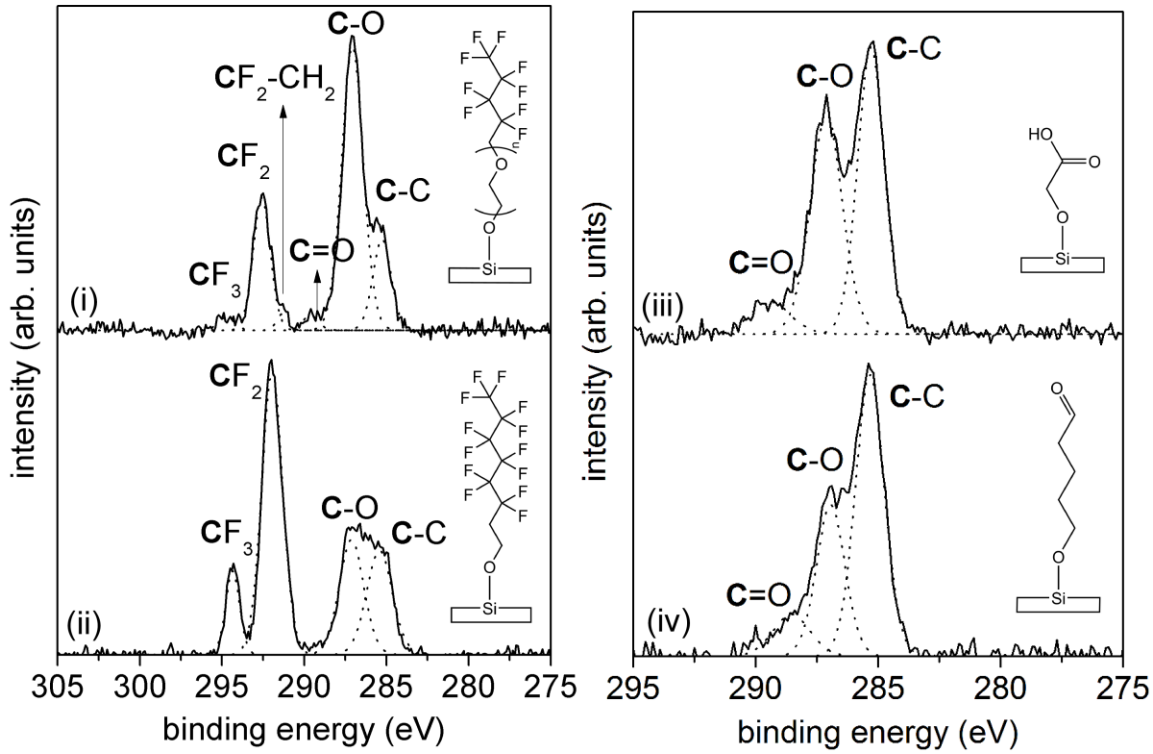

Figure 6.2. High-resolution C1s XPS of piranha cleaned silicon substrates after reacting with (i) Zonyl surfactant, (ii) 1*H*,1*H*,2*H*,2*H*-perfluoro-1-octanol, (iii) glycolic acid, and (iv) 5-hydroxypentanal. Reprinted with permission from Lee A. W. H. and Gates. B. D. *Langmuir* 2017 DOI: 10.1021/acs.langmuir.7b00820 ©2017 American Chemical Society.

Covalent Surface Modification of Silicon Oxides with Various Alcohol Compounds. A series of reactions were carried out to tune the surface chemistry of silicon oxides. These reactions analyzed various types of alcohol containing reagents that were dissolved in propylene carbonate. High resolution C_{1s} XPS results displayed distinguishable surface compositions for the substrates reacted with 1*H*,1*H*,2*H*,2*H*-perfluoro-1-octanol, Zonyl fluorosurfactant, glycolic acid, or 5-hydroxypentanal (Figure 6.2). The substrate coated with Zonyl fluorosurfactant exhibited a difluorocarbon (**C**F_2) peak at 292.6 eV and a trifluorocarbon (**C**F_3) peak at 294.7 eV.[129, 210, 247-249] This XPS analysis also indicated the presence of **C**−O species at 287.1 eV and C−C species at 285.3 eV. A shift in these binding energies relative to literature values was attributed to charging effects during the XPS analysis of the insulating layers of SiO_x and fluorocarbon-based monolayers.[203, 209] A higher intensity of the **C**−O peak in comparison to that of the

C−C peak was attributed to the poly(ethylene glycol) (PEG) content of the Zonyl-based monolayers.[250-251] An XPS analysis of the substrate coated with 1*H*,1*H*,2*H*,2*H*-perfluoro-1-octanol yielded a **C**F_2 peak at 291.9 eV, a **C**F_3 peak at 294.4 eV, a **C**−O peak at 287.1 eV, and a **C**−C peak at 285.4 eV. These peaks agree with the previously reported peak positions for these respective species based on the high resolution C_{1s} XPS of fluorinated monolayers.[208, 210, 227, 247-248] Monolayers derived from either glycolic acid or 5-hydroxypentanal contained three distinct peaks in their high resolution C_{1s} XPS analyses. For the substrate reacted with glycolic acid, the peaks attributed to **C**–C, **C**–O, and **C**=O were located at binding energies of 285.3, 287.1, and 289.4 eV, respectively. The binding energies of these peaks correlate with carboxyl-terminated SAMs previously reported on both stainless steel[252] and Si(111).[253] For the substrate reacted with 5-hydroxypentanal, the peaks attributed to **C**−C, **C**−O, and **C**=O were located at binding energies of 285.3, 286.9, and 288.5 eV, respectively. The binding energies of these peaks are in agreement with aldehyde-terminated, silane-based SAMs on silicon oxide surfaces.[254] The observed differences in binding energies of the **C**=O peaks for monolayers derived from glycolic acid and 5-hydroxypentanal (289.4 and 288.5 eV, respectively) was attributed to their differences in the groups adjacent to the terminal carbon species. In monolayers derived from 5-hydroxypentanal, the outermost carbon was the aldehyde moiety (H−C=O), whereas for monolayers derived from glycolic acids the outermost carbon was a carboxylic acid moiety (HO−C=O).

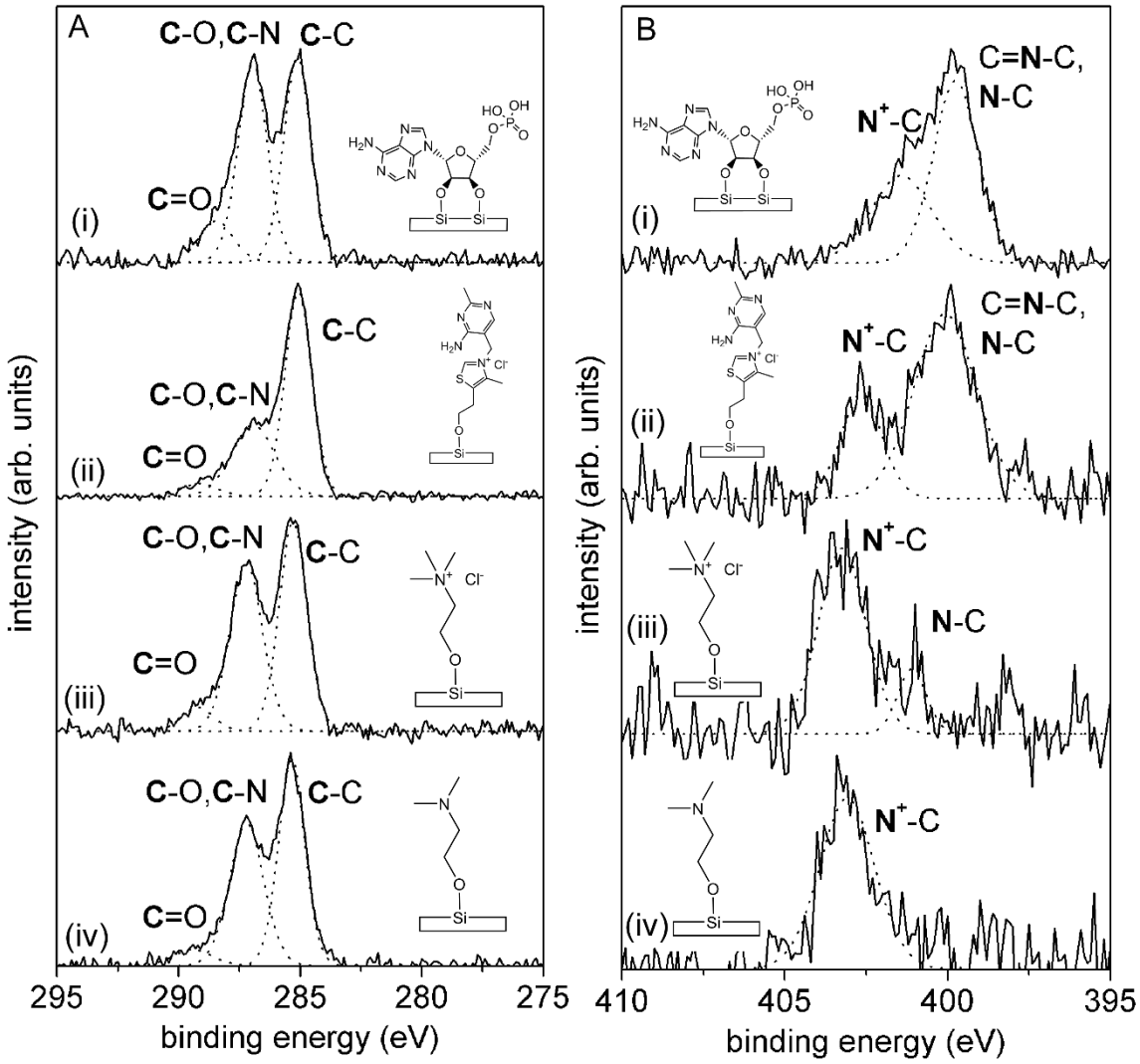

Figure 6.3. High-resolution (A) C1s and (B) N1s XPS of polished piranha-cleaned silicon substrates after reacting with (i) adenosine monophosphate (AMP), (ii) thiamine, (iii) choline chloride, and (iv) 2-dimethylaminoethanol. Reprinted with permission from Lee A. W. H. and Gates. B. D. *Langmuir* 2017 DOI: 10.1021/acs.langmuir.7b00820 ©2017 American Chemical Society.

Nitrogen containing alcohol-based compounds were also grafted onto the silicon oxide surfaces using the same strategy of dissolving these reagents in propylene carbonate and heating the mixture to 50 °C for 24 h. The selected reagents included adenosine 5'-monophosphate (AMP), thiamine, choline chloride, and 2-dimethylaminoethanol. The reacted substrates were characterized by high resolution C_{1s}

and N_{1s} XPS (Figure 6.3). The primary peaks in the C_{1s} spectra at binding energies 285.3 and 287.0 eV, respectively, are attributed to **C**−C and overlapping contributions from C−O and **C**−N. The peak intensity for the **C**−O and **C**−N species is relatively high due to a contribution from covalently attached carbon and nitrogen. The high resolution N_{1s} XPS analyses exhibited distinct binding energy profiles for each of these substrates. The XPS analysis of the substrates coated with AMP had N_{1s} peaks at 401.4 and 399.7 eV, which were attributed to the charged and uncharged nitrogen of the primary amine and the aromatic nitrogen of adenine.[255-256] The XPS analysis of the substrates coated with thiamine also exhibited two distinct nitrogen peaks but with binding energies of 402.7 and 400.1 eV.[257-258] A strong N_{1s} peak was observed for the substrates coated with either choline chloride or 2-dimethylaminoethanol at a binding energy of 403.2 eV. No significant shift in the N_{1s} binding energies between these two substrates suggested a positive charge associated within the terminal tertiary amine of the 2-dimethylaminoethanol-based monolayers. A weak N_{1s} peak was observed at a binding energy of 401.1 eV for the substrates coated with choline chloride. This peak was attributed to terminal quaternary ammonium groups in close proximity to the silicon oxide surfaces due to electrostatic interactions.[208] Overall, the silicon oxide surfaces were successfully modified after the reaction with various alcohol-containing reagents in propylene carbonate.

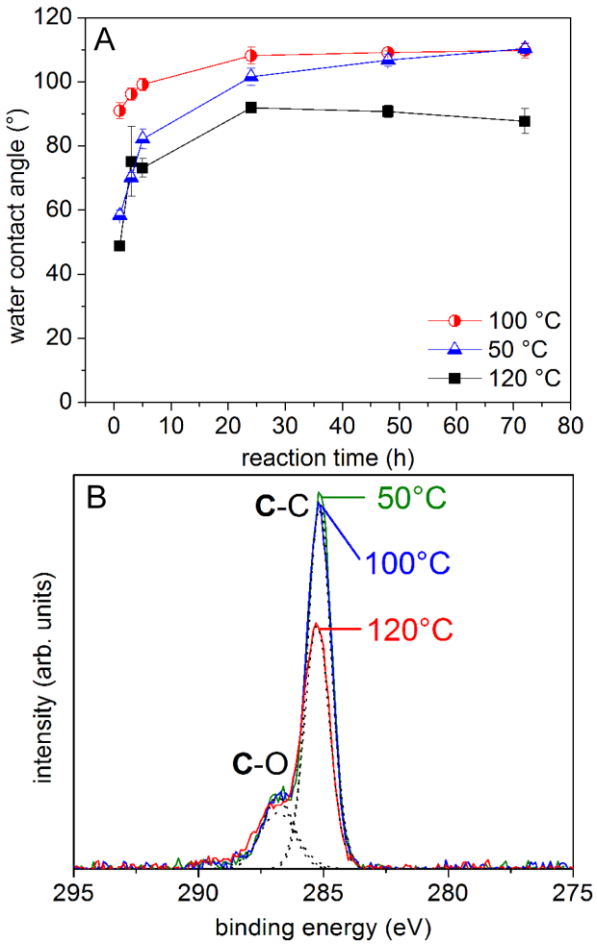

Figure 6.4. **(A) WCA measurements for piranha-cleaned silicon substrates reacted with 600 mM 1-octanol in propylene carbonate at different temperatures as indicated in the legend. (B) Normalized high resolution C1s XPS for the substrates reacted for 72 h at different temperatures as indicated by the labels on the plots. Reprinted with permission from Lee A. W. H. and Gates. B. D. *Langmuir* 2017 DOI: 10.1021/acs.langmuir.7b00820 ©2017 American Chemical Society.**

Formation of Monolayers Derived from Aliphatic Alcohols in Propylene Carbonate at Different Temperatures. The formation of alcohol-based monolayers was performed at different temperatures (i.e. 50 °C, 100 °C, and 120 °C) to investigate the influences of varying reaction conditions on the uniformity of the monolayers and the rate of their formation. The WCA values for piranha cleaned silicon substrates were measured after their reaction with 1-octanol for different durations, such as 1, 3, 5, 24, 48, and 72 h (Figure 6.4A). These WCA values increased with a longer reaction time until the WCA values plateaued at 110° for the substrates reacted at 50 and 100 °C. It took up to 24 h

for the WCA value to reach 110° for the reaction performed at 100 °C, while the reaction time up to 72 h were required to achieve similar results for the reaction held at 50 °C. The WCA values of ~110° indicate a relatively high surface coverage of the SAMs as the values are comparable to those reported in literature for methyl-terminated monolayers.[48, 208] This result demonstrated a comparable quality of monolayers to that of the monolayers prepared by a reaction of neat 1-octanol with polished silicon oxide surfaces using either convective heating at 196 °C for 2.5 h[65] or a microwave-assisted reaction at 180 °C for 30 min.[208] The ability to achieve relatively high quality monolayers at relatively low reaction temperatures (e.g., 50 or 100 °C) is attributed to the increased reaction time and to the increased solubility of both the reactants and byproducts in the polar aprotic medium. Propylene carbonate can enhance the molecular transport of water away from and 1-octanol molecules to the silicon oxide interfaces, which facilitates the formation of the alcohol-based monolayers. The WCA values plateaued at ~90° for the substrates held at 120 °C during the reaction, which was lower than the WCA values achieved at 50 and 100 °C. This result suggested the formation of lower quality, less uniform monolayers at 120 °C. It is likely that the mixture of propylene carbonate and 1-octanol underwent unwanted side reactions at temperatures of 120 °C.[259] This conclusion was supported in part from the change in color of the reaction mixture from a clear transparent solution to a light yellow solution. Further analyses were required to understand the results of the WCA measurements.

Chemical composition of the modified silicon substrates was analyzed using XPS. Correlation was sought between chemical composition of these surfaces and the reaction temperature. Two distinct peaks attributed to C−C and C−O were detected at binding energies of 285.1 and 286.8 eV, respectively, for all of the substrates. The substrates reacted at temperatures of 50, 100, and 120 °C for 72 h were analyzed by high-resolution C_{1s} XPS, which was normalized to Si_{2p} peak intensities obtained from each sample (Figure 6.4B). The relative intensities of the C−C peaks to the Si_{2p} peaks were similar (~0.15) for the samples reacted at 50 and 100 °C. On the other hand, the relative intensity for the sample reacted at 120 °C was 0.10, which was lower than the other two samples. This result agrees with the WCA measurements (Figure 6.4A) in which the hydrophobicity of the modified substrates was lower for the reactions carried out at 120 °C in comparison to those at 50 or 100 °C. The lower WCA values and the lower carbon content of the surface

modifications at 120 °C suggest that these monolayers were less uniform or otherwise compromised. Insight into these differences was sought from analyses of the changes in the surface topography of the substrates after reacting at the specified temperatures.

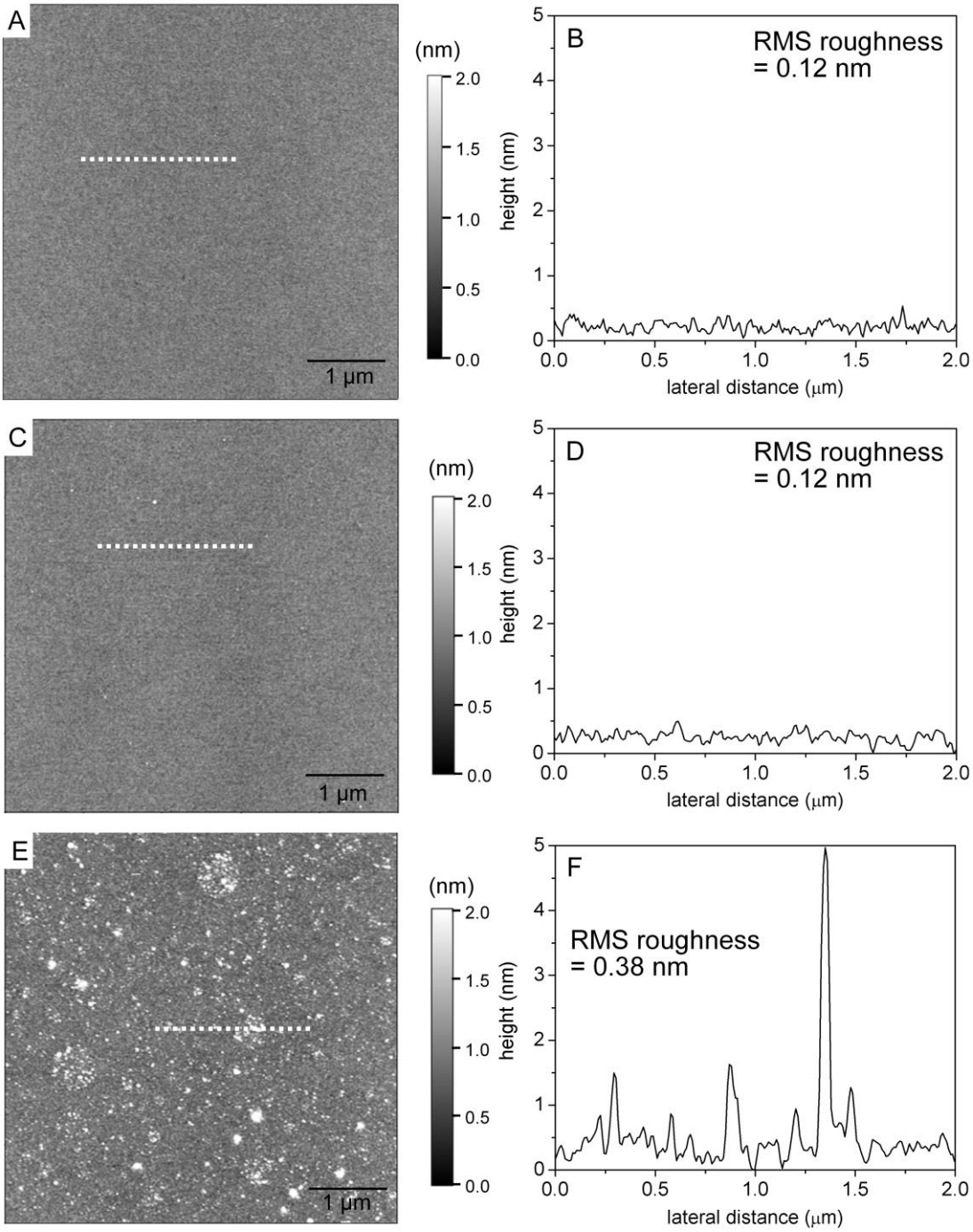

Figure 6.5. **Atomic force microscopy (AFM) images and representative cross-sectional profiles (corresponding to the white dashed lines) for silicon substrates after reacting with 600 mM 1-octanol in propylene carbonate at (A,B) 50 °C, (C,D) 100 °C, and (E,F) 120 °C for 72 h. Reprinted with permission from Lee A. W. H. and Gates. B. D. *Langmuir* 2017 DOI: 10.1021/acs.langmuir.7b00820 ©2017 American Chemical Society.**

The topography of the silicon substrates was assessed by AFM after reacting with 1-octanol in propylene carbonate. Each of these studies was performed on substrates that had been reacted for 72 h, and results were compared for reactions held at different temperatures. The substrates held at 50 and 100 °C exhibited relatively uniform surface topographies (Figure 6.5A, C). The measured RMS roughness for each of these substrates was 0.12 nm (Figure 6.5B, D), which is comparable to the RMS roughness of the native SiO_x surfaces. This result further suggested that these monolayers were uniform, as indicated by the WCA measurements. In contrast, the substrates reacted at 120 °C exhibited nonuniform surface topographies containing randomly distributed features with heights up to ~5 nm and an overall RMS roughness of 0.38 nm (Figure 6.5E, F). The increased surface roughness after performing the reaction at 120 °C was likely due to the deposition of byproducts produced from unwanted side reactions between the propylene carbonate and aliphatic alcohol.[259] In summary, the results of the WCA, XPS, and AFM analyses indicated that uniform monolayers of 1-octanol could be achieved for reactions at 50 and 100 °C within 72 h using propylene carbonate as the reaction medium. Higher reaction temperatures (e.g., 120 °C) could result in the formation of incomplete monolayers, which is attributed to side reactions or thermal degradation of the species in solution.

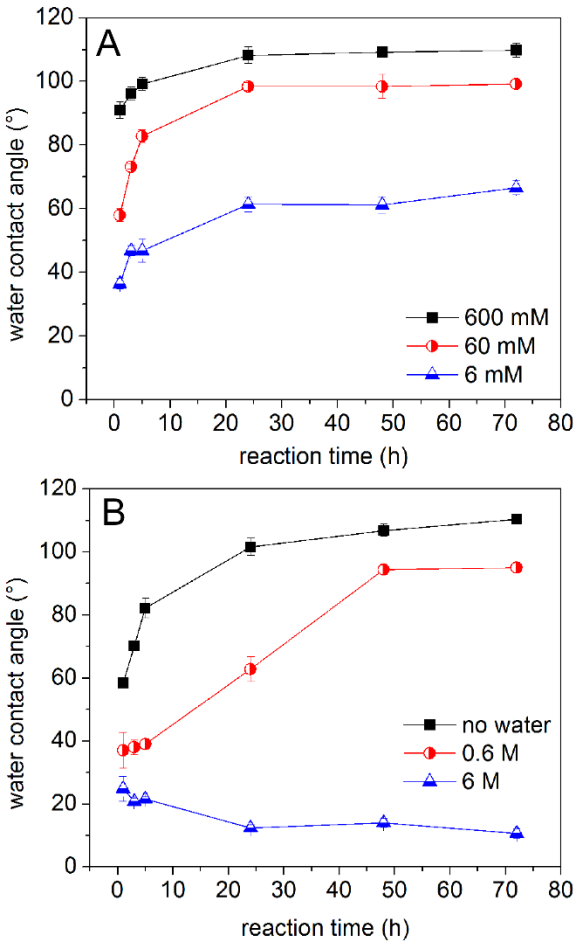

Figure 6.6. **WCA measurements for polished silicon substrates after reacting with a series of 1-octanol solutions in propylene carbonate. (A) In one series of reactions, the concentration of 1-octanol was varied from 6 to 600 mM while maintaining a reaction temperature of 100 °C. (B) In another series of reactions, increasing amounts of water (see legend) were added to solutions of 600 mM 1-octanol in propylene carbonate and subsequently reacted at 50 °C. Reprinted with permission from Lee A. W. H. and Gates. B. D. *Langmuir* 2017 DOI: 10.1021/acs.langmuir.7b00820 ©2017 American Chemical Society.**

Formation of Monolayers Derived from Aliphatic Alcohols in Propylene Carbonate: Impact of the Concentration of Alcohols and Water. A series of reactions were performed to study the changes in the concentration of an aliphatic alcohol on the formation of alcohol-based monolayers on silicon oxides. In the case of thiol-based monolayers on gold surfaces, their rate of formation increases with an increase in the concentration of precursors in solution.[1] It was anticipated that a similar relationship may

exist for the formation of aliphatic alcohol-based monolayers on silicon oxides. The hydrophobicity of substrates reacted at 100 °C in 600, 60, and 6 mM solutions of 1-octanol in propylene carbonate were analyzed as a function of reaction time through a series of WCA measurements (Figure 6.6A). The WCA values plateaued at ~110° for the substrates reacted in the 600 mM solution of 1-octanol, while the values plateaued at ~90° and ~65° for the 60 and 6 mM 1-octanol, respectively. The extent of monolayer formation increases with the increase in the concentration of the precursors in solution, which was analogous to the reaction kinetics observed for thiol-based SAMs.[1] For a given period of reaction time, the extent of the formation of the alcohol-based monolayers decreased at the lower concentrations of 1-octanol in the propylene carbonate. Uniform monolayers of alkylsilanes or thiols can be achieved for a wide range of concentrations of reactants (e.g., 0.1 to 100 mM) after a sufficient period of time.[1-2] The incomplete formation of monolayers derived from 1-octanol at the lower concentrations could be attributed in part to the mechanism of the condensation reaction between these alcohols and the silanols at the silicon oxide interface. The condensation reaction is a reversible reaction with water molecules created as a byproduct.[61-62, 65] If the concentration of aliphatic alcohols and water molecules in the solution is comparable, hydrolysis of the silyl ether bond to form silanol groups at the interface could compete with the condensation reaction of the alcohols.

Further investigation was conducted to understand the impact of water in the reaction mixture. Different amounts of water were added to a 600 mM 1-octanol solution and subsequently heated at 50 °C (Figure 6.6B). The lower reaction temperature was selected to minimize evaporation of water during the reaction. The addition of water molecules substantially impacted the formation of the alcohol-based monolayers. When the reaction was performed with 6 M of water, the substrates remained hydrophilic and the WCA values approached a plateau below 15°. Hydrophobicity of the substrates exhibited a more gradual increase when 600 mM water was added to the reaction mixture. This mixture yielded modified substrates that approached a plateau in its WCA of ~90° after 72 h. The rate of change in hydrophobicity as a function of reaction time suggested a slower formation of the monolayers due to the increase in water content of the solution. This result further suggested that monolayers formed on silicon oxides could be partially removed through hydrolysis of the silyl ether bond in the presence of water at elevated

temperatures. In summary, decreasing the concentration of 1-octanol leads to a decrease in the rate of formation of monolayers on silicon oxide surfaces. Furthermore, water content of the reaction mixture could further decrease the reaction rate and compromise the uniformity of these monolayers.

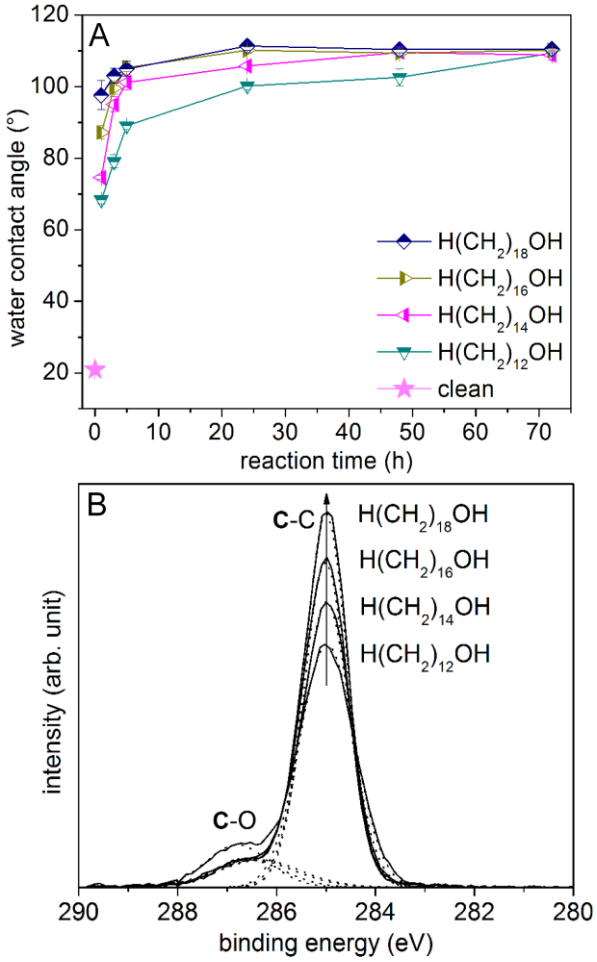

Figure 6.7. **(A) Water contact angle measurements for a series of silicon substrates reacted with different aliphatic alcohols. (B) High-resolution C1s XPS for the silicon substrates reacted with the aliphatic alcohols for 72 h. Each reaction was carried out at 100 °C in 50 mM of the respective alcohol reagent dissolved in propylene carbonate. Reprinted with permission from Lee A. W. H. and Gates. B. D. *Langmuir* 2017 DOI: 10.1021/acs.langmuir.7b00820 ©2017 American Chemical Society.**

Formation of Monolayers Derived from Aliphatic Alcohols in Propylene Carbonate: Effect of Alkyl Chain Length. Chain lengths of the aliphatic alcohols could play a key role in the rate of formation of the monolayers and influence their uniformity.

Differences in the intermolecular interactions, molecular transport, steric hindrance, and interactions with the solvent could each influence the efficiency of the formation of monolayers.[53] It is important to understand the impact of changes in the alkyl chain length on the rate of formation of these monolayers in propylene carbonate. A series of reactions were performed at 100 °C in solutions of 50 mM aliphatic alcohol in propylene carbonate (Figure 6.7A). The reactants included 1-dodecanol [$H(CH_2)_{12}OH$], 1-tetradecanol ([$H(CH_2)_{14}OH$], 1-hexadecanol [$H(CH_2)_{16}OH$], and 1-octadecanol[$H(CH_2)_{18}OH$]. The differences observed in the rate of increase in the WCA values with reaction time indicated that the monolayers were formed faster with an increase in the length of the alkyl chain. This result is in agreement with previous studies that reported a preferential adsorption of longer chain alkyl thiols on gold surfaces.[53] The trend suggests that the aliphatic alcohols, similar to their thiol analogues, are influenced by intermolecular interactions between the hydrocarbon chains during formation of the monolayers. These interactions could facilitate the formation of the monolayers. These results could also be attributed to the preferential adsorption of the longer chain alcohols due to a relatively lower solubility in the polar medium. Other factors, such as diffusion or steric constraints, were relatively insignificant as these factors should facilitate the formation of monolayers from shorter alkyl chains.[53] In conclusion, chain length of the aliphatic alcohols has a similar impact to their thiolate analogues with the rate of formation of the monolayers increasing in proportion to their chain lengths.

Composition of the silicon oxide surfaces after reacting for 72 h were analyzed using high-resolution C_{1s} XPS. Each C_{1s} XPS was normalized to the Si_{2p} intensities (Figure 6.7B). As the chain lengths of the alcohol precursors increased, the intensities of the C−C peak also progressively increased relative to the Si_{2p} intensity. The ratios between the C−C and Si_{2p} intensities were 0.54, 0.63, 0.74, and 0.83 for the substrates reacted with 1-dodecanol, 1-tetradecanol, 1-hexadecanol, and 1-octadecanol, respectively. This trend was attributed to the increasing carbon content of the aliphatic alcohols used to prepare the monolayers. All of the high-resolution spectra exhibited C−C and C−O peaks with binding energies at approximately 285.0 and 286.7 eV, respectively. The ratios of the C−C and C−O peaks were 4.9, 7.0, 10.7, and 14.0 for the substrates coated with 1-dodecanol, 1-tetradecanol, 1-hexadecanol, and 1-octadecanol, respectively. This trend of increasing peak area ratio was also attributed to the relative increase in the number of carbons in the

alkyl chain in comparison to that of the singular carbon attached to oxygen at the interface. Overall, the C_{1s} XPS analyses indicated an increase in carbon content with an increase in the length of the alkyl chains within the monolayers. These results suggest that the composition of the monolayers were consistent with changes in the composition of the precursors, which further demonstrated the uniformity of the monolayers.

6.5. Conclusions

In summary, we have demonstrated the formation of monolayers on silicon oxide surfaces using a variety of alcohol-containing compounds dissolved in propylene carbonate. The reactions performed in this polar aprotic medium enable a diverse array of surface modifications to the silicon oxides. The reagents included a series of readily available alcohols. The silicon oxides were successfully modified with monolayers containing fluorocarbons, aldehydes, carboxylic acids, quaternary ammonium cations, vitamins, or nucleic acids. The formation of monolayers from aliphatic alcohols was studied in further detail to investigate the influences of reaction temperature, concentrations of both reactants and moisture, and chain lengths of the reactants. It was determined that the increase in the reaction temperature up to 100 °C aided the formation of the alcohol-based monolayers. A further increase in reaction temperature to 120 °C results in an incomplete formation of monolayers due to possible side reactions in the reaction mixture. Increasing the concentration of the reactants increases the rate of monolayer formation, but the presence of relatively large amounts of water added to the propylene carbonate slow down or inhibit the formation of the monolayers. Chain length of the aliphatic alcohols can also have a large impact on the rate of formation of the monolayers. While uniform monolayers were formed using alcohols of varying alkyl chain length, their rate of formation increased in proportion to the lengths of the alkyl chains. This result implies that, similar to thiol-based SAMs, cohesive interactions between the hydrocarbon chains and solubility of the aliphatic alcohols in propylene carbonate had an impact on the formation of monolayers on silicon oxides. The use of propylene carbonate as a solvent for alcohol-based reagents increases the diversity of surface chemistries that can be prepared on silicon oxides. Although these condensation reactions draw a number of analogies to the reactions of alkanethiols on gold, there are a number of unique

attributes and limitations that are specific to the formation of alcohol-based monolayers. Understanding these features enables the design of further reactions aimed at tuning the surface chemistry of silicon oxides through the use of alcohol-containing reactants.

Chapter 7.

Summary and Outlook

This thesis work describes the use of microwaves as a tool to accelerate the formation of uniform monolayers on silicon oxide surfaces. Tailoring the surface properties of silicon oxides have been pursued for many applications including electronics, microfluidics, optics, separation science, nanotechnology, and biomedicine.[1-3] Traditional approaches in surface modification of silicon oxide surfaces include the usage of silanes or phosphonic acids. Challenges with the formation of the organic monolayers include susceptibility to ambient moisture, formation of multilayer coatings, as well as limited accessibility and difficulty in implementation of the traditional processing techniques. Defects in the monolayers can lead to detrimental failure of device or functional materials. The work presented in this study proposes several techniques to form uniform organic monolayers through the covalent surface modification of silicon oxides.

Chapter 1 reviews the methods to covalently modify surface properties through the use ofself-assembled monolayers (SAMs). Traditional types of organic precursors used in the formation of SAMs have been described in detail, including thiols, silanes, and phosphonic acids.[1-3, 37] Applicability, advantages, and limitations of each precursors have been compared based on literature findings. It also reviews the principle and applications of microwave heating. Microwave heating is a widely used technique in many areas of synthetic organic chemistry and material science.[37, 84-85, 94, 109] Its advantages and limitations are described for usage in these applications. Advantages of microwave heating have been proposed for the applications in surface chemistry. Finally, characterization methods to probe the quality of organic monolayers formed on surfaces have been described in the second part of the chapter. These methods including contact angle measurements for probing wettability of surfaces, X-ray photoelectron spectroscopy (XPS) for probing chemical compositions of surfaces, and atomic force microscopy (AFM) for probing morphology of surfaces.

In Chapter 2, a microwave-assisted reaction was demonstrated as a method for rapid formation of silane-based monolayers. Formation of uniform monolayers was

achieved by two strategies. First, rapid microwave heating of the system allows the condensation reaction of silanes on silicon oxide surfaces to accelerate. Such rapid heating methodology allows the formation of uniform silane based SAMs within 10 min of reaction or less. Second, monoreactive fluorinated alkylsilane molecules are used as precursors to minimize the formation of multilayers. Unlike trireactive silanes that can undergo intermolecular polymerization, which leads to the formation of multilayers, monoreactive silanes are less likely to form multilayers on surfaces.[46, 80] Microwave-assisted reaction is demonstrated as a technique to rapidly form uniform silane based monolayers to modify surface properties of silicon oxides.

Chapter 3 presents microwave-assisted formation of alcohol based monolayers on silicon oxide surfaces. Alcohol based precursors are prevalent laboratory reagents that are less moisture sensitive and non-toxic in comparison to traditional organic precursors, such as silanes and phosphonic acids. Challenges with formation of alcohol based monolayers include slow reaction kinetics of the condensation reaction between alcohols and silanol groups at silicon oxide surfaces. Microwave heating was utilized to address this challenge. Microwave heating, unlike conventional heating methods, effectively delivers the energy required to facilitate the molecular transport of surface adsorbed water and alcohol based reagents at the interface. As a result, the formation of uniform alcohol based monolayers with a WCA value of ~110° have been achieved within 10 min of reaction time. This result was repeatable on various types of silicon oxide surfaces including piranha cleaned silicon substrates with or without thermally grown oxide layer, soda-lime glass, and quartz substrates. Moreover, the technique introduced herein has been expanded to tune surface chemistry of silicon oxides with various alcohol containing reagents.

Chapter 4 focuses on the microwave-assisted formation of mixed alcohol based monolayers to tune the oleophobicity of silicon oxide surfaces. Formation of mixed monolayers has been pursued with thiol based precursors.[47, 53, 121] However, formation of such mixed monolayers could be challenging with reactive organic precursors, such as silanes because of its propensity for intermolecular polymerization. The results in this chapter demonstrate the formation of mixed monolayers derived from aliphatic and fluorinated alcohols. Results from contact angle measurements, as well as quantitative

XPS and AFM measurements, indicate that the surface composition of monolayers can be precisely tuned with a one pot reaction from a mixture of aliphatic and fluorinated alcohols.

Chapter 5 presents a detailed analysis of film thickness of the alcohol based monolayers on silicon oxide surfaces using angle-resolved X-ray photoelectron spectroscopy (ARXPS). In particular, aliphatic alcohol based monolayers with different alkyl chain lengths have been characterized using this technique. In the case of silane based compounds, it is difficult to achieve uniform monolayers with a consistent film thickness due to its tendency to form multilayers and micelles on surfaces. Film thickness characterization with ARXPS has been demonstrated with aliphatic alcohol based monolayers. The implications of this work suggests a correlation of the film thickness to the alkyl chain lengths of the alcohols used as reactants. The film thickness measured from the ARXPS has also been utilized to estimate the average tilt angle of the molecular coating. The tilt angle was found to be ~35°, which was comparable with previous literature studies in thiolate analogues.[66] The primary impact of the results presented in this chapter is the demonstrated ability to form a desirable film thickness with an appropriate choice of aliphatic alcohol with repeatability and consistency in the results of the final monolayers on silicon oxide.

Chapter 6 presents a reaction of alcohol containing compounds on silicon oxide surfaces in polar aprotic solvents. Specifically, the reactions performed in propylene carbonate were studied in detail for its ability to form uniform alcohol-based monolayers on silicon oxide surfaces. The alcohol-based reagents utilized for modifying surfaces of silicon oxides include 1*H*,1*H*,2*H*,2*H*-perfluoro-1-octanol, Zonyl fluorosurfactant, 5-hydroxypentanal, glycolic acid, adenosine 5'-monophosphate, thiamine, choline chloride, and 2-dimethylaminoethanol. The significance of this work includes the formation of alcohol based monolayers at relatively low reaction temperatures (e.g., 100 °C or lower). Such conditions enable the reaction of a variety of alcohol containing compounds with minimal side reactions or thermal degradation. The reaction with 1-octanol and silicon oxide substrates was investigated in detail to determine the impact of reaction temperature, as well as the concentrations of 1-octanol and water on the rate of formation of monolayers. Finally, the reaction with aliphatic alcohols with varying alkyl chain lengths

demonstrated that the alkyl chain lengths can affect the rate of formation of the monolayers.

Overall, the technique demonstrated in this thesis can be utilized to tune surface chemistry of various silicon oxide surfaces. The work presented in this thesis demonstrated a variety of alternative techniques that can be implemented to effectively tune the surface chemistry of silicon oxides through covalent attachment of prevalent laboratory reagents that are relatively non-toxic with a reasonable chemical stability against ambient moisture. The molecular structure and orderliness of the silane or alcohol based precursors and their correlation with wettability can be further studied in comparison to alkanethiol based monolayers on gold surfaces to investigate the quality of these monolayers formed under different processing conditions.[189, 204] Difference in the molecular structure and orderliness can also be further investigated between monolayers formed with linear alcohol molecules in comparison to those formed with non-linear alcohol molecules. Applications of the covalent surface modification techniques can be investigated in future. Specifically, further studies on various applications of charged silicon oxide surfaces for biological surfaces can be pursued in future studies.[13-14, 31, 38, 44, 157] Another aspect of future studies can be further pursued on the applicability of alcohol based monolayers in microscale devices, such as MEMS or molecular electronic devices.[3, 5-6, 226] The surface modification techniques developed in this thesis can also be investigated for their applicability in tuning surface chemistry of micro- and nano-particles for their use in separation science and drug delivery.[1, 25-27, 67, 168] Finally, scalability of the processing, as well as durability of the coating technology can be pursued for widespread applicability to silicon oxide panels towards creation of hydrophobic, self-cleaning surfaces.[2-3, 260-265]

References

(1) Love, J. C.; Estroff, L. A.; Kriebel, J. K.; Nuzzo, R. G.; Whitesides, G. M. Self-Assembled Monolayers of Thiolates on Metals as a Form of Nanotechnology. *Chem. Rev.* **2005,** *105*, 1103-1169.

(2) Pujari, S. P.; Scheres, L.; Marcelis, A. T. M.; Zuilhof, H. Covalent Surface Modification of Oxide Surfaces. *Angew. Chem. Int. Ed.* **2014,** *53*, 6322-6356.

(3) Onclin, S.; Ravoo, B. J.; Reinhoudt, D. N. Engineering Silicon Oxide Surfaces Using Self-Assembled Monolayers. *Angew. Chem. Int. Ed.* **2005,** *44*, 6282-6304.

(4) Haensch, C.; Hoeppener, S.; Schubert, U. S. Chemical Modification of Self-Assembled Silane Based Monolayers by Surface Reactions. *Chem. Soc. Rev.* **2010,** *39*, 2323-2334.

(5) Liao, K.-C.; Bowers, C. M.; Yoon, H. J.; Whitesides, G. M. Fluorination, and Tunneling across Molecular Junctions. *J. Am. Chem. Soc.* **2015,** *137*, 3852-3858.

(6) Doms, M.; Feindt, H.; Kuipers, W. J.; Shewtanasoontorn, D.; Matar, A. S.; Brinkhues, S.; Welton, R. H.; Mueller, J. Hydrophobic Coatings for MEMS Applications. *J. Micromech. Microeng.* **2008,** *18*, 055030.

(7) Gergel-Hackett, N.; Aguilar, I.; Richter, C. A. Engineering the Electron Transport of Silicon-Based Molecular Electronic Devices via Molecular Dipoles. *J. Phys. Chem. C* **2010,** *114*, 21708-21714.

(8) Richter, C. A.; Hacker, C. A.; Richter, L. J.; Kirillov, O. A.; Suehle, J. S.; Vogel, E. M. Interface Characterization of Molecular-Monolayer/SiO_2 Based Molecular Junctions. *Solid-State Electron.* **2006,** *50*, 1088-1096.

(9) Gergel-Hackett, N.; Zangmeister, C. D.; Hacker, C. A.; Richter, L. J.; Richter, C. A. Demonstration of Molecular Assembly on Si (100) for CMOS-Compatible Molecule-Based Electronic Devices. *J. Am. Chem. Soc.* **2008,** *130*, 4239-4261.

(10) Puniredd, S. R.; Jayaraman, S.; Yeong, S. H.; Troadec, C.; Srinivasan, M. P. Stable Organic Monolayers on Oxide-Free Silicon/Germanium in a Supercritical Medium: A New Route to Molecular Electronics. *J. Phys. Chem. Lett.* **2013,** *4*, 1397-1403.

(11) Lamb, B. M.; Park, S.; Yousaf, M. N. Microfluidic Permeation Printing of Self-Assembled Monolayer Gradients on Surfaces for Chemoselective Ligand Immobilization Applied to Cell Adhesion and Polarization. *Langmuir* **2010,** *26*, 12817-12823.

(12) Carvalho, R. R.; Pujari, S. P.; Gahtory, D.; Vrouwe, E. X.; Albada, B.; Zuilhof, H. Mild Photochemical Biofunctionalization of Glass Microchannels. *Langmuir* **2017,** *33*, 8624-8631 DOI: 10.1021/acs.langmuir.6b03931.

(13) Pulsipher, A.; Westcott, N. P.; Luo, W.; Yousaf, M. N. Rapid Microfluidic Generation of Patterned Aldehydes from Hydroxy-Terminated Self-Assembled Monolayers for Ligand and Cell Immobilization on Optically Transparent Indium Tin Oxide Surfaces. *Adv. Mater.* **2009,** *21*, 3082-3086.

(14) Tetala, K. K. R.; Vijayalakshmi, M. A. A Review on Recent Developments for Biomolecule Separation at Analytical Scale Using Microfluidic Devices. *Anal. Chim. Acta* **2016,** *906*, 7-21.

(15) Srivastava, S.; Solanki, P. R.; Kaushik, A.; Md.Ali, A.; Srivastavab, A.; Malhotra, B. D. A Self Assembled Monolayer Based Microfluidic Sensor for Urea Detection. *Nanoscale* **2011,** *3*, 2971-2977.

(16) Perelaer, J.; Hendriks, C. E.; deLaat, A. W. M.; Schubert, U. S. One-Step Inkjet Printing of Conductive Silver Tracks on Polymer Substrates. *Nanotechnology* **2009,** *20*, 165303.

(17) Son, Y.; Kim, C.; Yang, D. H.; Ahn, D. J. Spreading of an Inkjet Droplet on a Solid Surface with a Controlled Contact Angle at Low Weber and Reynolds Numbers. *Langmuir* **2008,** *24*, 2900-2907.

(18) Tang, W.; Feng, L.; Jiang, C.; Yao, G.; Zhao, J.; Cui, Q.; Guo, X. Controlling the Surface Wettability of the Polymer Dielectric for Improved Resolution of Inkjet-Printed Electrodes and Patterned Channel Regions in Low-Voltage Solution-Processed Organic Thin Film Transistors. *J. Mater. Chem. C* **2014,** *2*, 5553-5558.

(19) Chen, M.; Peng, R.; Xiong, X.; Chen, S.; Zhang, G.; Lu, H.; Wang, X.; Qiu, L. Inkjet Printed Poly(3-hexylthiophene) Thin-Film Transistors: Effect of Self-Assembled Monolayer. *Mol. Cryst. Liq. Cryst.* **2014,** *593*, 201-213.

(20) Nguyen, P. Q. M.; Yeo, L.-P.; Lok, B.-K.; Lam, Y.-C. Patterned Surface with Controllable Wettability for Inkjet Printing of Flexible Printed Electronics. *ACS Appl. Mater. Interfaces* **2014,** *6*, 4011-4016.

(21) Geissler, M.; Schmid, H.; Bietsch, A.; Michel, B.; Delamarche, E. Defect-Tolerant and Directional Wet-Etch Systems for Using Monolayers as Resists. *Langmuir* **2002,** *18*, 2374-2377.

(22) Preiner, M. J.; Melosh, N. A. Identification and Passivation of Defects in Self-Assembled Monolayers. *Langmuir* **2009,** *25*, 2585-2587.

(23) Geissler, M.; Schmid, H.; Michel, B.; Delamarche, E. Selective Wet-Etching of Microcontact-Printed Cu Substrates with Control over the Etch Profile. *Microelectron. Eng.* **2003,** *67-68*, 326-332.

(24) Li, D.; Chen, S.; Zhao, S.; Ma, H. The Corrosion Inhibition of the Self-Assembled Au, and Ag Nanoparticles Films on the Surface of Copper. *Colloids Surf., A* **2006,** *273*, 16-23.

(25) Zhao, X.-M.; Wilbur, J. L.; Whitesides, G. M. Using Two-Stage Chemical Amplification To Determine the Density of Defects in Self-Assembled Monolayers of Alkanethiolates on Gold. *Langmuir* **1996,** *12*, 3257-3264.

(26) Wirth, M. J.; Fairbank, R. W. P.; Fatunmbi, H. O. Mixed Self-Assembled Monolayers in Chemical Separations. *Science* **1997,** *275*, 44-47.

(27) Ke, X.; Huang, Y.; Dargaville, T. R.; Fan, Y.; Cui, Z.; Zhu, H. Modified Alumina Nanofiber Membranes for Protein Separation. *Sep. Purif. Technol.* **2013,** *120*, 239-244.

(28) Azzouz, I.; Vial, J.; Thiébaut, D.; Haudebourg, R.; Danaie, K.; Sassiat, P.; Breviere, J. Review of Stationary Phases for Microelectromechanical Systems in Gas Chromatography: Feasibility and Separations. *Anal. Bioanal. Chem.* **2014,** *406*, 981-994.

(29) Shakeel, H.; Rice, G. W.; Agah, M. Semipacked Columns with Atomic Layer-Deposited Alumina as a Stationary Phase. *Sens. Actuators, B* **2014,** *203*, 641-646.

(30) Radhakrishnan, R.; Pali, M.; Lee, H. J.; Lee, T. R.; Suni, I. I. Impedance Biosensor Incorporating a Carboxylate-Terminated Bidentate Thiol for Antibody Immobilization. *Journal of Electrochemical Society* **2016,** *163*, B125-B130.

(31) Mandler, D.; Kraus-Ophir, S. Self-Assembled Monolayers (SAMs) for Electrochemical Sensing. *J. Solid State Electrochem.* **2011,** *15*, 1535-1558.

(32) Gooding, J. J.; Mearns, F.; Yang, W.; Liu, J. Self-Assembled Monolayers into the 21st Century: Recent Advances and Applications. *Electroanal.* **2003,** *15*, 81-96.

(33) Perrotta, P. R.; Vettorazzi, N. R.; Arevalo, F. J.; Granero, A. M.; Chulze, S. N.; Zon, M. A.; Fernandez, H. Electrochemical Studies of Ochratoxin A Mycotoxin at Gold Electrodes Modified with Cysteamine Self-Assembled Monolayers Its Ultrasensitive Quantification in Red Wine Samples. *Electroanal.* **2011,** *23*, 1585-1592.

(34) Porter, R.; vanderLogt, P.; Howell, S.; Kyrolainen-Reay, M.; Badley, A. An Electro-Active System of Immuno-assay (EASI assay) utilising Self Assembled Monolayer Modified Electrodes. *Biosens. Bioelectron.* **2001,** *16*, 875-885.

(35) Eckermann, A. L.; Feld, D. J.; Shaw, J. A.; Meade, T. J. Electrochemistry of Redox-Active Self-Assembled Monolayers. *Coord. Chem. Rev.* **2010,** *254*, 1769-1802.

(36) Nicholson, R. L.; Ladlow, M. L.; Spring, D. R. Fluorous Tagged Small Molecule Microarrays. *Chem. Commun.* **2007**, 3906-3908.

(37) Ulman, A. Formation and Structure of Self-Assembled Monolayers. *Chem. Rev.* **1996,** *96*, 1533-1554.

(38) Holmlin, R. E.; Chen, X.; Chapman, R. G.; Takayama, S.; Whitesides, G. M. Zwitterionic SAMs that Resist Nonspecific Adsorption of Protein from Aqueous Buffer. *Langmuir* **2001,** *17*, 2841-2850.

(39) Huang, C.-J.; Chu, S.-H.; Wang, L.-C.; Li, C.-H.; Lee, T. R. Bioinspired Zwitterionic Surface Coatings with Robust Photostability and Fouling Resistance. *ACS Appl. Mater. Interfaces* **2015,** *7*, 23776-23786.

(40) Chatzipetrou, M.; Massaouti, M.; Tsekenis, G.; Trilling, A. K.; vanAndel, E.; Scheres, L.; Smulders, M. M. J.; Zuilhof, H.; Zergioti, I. Direct Creation of Biopatterns via a Combination of Laser-Based Techniques and Click Chemistry. *Langmuir* **2017,** *33*, 848-853.

(41) Lin, P.; Ding, L.; Lin, C.-W.; Gu, F. Nonfouling Property of Zwitterionic Cysteine Surface. *Langmuir* **2014,** *30*, 6497-6507.

(42) Banerjee, I.; Pangule, R. C.; Kane, R. S. Antifouling Coatings: Recent Developments in the Design of Surfaces That Prevent Fouling by Proteins, Bacteria, and Marine Organisms. *Adv. Mater.* **2011,** *23*, 690-718.

(43) Reverté, L.; Iglesia, P. d. l.; Río, V. d.; Campbell, K.; Elliott, C. T.; Kawatsu, K.; Katikou, P.; Diogène, J.; Campàs, M. n. Detection of Tetrodotoxins in Puffer Fish by a Self-Assembled Monolayer-Based Immunoassay and Comparison with Surface Plasmon Resonance, LC-MS/MS, and Mouse Bioassay. *Anal. Chem.* **2015,** *87*, 10839-10847.

(44) Wei, Q.; Becherer, T.; Angioletti-Uberti, S.; Dzubiella, J.; Wischke, C.; Neffe, A. T.; Lendlein, A.; Ballauff, M.; Haag, R. Protein Interactions with Polymer Coatings and Biomaterials. *Angew. Chem. Int. Ed.* **2014,** *53*, 8004-8031.

(45) Vutukuru, S.; Kane, R. S. Surface Plasmon Resonance Spectroscopy-Based High-Throughput Screening of Ligands for Use in Affinity and Displacement Chromatography. *Langmuir* **2008,** *24*, 11784-11789.

(46) Wang, Y.; Lieberman, M. Growth of Ultrasmooth Octadecyltrichlorosilane Self-Assembled Monolayers on SiO_2. *Langmuir* **2003,** *19*, 1159-1167.

(47) Bain, C. D.; Evall, J.; Whitesides, G. M. Formation of Monolayers by the Coadsorption of Thiols on gold: Variation in the Head Group, Tail Group, and Solvent. *J. Am. Chem. Soc.* **1989,** *111*, 7155-7164.

(48) Bain, C. D.; Troughton, E. B.; Tao, Y.-T.; Evall, J.; Whitesides, G. M.; Nuzzo, R. G. Formation of Monolayer Films by the Spontaneous Assembly of Organic Thiols from Solution onto Gold. *J. Am. Chem. Soc.* **1989,** *111*, 321-335.

(49) Ulman, A.; Eilers, J. E.; Tillman, N. Packing and Molecular Orientation of Alkanethiol Monolayers on Gold Surfaces. *Langmuir* **1989,** *5*, 1147-1152.

(50) Brzoska, J. B.; Azouz, I. B.; Rondelez, F. Silanization of Solid Substrates: A Step toward Reproducibility. *Langmuir* **1994,** *10*, 4367-4373.

(51) Desbief, S.; Patrone, L.; Goguenheim, D.; rind, D. G.; Vuillaume, D. Impact of Chain Length, Temperature, and Humidity on the Growth of Long Alkyltrichlorosilane Self-Assembled Monolayers. *PCCP* **2011,** *13*, 2870-2879.

(52) Vega, A.; Thissen, P.; Chabal, Y. J. Environment-Controlled Tethering by Aggregation and Growth of Phosphonic Acid Monolayers on Silicon Oxide. *Langmuir* **2012,** *28*, 8046-8051.

(53) Bain, C. D.; Whitesides, G. M. Formation of Monolayers by the Coadsorption of Thiols on gold: Variation in the Length of the Alkyl Chain. *J. Am. Chem. Soc.* **1989,** *111*, 7164-7175.

(54) Parker, J. E.; Clarke, S. M.; Perdigon, A. C. Preferential Adsorption of Solid Monolayers of Hydrocarbons over Fluorocarbons at the Solid/liquid Interface. *Surf. Sci.* **2007,** *601*, 4149-4153.

(55) Wang, M.; Liechti, K. M.; Wang, Q.; White, J. M. Self-Assembled Silane Monolayers: Fabrication with Nanoscale Uniformity. *Langmuir* **2005,** *21*, 1848-1857.

(56) Nuzzo, R. G.; Allara, D. L. Adsorption of Bifunctional Organic Disulfides on Gold Surfaces. *J. Am. Chem. Soc.* **1983,** *105*, 4481-4483.

(57) Nie, H. Y.; Walzak, M. J.; McIntyre, N. S. Bilayer and Odd-Numbered Multilayers of Octadecylphosphonic Acid Formed on a Si Substrate Studied by Atomic Force Microscopy. *Langmuir* **2002,** *18*, 2955-2958.

(58) Dubey, M.; Weidner, T.; Gamble, L. J.; Castner, D. G. Structure and Order of Phosphonic Acid-Based Self-Assembled Monolayers on Si(100). *Langmuir* **2010,** *26* (18), 14747-14754.

(59) Paul, J.; Meltzer, C.; Braunschweig, B.; Peukert, W. Lubrication of Individual Microcontacts by a Self-Assembled Alkyl Phosphonic Acid Monolayer on α-Al_2O_3(0001). *Langmuir* **2016,** *32*, 8298-8306.

(60) Sagiv, J. Organized Monolayers by Adsorption, I . Formation and Structure of Oleophobic Mixed Monolayers on Solid Surfaces. *J. Am. Chem. Soc.* **1980,** *102* (1), 92-98.

(61) Ballard, C. C.; Broge, E. C.; Iler, R. K.; John, D. S.; McWhorter, J. R. Esterification of the Surface of Amorphous Silica. *J. Phys. Chem.* **1961,** *65*, 20-25.

(62) Sprung, M. M.; Guenther, F. O. The Reaction of Some Silanols and Siloxanes with n-Octyl Alcohol. *J. Org. Chem.* **1961,** *26*, 552-557.

(63) Kim, N. Y.; Laibinis, P. E. Thermal Derivatization of Porous Silicon with Alcohols. *J. Am. Chem. Soc.* **1997,** *119*, 2297-2298.

(64) Boukherroub, R.; Morin, S.; Sharpe, P.; Wayner, D. D. M. Insights into the Formation Mechanisms of Si-OR Monolayers from the Thermal Reactions of Alcohols and Aldehydes with Si(111)-H. *Langmuir* **2000,** *16*, 7429-7434.

(65) Dion, M.; Rapp, M.; Rorrer, N.; Shin, D. H.; Martin, S. M.; Ducker, W. A. The Formation of Hydrophobic Films on Silica with Alcohols. *Colloids Surf., A* **2010,** *362*, 65-70.

(66) Laibinis, P. E.; Whitesides, G. M.; Allara, D. L.; Tao, Y. T.; Parikh, A. N.; Nuzzo, R. G. Comparison of the Structures and Wetting Properties of Self-Assembled Monolayers of n-Alkanethiols on the Coinage Metal Surfaces, Copper, Silver, and Gold. *J. Am. Chem. Soc.* **1991,** *113*, 7152-7167.

(67) Sarathy, K. V.; Raina, G.; Yadav, R. T.; Kulkarni, G. U.; Rao, C. N. R. Thiol-Derivatized Nanocrystalline Arrays of Gold, Silver, and Platinum. *J. Phys. Chem. B* **1997,** *101*, 9876-9880.

(68) Laiho, T.; Lukkari, J.; Meretoja, M.; Laajalehto, K.; Kankare, J.; Leiro, J. A. Chemisorption of Alkyl Thiols and S-Alkyl Thiosulfates on Pt(1 1 1) and Polycrystalline Platinum Surfaces. *Surf. Sci.* **2005,** *584*, 83-89.

(69) Petrovykh, D. Y.; Kimura-Suda, H.; Opdahl, A.; Richter, L. J.; Tarlov, M. J.; Whitman, L. J. Alkanethiols on Platinum: Multicomponent Self-Assembled Monolayers. *Langmuir* **2006,** *22*, 2578-2587.

(70) Vericat, C.; Vela, M. E.; Benitez, G.; Carro, P.; Salvarezza, R. C. Self-Assembled Monolayers of Thiols and Dithiols on Gold: New Challenges for a Well-Known System. *Chem. Soc. Rev.* **2010,** *39*, 1805-1834.

(71) Chandekar, A.; Sengupta, S. K.; Whitten, J. E. Thermal Stability of Thiol and Silane Monolayers: A Comparative Study. *Appl. Surf. Sci.* **2010,** *256*, 2742-2749.

(72) Bhairamadgi, N. S.; Pujari, S. P.; Trovela, F. G.; Debrassi, A.; Khamis, A. A.; Alonso, J. M.; AlZahrani, A. A.; Wennekes, T.; Al-Turaif, H. A.; vanRijn, C.; Alhamed, Y. A.; Zuilhof, H. Hydrolytic and Thermal Stability of Organic Monolayers on Various Inorganic Substrates. *Langmuir* **2014,** *30* (20), 5829-5839.

(73) Hu, M.; Noda, S.; Okubo, T.; Yamaguchi, Y.; Komiyama, H. Structure and Morphology of Self-Assembled 3-Mercaptopropyltrimethoxysilane Layers on Silicon Oxide. *Appl. Surf. Sci.* **2001,** *181*, 307-316.

(74) Queffélec, C. m.; Petit, M.; Janvier, P.; Knight, D. A.; Bujoli, B. Surface Modification Using Phosphonic Acids and Esters. *Chem. Rev.* **2012,** *112*, 3777-3087.

(75) Thissen, P.; Valtiner, M.; Grundmeier, G. Stability of Phosphonic Acid Self-Assembled Monolayers on Amorphous and Single-Crystalline Aluminum Oxide Surfaces in Aqueous Solution. *Langmuir* **2010,** *26*, 156-164.

(76) RiesJr, H. E.; Cook, H. D. Monomolecular Films of Mixtures: I. Stearic Acid with Isostearic Acid and with tri-p-cresyl Phosphate. Comparison of Components with Octadecylphosphonic acid and with tri-o-xenyl Phosphate. *Journal of Colloid Science* **1954,** *9*, 535-546.

(77) Hoque, E.; DeRose, J. A.; Hoffmann, P.; Bhushan, B.; Mathieu, H. J. Alkylperfluorosilane Self-Assembled Monolayers on Aluminum: A Comparison with Alkylphosphonate Self-Assembled Monolayers. *J. Phys. Chem. C* **2007,** *111*, 3956-3962.

(78) Hanson, E. L.; Schwartz, J.; Nickel, B.; Koch, N.; Danisman, M. F. Bonding Self-Assembled, Compact Organophosphonate Monolayers to the Native Oxide Surface of Silicon. *J. Am. Chem. Soc.* **2003,** *125*, 16074-16080.

(79) Gouzman, I.; Dubey, M.; Carolus, M. D.; Schwartz, J.; Bernasek, S. L. Monolayer vs. Multilayer Self-Assembled Alkylphosphonate Films: X-ray Photoelectron Spectroscopy Studies. *Surf. Sci.* **2006,** *600*, 773-781.

(80) Campos, R.; Guenthner, A. J.; Haddad, T. S.; Mabry, J. M. Fluoroalkyl-Functionalized Silica Particles: Synthesis, Characterization, and Wetting Characteristics. *Langmuir* **2011,** *27*, 10206-10215.

(81) Hacker, C. A.; Anderson, K. A.; Richter, L. J.; Richter, C. A. Comparison of Si-O-C Interfacial Bonding of Alcohols and Aldehydes on Si(111) Formed from Dilute Solution with Ultraviolet Irradiation. *Langmuir* **2005,** *21*, 882-889.

(82) Chandrasekaran, S.; Ramanathan, S.; Basak, T. Microwave Food Processing—A Review. *Food Res. Int.* **2013,** *52*, 243-261.

(83) Lidstrom, P.; Tierney, J.; Wathey, B.; Westman, J. Microwave Assisted Organic Synthesis - a Review. *Tetrahedron* **2001,** *57*, 9225-9283.

(84) Kappe, C. O. Microwave Dielectric Heating in Synthetic Organic Chemistry. *Chem. Soc. Rev.* **2008,** *37*, 1127-1139.

(85) Caddick, S.; Fitzmaurice, R. Microwave Enhanced Synthesis. *Tetrahedron* **2009,** *65*, 3325-3355.

(86) Gawande, M. B.; Shelke, S. N.; Zboril, R.; Varma, R. S. Microwave-Assisted Chemistry: Synthetic Applications for Rapid Assembly of Nanomaterials and Organics. *Acc. Chem. Res.* **2014,** *47*, 1338-1348.

(87) Kappe, C. O.; Dallinger, D. Controlled Microwave Heating in Modern Organic Synthesis: Highlights from the 2004-2008 Literature. *Molecular Diversity* **2009,** *3*, 71-193.

(88) Stuerga, D.; Gaillard, P. Microwave Heating as a New Way to Induce Localized Enhancements of Reaction Rate Non-Isothermal and Heterogeneous Kinetics. *Tetrahedron* **1996,** *52* (15), 5505-5510.

(89) Warren, B.; Awida, M. H.; Fathy, A. E. Microwave Heating of Metals. *IET Microw. Antennas Propag.* **2012,** *6*, 196-205.

(90) Rybakov, K. I.; Olevsky, E. A.; Krikun, E. V. Microwave Sintering: Fundamentals and Modeling. *Journal of American Chemical society* **2013,** *96*, 1003-1020.

(91) Mishra, R. R.; Sharma, A. K. A Review of Research Trends in Microwave Processing of Metal-Based Materials and Opportunities in Microwave Metal Casting. *Crit. Rev. Solid State Mater. Sci.* **2016,** *41*, 217-255.

(92) Eugene, W. W. L.; Gupta, M. Characteristics of Aluminum and Magnesium Based Nanocomposites Processed Using Hybrid Microwave Sintering. *Journal of Microwave Power and Electromagnetic Energy* **2010,** *44*, 14-27.

(93) Chandrasekaran, S.; Basak, T.; Ramanathan, S. Experimental and Theoretical Investigation on Microwave Melting of Metals. *J. Mater. Process. Technol.* **2011,** *211*, 482-487.

(94) Mishra, R. R.; Sharma, A. K. Microwave–Material Interaction Phenomena: Heating Mechanisms, Challenges and Opportunities in Material Processing. *Composites: Part A* **2016,** *81*, 78-97.

(95) Tun, K. S.; Jayaramanavar, P.; Nguyen, Q. B.; Chan, J.; Kwok, R.; Gupta, M. Investigation into Tensile and Compressive Responses of Mg–ZnO Composites. *Mater. Sci. Technol.* **2012,** *28*, 582-588.

(96) Peng, Z.; Hwang, J.-Y. Microwave-Assisted Metallurgy. *Int. Mater. Rev.* **2015,** *60*, 30-63.

(97) Schwenke, A. M.; Hoeppener, S.; Schubert, U. S. Synthesis and Modification of Carbon Nanomaterials Utilizing Microwave Heating. *Adv. Mater.* **2015,** *27*, 4113-4141.

(98) Baghbanzadeh, M.; Carbone, L.; Cozzoli, D. P. D.; Kappe, C. O. Microwave-Assisted Synthesis of Colloidal Inorganic Nanocrystals. *Angew. Chem. Int. Ed.* **2011,** *50*, 11312-11359.

(99) Zhu, Y.-J.; Chen, F. Microwave-Assisted Preparation of Inorganic Nanostructures in Liquid Phase. *Chem. Rev.* **2014,** *114* (12), 6462-6555.

(100) Yin, X.; Xue, Y.; Zhang, L.; Cheng, L. Dielectric, Electromagnetic Absorption and Interference Shielding Properties of Porous Yttria-Stabilized Zirconia/Silicon Carbide Composites. *Ceram. Int.* **2012,** *38*, 2421-2427.

(101) Liu, X.; Cao, H.; Yin, J. Generation and Photocatalytic Activities of $Bi@Bi_2O_3$ Microspheres. *Nano Res.* **2011,** *4*, 470-482.

(102) Whittaker, A. G.; Mingos, D. M. P. Microwave-Assisted Solid-State Reactions Involving Metal Powders. *J. Chem. Soc. Dalton Trans.* **1995**, 2073-2079.

(103) Sun, J.; Wang, W.; Yue, Q.; Ma, C.; Zhang, J.; Zhao, X.; Song, Z. Review on Microwave–Metal Discharges and their Applications in Energy and Industrial Processes. *Appl. Energy* **2016,** *175*, 141-157.

(104) Singh, S.; Gupta, D.; Jain, V. Novel Microwave Composite Casting Process: Theory, Feasibility and Characterization. *Mater. Des.* **2016,** *111*, 51-59.

(105) Luo, J.; Hunyar, C.; Feher, L.; Link, G.; Thumm, M.; Pozzo, P. Potential Advantages for Millimeter-Wave Heating of Powdered Metals. *Int. J. Infrared Milli.* **2004,** *25*, 1271-1283.

(106) Ignatenko, M.; Tanaka, M.; Sato, M. Absorption of Microwave Energy by a Spherical Nonmagnetic Metal Particle. *Jpn. J. Appl. Phys.* **2009,** *48*, 067001.

(107) Galema, S. A. Microwave Chemistry. *Chem. Soc. Rev.* **1997,** *26*, 233-238.

(108) Gabriel, C.; Gabriel, S.; Grant, E. H.; Halstead, B. S. J.; Mingos, D. M. P. Dielectric Parameters Relevant to Microwave Dielectric Heating. *Chem. Soc. Rev.* **1998,** *27*, 213-223.

(109) Gupta, M.; Leong, E. W. W. *Microwaves and Metals*; Wiley 2007.

(110) A. C. Metaxas; Meredith, R. J. *Industrial Microwave Heating*; Peter Peregrinus Ltd.: London, United Kingdom, 1983.

(111) Farag, S.; Sobhy, A.; Akyel, C.; Doucet, J.; Chaouki, J. Temperature Profile Prediction within Selected Materials Heated by Microwaves at 2.45GHz. *Appl. Therm. Eng.* **2012,** *36*, 360-369.

(112) Durka, T.; Gerven, T. V.; Stankiewicz, A. Microwaves in Heterogeneous Gas-Phase Catalysis: Experimental and Numerical Approaches. *Chem. Eng. Technol.* **2009,** *32*, 1301-1312.

(113) Reeja-Jayan, B.; Harrison, K. L.; Yang, K.; Wang, C.-L.; Yilmaz, A. E.; Manthiram, A. Microwave-Assisted Low-Temperature Growth of Thin Films in Solution. *Sci. Rep.* **2012,** *2*, 1003.

(114) Yuan, Y.; Lee, T. R. Contact Angle and Wetting Properties. In *Surface Science Techniques*, Bracco, G.; Holst, B., Eds.; Springer: Berlin, 2013; Vol. 51, pp 3-34.

(115) Choi, J.; Kato, T. Self-Assembled Monolayers as Lubricants for Magnetic Disk Drives. *IEEE Trans. Magn.* **2005,** *41*, 599-603.

(116) Zhao, X.; Blunt, M. J.; Yao, J. Pore-Scale Modeling: Effects of Wettability on Waterflood Oil Recovery. *J. Pet. Sci. Eng.* **2010,** *71*, 169-178.

(117) Xue, Z.; Cao, Y.; Liu, N.; Feng, L.; Jiang, L. Special Wettable Materials for Oil/Water Separation. *J. Mater. Chem. A* **2014,** *2*, 2445-2460.

(118) Kota, A. K.; Kwon, G.; Choi, W.; Mabry, J. M.; Tuteja, A. Hygro-Responsive Membranes for Effective Oil–Water Separation. *Nat. Commun.* **2012,** *3*, 1025.

(119) Kwok, D. Y.; Lin, R.; Mui, M.; Neumann, A. W. Low-Rate Dynamic and Static Contact Angles and the Determination of Solid Surface Tensions. *Colloids Surf., A* **1996,** *116*, 63-77.

(120) Colorado, R.; Lee, T. R. Wettabilities of Self-Assembled Monolayers on Gold Generated from Progressively Fluorinated Alkanethiols. *Langmuir* **2003,** *19*, 3288-3296.

(121) Colorado, R.; Lee, T. R. Physical Organic Probes of Interfacial Wettability Reveal the Importance of Surface Dipole Effects. *J. Phys. Org. Chem.* **2000,** *13*, 796-807.

(122) Johnson, R. E.; Dettre, R. H. Contact Angle Hysteresis. III. Study of an Idealized Heterogeneous Surface. *J. Phys. Chem.* **1964,** *68*, 1744-1750.

(123) Joanny, J. F.; deGennes, P. G. A Model for Contact Angle Hysteresis. *J. Chem. Phys.* **1984,** *81*, 552-562.

(124) Schwartz, L. W.; Garoff, S. Contact Angle Hysteresis on Heterogeneous Surfaces. *Langmuir* **1985,** *1*, 219-230.

(125) Petrovykh, D. Y.; Kimura-Suda, H.; Whitman, L. J.; Tarlov, M. J. Quantitative Analysis and Characterization of DNA Immobilized on Gold. *J. Am. Chem. Soc.* **2003,** *125*, 5219-5226.

(126) Cerofolini, G. F.; Galati, C.; Reina, S.; Renna, L. Quantitative XPS Analysis of Hydrosilated 1-alkene and 1-alkyne at Terraced, Dihydrogen-Terminated, 1×1 (100) Silicon. *Surf. Interface Anal.* **2006,** *38*, 126-138.

(127) Colorado, R.; Lee, T. R. Attenuation Lengths of Photoelectrons in Fluorocarbon Films. *J. Phys. Chem. B* **2003,** *107*, 10216-10220.

(128) Rittikulsittichai, S.; Jamison, A. C.; Lee, T. R. Self-Assembled Monolayers Derived from Alkoxyphenylethanethiols Having One, Two, and Three Pendant Chains. *Langmuir* **2011,** *27*, 9920-9927.

(129) Lee, H. J.; Jamison, A. C.; Lee, T. R. Two Are Better than One: Bidentate Adsorbates Offer Precise Control of Interfacial Composition and Properties. *Chem. Mater.* **2016,** *28*, 5356-5364.

(130) vanderHeide, P. *X-ray Photoelectron Spectroscopy: An introduction to Principles and Practices*; Wiley: Hoboken, NJ, 2011.

(131) Fradley, C. S. Angle-resolved X-ray photoelectron spectroscopy. *Prog. Surf. Sci.* **1984,** *16* (3), 275-388.

(132) Wei, Q.; Tajima, K.; Tong, Y.; Ye, S.; Hashimoto, K. Surface-Segregated Monolayers: A New Type of Ordered Monolayer for Surface Modification of Organic Semiconductors. *J. Am. Chem. Soc.* **2009,** *131* (48), 17597-17604.

(133) Cumpson, P. J. The Thickogram: a Method for Easy Film Thickness Measurement in XPS. *Surf. Interface Anal.* **2000,** *29*, 403-406.

(134) Eaton, P.; West, P. *Atomic Force Microscopy*; Oxford University Press2010.

(135) Jalili, N.; Laxminarayana, K. A Review of Atomic Force Microscopy Imaging Systems: Application to Molecular Metrology and Biological Sciences. *Mechatronics* **2004,** *14* (8), 907-945.

(136) Burnham, N. A.; Chen, X.; Hodges, C. S.; Matei, G. A.; Thoreson, E. J.; Roberts, C. J.; Davies, M. C.; Tendler, S. J. B. Comparison of Calibration Methods for Atomic-Force Microscopy Cantilevers. *Nanotechnology* **2003,** *14*, 1-6.

(137) Carpick, R. W.; Salmeron, M. Scratching the Surface: Fundamental Investigations of Tribology with Atomic Force Microscopy. *Chem. Rev.* **1997,** *97* (4), 1163-1194.

(138) Giessibl, F. J. Advances in Atomic Force Microscopy. *Rev. Mod. Phys.* **2003,** *75*, 949-983.

(139) Sugimoto, Y.; Pou, P.; Abe, M.; Jelinek, P.; Pérez, R.; Morita, S.; Custance, Ó. Chemical Identification of Individual Surface Atoms by Atomic Force Microscopy. *Nature* **2007,** *446*, 64-67.

(140) Whited, A. M.; Park, P. S.-H. Atomic Force Microscopy: A Multifaceted Tool to Study Membrane Proteins and Their Interactions with Ligands. *Biochim. Biophys. Acta* **2014,** *1838* (1), 56-68.

(141) Morita, S.; Wiesendanger, R.; Meyer, E. *Noncontact Atomic Force Microscopy*; Springer2002.

(142) Schwartz, D. K. Mechanisms and Kinetics of Self-Assembled Monolayer Formation. *Annu. Rev. Phys. Chem.* **2001,** *52*, 107-137.

(143) Aswal, D. K.; Lenfant, S.; Guerin, D.; Yakhmi, J. V.; Vuillaume, D. Self Assembled Monolayers on Silicon for Molecular Electronics. *Anal. Chim. Acta* **2006,** *568*, 84-108.

(144) Manifar, T.; Rezaee, A.; Sheikhzadeh, M.; Mittler, S. Formation of Uniform Self-Assembly Monolayers by Choosing the Right Solvent: OTS on Silicon Wafer, a Case Study. *Appl. Surf. Sci.* **2008,** *254*, 4611-4619.

(145) McGovern, M. E.; Kallury, K. M. R.; Thompson, M. Role of Solvent on the Silanization of Glass with Octadecyltrichlorosilane. *Langmuir* **1994,** *10*, 3607-3614.

(146) Devaprakasam, D.; Sampath, S.; Biswas, S. K. Thermal Stability of Perfluoroalkyl Silane Self-Assembled on a Polycrystalline Aluminum Surface. *Langmuir* **2004,** *20* (4), 1329-1334.

(147) Hoque, E.; DeRose, J. A.; Houriet, R.; Hoffmann, P.; Mathieu, H. J. Stable Perfluorosilane Self-Assembled Monolayers on Copper Oxide Surfaces: Evidence of Siloxy-Copper Bond Formation. *Chem. Mater.* **2007,** *19*, 798-804.

(148) Goldmann, M.; Davidovits, J. V.; Silberzan, P. Kinetics of self-assembled silane monolayers at various temperatures: evidence of 2D foam. *Thin Solid Films* **1998,** *327-329*, 166-171.

(149) Sung, I.-H.; Yang, J.-C.; Kim, D.-E.; Shin, B.-S. Micro/nano-Tribological Characteristics of Self-Assembled Monolayer and Its Application in Nano-Structure Fabrication. *Wear* **2003,** *255* (7), 808-818.

(150) Bush, B. G.; DelRio, F. W.; Opatkiewicz, J.; Maboudian, R.; Carraro, C. Effect of Formation Temperature and Roughness on Surface Potential of Octadecyltrichlorosilane Self-Assembled Monolayer on Silicon Surfaces. *J. Phys. Chem. A* **2007,** *111*, 12339-12343.

(151) Srinivasan, U.; Houston, M. R.; Howe, R. T.; Maboudian, R. Alkyltrichlorosilane-based self-assembled monolayer films for stiction reduction in silicon micromachines. *Journal of Microelectromechanical Systems* **1998,** *7* (2), 252-260.

(152) Maboudian, R.; Ashurst, W. R.; Carraro, C. Self-Assembled Monolayers as Anti-Stiction Coatings for MEMS: Characteristics and Recent Developments. *Sens. Actuators, A* **2000,** *82*, 219-223.

(153) Gong, Y.; Wang, M. C. P.; Zhang, X.; Ng, H. W.; Gates, B. D. Optimizing the Quality of Monoreactive Perfluoroalkylsilane-Based Self-Assembled Monolayers. *Langmuir* **2012,** *28*, 11790-11801.

(154) Jalali, H.; Gates, B. D. Monitoring and Mapping Imperfections in Silane-Based Self-Assembled Monolayers by Chemical Amplification. *Langmuir* **2009,** *25* (16), 9078-9084.

(155) Kumar, N.; Maldarelli, C.; Steiner, C.; Couzis, A. Formation of Nanometer Domains of One Chemical Functionality in a Continuous Matrix of a Second Chemical Functionality by Sequential Adsorption of Silane Self-Assembled Monolayers. *Langmuir* **2001,** *17*, 7789-7797.

(156) Kappe, C. O. Controlled Microwave Heating in Modern Organic Synthesis. *Angew. Chem. Int. Ed.* **2004,** *43*, 6250-6284.

(157) Lee, J. H.; Hyun, H.; Cross, C. J.; Henary, M.; Nasr, K. A.; Oketokoun, R.; Choi, H. S.; Frangioni, J. V. Rapid and Facile Microwave-Assisted Surface Chemistry for Functionalized Microarray Slides. *Adv. Funct. Mater.* **2012,** *22*, 872-878.

(158) vandenBerg, S. A.; Alonso, J. M.; Wadhwa, K.; Franssen, M. C. R.; Wennekes, T.; Zuilhof, H. Microwave-Assisted Formation of Organic Monolayers from 1-Alkenes on Silicon Carbide. *Langmuir* **2014,** *30*, 10562-10565.

(159) Grell, T. A. J.; Alabanza, A. M.; Gaskell, K.; Aslan, K. Microwave-Accelerated Surface Modification of Plasmonic Gold Thin Films with Self-Assembled Monolayers of Alkanethiols. *Langmuir* **2013,** *29*, 13209-13216.

(160) Lovingood, D. D.; Salter, W. B.; Griffith, K. R.; Simpson, K. M.; Hearn, J. D.; Owens, J. R. Fabrication of Liquid and Vapor Protective Cotton Fabrics. *Langmuir* **2013,** *29*, 15043-15050.

(161) deGennes, P. G. Wetting: Statics and Dynamics. *Rev. Mod. Phys.* **1985,** *57*, 827-863.

(162) Sugimur, H.; Ushiyam, K.; Hozumi, A.; Takai, O. Lateral Force on Fluoroalkylsilane Self-Assembled Monolayers Dependent on Molecular Ordering. *J. Vac. Sci. Technol., B* **2002,** *20* (1), 393-395.

(163) Paso, K.; M.L., R.; Helberg; Raaen, S.; Sjöblom, J. Hydrophobic Monolayer Preparation by Langmuir-Blodgett and Chemical Adsorption Techniques. *J. Colloid Interface Sci.* **2008,** *325*, 228-235.

(164) Coll, M.; Miller, L. H.; Richter, L. J.; Hines, D. R.; Jurchescu, O. D.; Gergel-Hackett, N.; Richter, C. A.; Hacker, C. A. Formation of Silicon-Based Molecular Electronic Structures Using Flip-Chip Lamination. *J. Am. Chem. Soc.* **2009,** *131*, 12451-12457.

(165) Besson, E.; Gue, A.-M.; Sudor, J.; Korri-Youssoufi, H.; Jaffrezic, N.; Tardy, J. A Novel and Simplified Procedure for Patterning Hydrophobic and Hydrophilic SAMs for Microfluidic Devices by Using UV Photolithography. *Langmuir* **2006,** *22*, 8346-8352.

(166) Carlos, L. D.; Ferreira, R. A. S.; Bermudez, V. Z.; Ribeiro, S. J. L. Lanthanide-Containing Light-Emitting Organic–Inorganic Hybrids: A Bet on the Future. *Adv. Mater.* **2009,** *21*, 509-534.

(167) Zamboulis, A.; Moitra, N.; Moreau, J. J. E.; Cattoen, X.; Man, M. W. C. Hybrid Materials: Versatile Matrices for Supporting Homogeneous Catalysts. *J. Mater. Chem.* **2010,** *20*, 9322-9338.

(168) Coti, K. K.; Belowich, M. E.; Liong, M.; Ambrogio, M. W.; Lau, Y. A.; Khatib, H. A.; Zink, J. I.; Khashab, N. M.; Stoddart, J. F. Mechanised Nanoparticles for Drug Delivery. *Nanoscale* **2009,** *1*, 16-39.

(169) Hong, Q.; Rogero, C.; Lakey, J. H.; Connolly, B. A.; Houltona, A.; Horrocks, B. R. Immobilisation of Proteins at Silicon Surfaces Using Undecenylaldehyde: Demonstration of the Retention of Protein Functionality and Detection Strategies. *Analyst* **2009,** *134*, 593-601.

(170) Perez, E.; Lahlil, K.; Rougeau, C.; Moraillon, A.; Chazalviel, J.-N. l.; Ozanam, F.; Gouget-Laemmel, A. C. Influence of the Molecular Design on the Antifouling Performance of Poly(ethylene glycol) Monolayers Grafted on (111) Si. *Langmuir* **2012,** *28*, 14654-14664.

(171) Cecchet, F.; DeMeersman, B.; Demoustier-Champagne, S.; Nysten, B.; Jonas, A. M. One Step Growth of Protein Antifouling Surfaces: Monolayers of Poly(ethylene oxide) (PEO) Derivatives on Oxidized and Hydrogen-Passivated Silicon Surfaces. *Langmuir* **2006,** *22*, 1173-1181.

(172) Bierbaum, K.; Grunze, M.; Baski, A. A.; Chi, L. F.; Schrepp, W.; Fuchs, H. Growth of Self-Assembled n-Alkyltrichlorosilane Films on Si(100) Investigated by Atomic Force Microscopy. *Langmuir* **1995,** *11*, 2143-2150.

(173) Heise, A.; Stamm, M.; Rauscher, M.; Duschner, H.; Menzela, H. Mixed Silane Self Assembled Monolayers and Their in situ Modification. *Thin Solid Films* **1998,** *327-329*, 199-203.

(174) Zhong, Y. L.; Bernasek, S. L. Direct Photochemical Functionalization of Si(111) with Undecenol. *Langmuir* **2011,** *27* (5), 1796-1802.

(175) Barrelet, C. J.; Robinson, D. B.; Cheng, J.; Hunt, T. P.; Quate, C. F.; Chidsey, C. E. D. Surface Characterization and Electrochemical Properties of Alkyl, Fluorinated Alkyl, and Alkoxy Monolayers on Silicon. *Langmuir* **2001,** *17*, 3460-3465.

(176) Sweryda-Krawiec, B.; Cassagneau, T.; Fendler, J. H. Surface Modification of Silicon Nanocrystallites by Alcohols. *J. Phys. Chem. B* **1999,** *103*, 9524-9529.

(177) Moitra, N.; Kamei, T.; Kanamori, K.; Nakanishi, K.; Takeda, K.; Shimada, T. Recyclable Functionalization of Silica with Alcohols via Dehydrogenative Addition on Hydrogen Silsesquioxane. *Langmuir* **2013,** *29*, 12243-12253.

(178) Mingos, D. M. P.; Baghurst, D. R. Applications of Microwave Dielectric Heating Effects to Synthetic Problems in Chemistry. *Chem. Soc. Rev.* **1991,** *20*, 1-47.

(179) Druzhinina, T.; Weltjens, W.; Hoeppener, S.; Schubert, U. S. The Selective Heating of Iron Nanoparticles in a Single-Mode Microwave for the Patterned Growths of Carbon Nanofibers and Nanotubes. *Adv. Funct. Mater.* **2009,** *19*, 1287-1292.

(180) Lee, A. W. H.; Pilapil, B. K.; Ng, H. W.; Gates, B. D. Microwave Assisted Formation of Monoreactive Perfluoroalkylsilane-Based Self-Assembled Monolayers. *Chem. Commun.* **2015,** *51*, 2060-2063.

(181) Petit, A.; Delmotte, M.; Loupy, A.; Chazalviel, J.-N.; Ozanam, F.; Boukherroub, R. Microwave Effects on Chemical Functionalization of Hydrogen-Terminated Porous Silicon Nanostructures. *J. Phys. Chem. C* **2008,** *112*, 16622-16628.

(182) Boukherroub, R.; Petit, A.; Loupy, A.; Chazalviel, J.-N.; Ozanam, F. Microwave-Assisted Chemical Functionalization of Hydrogen-Terminated Porous Silicon Surfaces. *J. Phys. Chem. B* **2003,** *107*, 13459-13462.

(183) Vossen, D. L. J.; deDood, M. J. A.; vanDillen, T.; Zijlstra, T.; Drift, E. v. d.; Polman, A.; vanBlaaderen, A. Novel Method for Solution Growth of Thin Silica Films from Tetraethoxysilane. *Adv. Mater.* **2000,** *12* (19), 1434-1437.

(184) vandeKruijs, B. H. P.; Dressen, M. H. C. L.; Meuldijk, J.; Vekemans, J. A. J. M.; Hulshof, L. A. Microwave-Induced Electrostatic Etching: Generation of Highly Reactive Magnesium for Application in Grignard Reagent Formation. *Org. Biomol. Chem.* **2010,** *8*, 1688-1694.

(185) Corey, E. J.; Venkateswarlu, A. Protection of Hydroxyl Groups as tert-Butyldimethylsilyl Derivatives. *J. Am. Chem. Soc.* **1972,** *94* (17), 6190-6191.

(186) Aureau, D.; Rappich, J.; Moraillon, A.; Allongue, P.; Ozanam, F.; Chazalviel, J.-N. In Situ Monitoring of the Electronic Properties and the pH Stability of Grafted Si(1 1 1). *J. Electroanal. Chem.* **2010,** *646*, 33-42.

(187) Yu, J.; Guan, M.; Li, F.; Zhang, Z.; Wang, C.; Shu, C.; Wei, H.; Zhang, X.-E. Effects of Fullerene Derivatives on Bioluminescence and Application for Protease Detection. *Chem. Commun.* **2012,** *48*, 11011-11013.

(188) Glavan, A. C.; Martinez, R. V.; Subramaniam, A. B.; Yoon, H. J.; Nunes, R. M. D.; Lange, H.; Thuo, M. M.; Whitesides, G. M. Omniphobic "R^F Paper" Produced by Silanization of Paper with Fluoroalkyltrichlorosilanes *Adv. Funct. Mater.* **2014,** *24*, 60-70.

(189) Zenasni, O.; Jamison, A. C.; Lee, T. R. The Impact of Fluorination on the Structure and Properties of Self-Assembled Monolayer Films. *Soft Matter* **2013,** *9*, 6356-6370.

(190) Kim, J.-M.; Baek, C.-W.; Park, J.-H.; Shin, D.-S.; Lee, Y.-S.; Kim, Y.-K. Continuous Anti-Stiction Coatings Using Self-Assembled Monolayers for Gold Microstructures. *J. Micromech. Microeng.* **2002,** *12*, 688-695.

(191) Knieling, T.; Lang, W.; Benecke, W. Gas Phase Hydrophobisation of MEMS Silicon Structures with Self-Assembling Monolayers for Avoiding in-use Sticking. *Sens. Actuators, B* **2007,** *126*, 13-17.

(192) Santos, C. M.; Kumar, A.; Zhang, W.; Cai, C. Functionalization of Fluorous Thin Films via "Click" Chemistry. *Chem. Commun.* **2009**, 2854-2856.

(193) Klein, E.; Kerth, P.; Lebeau, L. Enhanced Selective Immobilization of Biomolecules onto Solid Supports Coated with Semifluorinated Self-Assembled Monolayers. *Biomaterials* **2008,** *29*, 204-214.

(194) Janssen, D.; DePalma, R.; Verlaak, S.; Heremans, P.; Dehaen, W. Static Solvent Contact Angle Measurements, Surface Free Energy and Wettability Determination of Various Self-Assembled Monolayers on Silicon Dioxide. *Thin Solid Films* **2006,** *515*, 1433-1438.

(195) Chen, J.; Wang, Z.; Oyola-Reynoso, S.; Gathiaka, S. M.; Thuo, M. Limits to the Effect of Substrate Roughness or Smoothness on the Odd−Even Effect in Wetting Properties of n-Alkanethiolate Monolayers. *Langmuir* **2015,** *31*, 7047-7054.

(196) Kim, E.-K.; Lee, C.-S.; Kim, S. S. Superhydrophobicity of Electrospray-Synthesized Fluorinated Silica Layers. *J. Colloid Interface Sci.* **2012,** *368*, 599-602.

(197) Yang, L.; Guihen, E.; Glennon, J. D. Alkylthiol Gold Nanoparticles in Sol-Gel-Based Open Tubular Capillary Electrochromatography. *J. Sep. Sci.* **2005,** *28*, 757-766.

(198) Zhang, Z.; Wang, Z.; Liao, Y.; Liu, H. Applications of Nanomaterials in Liquid Chromatography: Opportunities for Separation with High Efficiency and Selectivity. *J. Sep. Sci.* **2006,** *29*, 1872-1878.

(199) Kobayashi, K.; Kitagawa, S.; Ohtani, H. Development of Capillary Column Packed with Thiol-Modified Gold-Coated Polystyrene Particles and Its Selectivity for Aromatic Compounds. *J. Chromatogr. A* **2006,** *1110*, 95-101.

(200) Gross, G. M.; Nelson, D. A.; Grate, J. W.; Synovec, R. E. Monolayer-Protected Gold Nanoparticles as a Stationary Phase for Open Tubular Gas Chromatography. *Anal. Chem.* **2003,** *75*, 4558-4564.

(201) Wang, D.; Oleschuk, R. D.; Horton, J. H. Surface Modification of Poly(dimethylsiloxane) with a Perfluorinated Alkoxysilane for Selectivity toward Fluorous Tagged Peptides. *Langmuir* **2008,** *24*, 1080-1086.

(202) Wu, K.; Bailey, T. C.; Willson, C. G.; Ekerdt, J. G. Surface Hydration and Its Effect on Fluorinated SAM Formation on SiO_2 Surfaces. *Langmuir* **2005,** *21*, 11795-11801.

(203) Zenasni, O.; Marquez, M. D.; Jamison, A. C.; Lee, H. J.; Czader, A.; Lee, T. R. Inverted Surface Dipoles in Fluorinated Self-Assembled Monolayers. *Chem. Mater.* **2015,** *27*, 7433-7446.

(204) Kim, H. I.; Graupe, M.; Oloba, O.; Koini, T.; Imaduddin, S.; Lee, T. R.; Perry, S. S. Molecularly Specific Studies of the Frictional Properties of Monolayer Films: A Systematic Comparison of CF_3-, $(CH_3)_2CH$-, and CH_3-Terminated Films. *Langmuir* **1999,** *15*, 3179-3185.

(205) Li, S.; Cao, P.; Colorado, R.; Yan, X.; Wenzl, I.; Shmakova, O. E.; Graupe, M.; Lee, T. R.; Perry, S. S. Local Packing Environment Strongly Influences the Frictional Properties of Mixed CH_3- and CF_3-Terminated Alkanethiol SAMs on Au(111). *Langmuir* **2005,** *21*, 933-936.

(206) Zenasni, O.; Jamison, A. C.; Marquez, M. D.; Lee, T. R. Self-Assembled Monolayers on Gold Generated from Terminally Perfluorinated Alkanethiols Bearing Propyl vs. Ethyl Hydrocarbon Spacers. *J. Fluorine Chem.* **2014,** *168*, 128-136.

(207) Tamada, K.; Ishida, T.; Knoll, W.; Fukushima, H. Molecular Packing of Semifluorinated Alkanethiol Self-Assembled Monolayers on Gold: Influence of Alkyl Spacer Length. *Langmuir* **2001,** *17*, 1913-1921.

(208) Lee, A. W. H.; Gates, B. D. Rapid Covalent Modification of Silicon Oxide Surfaces through Microwave-Assisted Reactions with Alcohols. *Langmuir* **2016,** *32*, 7284-7293.

(209) Yu, X.; Hantsche, H. Some Aspects of the Charging Effect in Monochromatized Focused XPS. *Fresenius J. Anal. Chem.* **1993,** *346*, 233-236.

(210) Briggs, D.; Beamson, G. *High Resolution XPS of Organic Polymers: The Scienta ESCA300 Database*; John Wiley & Sons: Chichester, U.K., 1992.

(211) Venkataraman, N. V.; Zurcher, S.; Rossi, A.; Lee, S.; Naujoks, N.; Spencer, N. D. Spatial Tuning of the Metal Work Function by Means of Alkanethiol and Fluorinated Alkanethiol Gradients. *J. Phys. Chem. C* **2009,** *113*, 5620-5628.

(212) Fujihira, M.; Tani, Y.; Furugori, M.; Akiba, U.; Okabe, Y. Chemical Force Microscopy of Self-Assembled Monolayers on Sputtered Gold Films Patterned by Phase Separation. *Ultramicroscopy* **2001,** *86*, 63-73.

(213) Fujihira, M. Kelvin Probe Force Microscopy of Molecular Surfaces. *Annu. Rev. Mater. Sci.* **1999,** *29*, 353-380.

(214) Hayes, W. A.; Kim, H.; Yue, X.; Perry, S. S.; Shannon, C. Nanometer-Scale Patterning of Surfaces Using Self-Assembly Chemistry. 2. Preparation, Characterization, and Electrochemical Behavior of Two-Component Organothiol Monolayers on Gold Surfaces. *Langmuir* **1997,** *13*, 2511-2518.

(215) Stranick, S. J.; Atre, S. V.; Parikh, A. N.; Wood, M. C.; Allara, D. L.; Winograd, N.; Weiss, P. S. Nanometer-Scale Phase Separation in Mixed Composition Self-Assembled Monolayers. *Nanotechnology* **1996,** *7*, 438-442.

(216) Salaita, K.; Amarnath, A.; Maspoch, D.; Higgins, T. B.; Mirkin, C. A. Spontaneous "Phase Separation" of Patterned Binary Alkanethiol Mixtures. *J. Am. Chem. Soc.* **2005,** *127*, 11283-11287.

(217) Yagi, K.; Fujihira, M. Study of Mixed Langmuir–Blodgett Films of Hydrocarbon and Fluorocarbon Amphiphilic Compounds by Scanning Surface Potential Microscopy and Friction Force Microscopy. *Appl. Surf. Sci.* **2000,** *157*, 405-411.

(218) Yamada, R.; Wano, H.; Uosaki, K. Effect of Temperature on Structure of the Self-Assembled Monolayer of Decanethiol on Au(111) Surface. *Langmuir* **2000,** *16*, 5523-5525.

(219) Bumm, L. A.; Arnold, J. J.; Charles, L. F.; Dunbar, T. D.; Allara, D. L.; Weiss, P. S. Directed Self-Assembly to Create Molecular Terraces with Molecularly Sharp Boundaries in Organic Monolayers. *J. Am. Chem. Soc.* **1999,** *121*, 8017-8021.

(220) Ballav, N.; Terfort, A.; Zharnikov, M. Mixing of Nonsubstituted and Partly Fluorinated Alkanethiols in a Binary Self-Assembled Monolayer. *J. Phys. Chem. C* **2009,** *113*, 3697-3706.

(221) Wu, K.-Y.; Yu, S.-Y.; Tao, Y.-T. Continuous Modulation of Electrode Work Function with Mixed Self-Assembled Monolayers and Its Effect in Charge Injection. *Langmuir* **2009,** *25* (11), 6232-6238.

(222) Alves, C. A.; Porter, M. D. Atomic Force Microscopic Characterization of a Fluorinated Alkanethiolate Monolayer at Gold and Correlations to Electrochemical and Infrared Reflection Spectroscopic Structural Descriptions. *Langmuir* **1993,** *9*, 3507-3512.

(223) Shaporenko, A.; Cyganik, P.; Buck, M.; Ulman, A.; Zharnikov, M. Self-Assembled Monolayers of Semifluorinated Alkaneselenolates on Noble Metal Substrates. *Langmuir* **2005,** *21*, 8204-8213.

(224) Fan, F.-R. F.; Yang, J.; Cai, L.; Price, D. W.; Dirk, S. M.; Kosynkin, D. V.; Yao, Y.; Rawlett, A. M.; Tour, J. M.; Bard, A. J. Charge Transport through Self-Assembled Monolayers of Compounds of Interest in Molecular Electronics. *J. Am. Chem. Soc.* **2002,** *124*, 5550-5560.

(225) DiBenedetto, S. A.; Facchetti, A.; Ratner, M. A.; Marks, T. J. Molecular Self-Assembled Monolayers and Multilayers for Organic and Unconventional Inorganic Thin-Film Transistor Applications. *Adv. Mater.* **2009,** *21*, 1407-1433.

(226) Gau, J.-J.; Lan, E. H.; Dunn, B.; Ho, C.-M.; Woo, J. C. S. A MEMS Based Amperometric Detector for E. Coli Bacteria Using Self-Assembled Monolayers. *Biosens. Bioelectron.* **2001,** *16*, 745-755.

(227) Lee, A. W. H.; Gates, B. D. Tuning Oleophobicity of Silicon Oxide Surfaces with Mixed Monolayers of Aliphatic and Fluorinated Alcohols. *Langmuir* **2016,** *32*, 13030-13039.

(228) Ton-That, C.; Shard, A. G.; Bradley, R. H. Thickness of Spin-Cast Polymer Thin Films Determined by Angle-Resolved XPS and AFM Tip-Scratch Methods. *Langmuir* **2000,** *16*, 2281-2284.

(229) Hill, J. M.; Royce, D. G.; Fadley, C. S.; Wagner, L. F.; Grunthaner, F. J. Properties of Oxidized Silicon as Determined by Angular-Dependent X-ray Photoelectron Spectroscopy. *Chem. Phys. Lett.* **1976,** *44* (2), 225-231.

(230) Love, J. C.; Estroff, L. A.; Kriebel, J. K.; Nuzzo, R. G.; Whitesides, G. M. Self-Assembled Monolayers of Thiolates on Metals as a Form of Nanotechnology. *Chem. Rev.* **2005,** *105*, 1103-1169.

(231) Zhang, Q.; Huang, H.; He, H.; Chen, H.; Shao, H.; Liu, Z. Determination of Locations of Sulfur, Amide-Nitrogen and Azo-Nitrogen in Self-Assembled Monolayers of Alkanethiols and Azobenzenethiols on Au (111) and GaAs (100) by Angle-Resolved X-ray Photoelectron Spectroscopy. *Surf. Sci.* **1999,** *1999*, 142-150.

(232) Merzlikin, S. V.; Tolkachev, N. N.; Strunskus, T.; Witte, G.; Glogowski, T.; Woll, C.; Grunert, W. Resolving the Depth Coordinate in Photoelectron Spectroscopy – Comparison of Excitation Energy Variation vs. Angular-Resolved XPS for the Analysis of a Self-Assembled Monolayer Model System. *Surf. Sci.* **2008,** *602*, 755-767.

(233) Porter, M. D.; Bright, T. B.; Allara, D. L.; Chidsey, C. E. D. Spontaneously Organized Molecular Assemblies. 4. Structural Characterization of n-Alkyl Thiol Monolayers on Gold by Optical Ellipsometry, Infrared Spectroscopy, and Electrochemistry. *J. Am. Chem. Soc.* **1986,** *109*, 3559-3573.

(234) Huang, X.; Huang, H.; Wu, N.; Hu, R.; Zhu, T.; Liu, Z. Investigation of Structure and Chemical States of Self-Assembled Au Nanoscale Particles by Angle-Resolved X-ray Photoelectron Spectroscopy. *Surf. Sci.* **2000,** *183-190*.

(235) Tidswell, I. M.; Ocko, B. M.; Pershan, P. S.; Wasserman, S. R.; Whitesides, G. M.; Axe, J. D. X-ray Specular Reflection Studies of Silicon Coated by Organic Mono]ayers (Alkylsiloxanes). *Phys. Rev. B: Condens. Matter* **1990,** *41*, 1111-1128.

(236) Srivastava, S.; Solanki, P. R.; Kaushik, A.; Md.Ali, A.; Srivastava, A.; Malhotra, B. D. A Self Assembled Monolayer Based Microfluidic Sensor for Urea Detection. *Nanoscale* **2011,** *3*, 2971-2977.

(237) Linford, M. R.; Fenter, P.; Eisenberger, P. M.; Chidsey, C. E. D. Alkyl Monolayers on Silicon Prepared from 1-Alkenes and Hydrogen-Terminated Silicon. *J. Am. Chem. Soc.* **1995,** *117*, 3145-3155.

(238) Lange, S. C.; vanAndel, E.; Smulders, M. M. J.; Zuilhof, H. Efficient and Tunable Three-Dimensional Functionalization of Fully Zwitterionic Antifouling Surface Coatings. *Langmuir* **2016,** *32*, 10199-10205.

(239) Alonso, J. M.; Bielen, A. A. M.; Olthuis, W.; Kengen, S. W. M.; Zuilhof, H.; Franssen, M. C. R. Self-Assembled Monolayers of 1-alkenes on Oxidized Platinum Surfaces as Platforms for Immobilized Enzymes for Biosensing. *Appl. Surf. Sci.* **2016,** *383*, 283-293.

(240) Zaba, T.; Noworolska, A.; Bowers, C. M.; Breiten, B.; Whitesides, G. M.; Cyganik, P. Formation of Highly Ordered Self-Assembled Monolayers of Alkynes on Au(111) Substrate. *J. Am. Chem. Soc.* **2014,** *136*, 11918-11921.

(241) Chen, J.; Franking, R.; Ruther, R. E.; Tan, Y.; He, X.; Hogendoorn, S. R.; Hamers, R. J. Formation of Molecular Monolayers on TiO_2 Surfaces: A Surface Analogue of the Williamson Ether Synthesis. *Langmuir* **2011,** *27*, 6879-6889.

(242) Pujari, S. P.; vanAndel, E.; Yaffe, O.; Cahen, D.; Weidner, T.; vanRijn, C. J. M.; Zuilhof, H. Mono-Fluorinated Alkyne-Derived SAMs on Oxide-Free Si(111) Surfaces: Preparation, Characterization and Tuning of the Si Workfunction. *Langmuir* **2013,** *29*, 570-580.

(243) Scheres, L.; Giesbers, M.; Zuilhof, H. Self-Assembly of Organic Monolayers onto Hydrogen-Terminated Silicon: 1-Alkynes Are Better Than 1-Alkenes. *Langmuir* **2010,** *26*, 10924-10929.

(244) Paoprasert, P.; Kandala, S.; Sweat, D. P.; Ruther, R.; Gopalan, P. Versatile Grafting Chemistry for Creation of Stable Molecular Layers on Oxides. *J. Mater. Chem.* **2012,** *22*, 1046-1053.

(245) Henderson, R. K.; Jimenez-Gonzalez, C.; Constable, D. J. C.; Alston, S. R.; Inglis, G. G. A.; Fisher, G.; Sherwood, J.; Binks, S. P.; Curzons, A. D. Expanding GSK's Solvent Selection Guide – Embedding Sustainability into Solvent Selection Starting at Medicinal Chemistry. *Green Chem.* **2011,** *13*, 854-862.

(246) Patschinski, P.; Zhang, C.; Zipse, H. The Lewis Base-Catalyzed Silylation of Alcohols-A Mechanistic Analysis. *J. Org. Chem.* **2014,** *79*, 8348-8357.

(247) Ballarin, B.; Barreca, D.; Cassani, M. C.; Carraro, G.; Maccato, C.; Mignani, A.; Lazzari, D.; Bertola, M. Fluoroalkylsilanes with Embedded Functional Groups as Building Blocks for Environmentally Safer Self-Assembled Monolayers. *Langmuir* **2015,** *31*, 6988-6994.

(248) Motta, A.; Cannelli, O.; Boccia, A.; Zanoni, R.; Raimondo, M.; Caldarelli, A.; Veronesi, F. A Mechanistic Explanation of the Peculiar Amphiphobic Properties of Hybrid Organic−Inorganic Coatings by Combining XPS Characterization and DFT Modeling. *ACS Appl. Mater. Interfaces* **2015,** *7*, 19941-19947.

(249) Chinwangso, P.; Lee, H. J.; Lee, T. R. Self-Assembled Monolayers Generated from Unsymmetrical Partially Fluorinated Spiroalkanedithiols. *Langmuir* **2015,** *31*, 13341-13349.

(250) Kovach, K. M.; Capadon, J. R.; Gupta, A. S.; Potkay, J. A. The Effects of PEG-based Surface Modification of PDMS Microchannels on Long-Term Hemocompatibility. *J. Biomed. Mater. Res. A* **2014,** *102*, 4195-4205.

(251) Britcher, L.; Barnes, T. J.; Griesser, H. J.; Prestidge, C. A. PEGylation of Porous Silicon Using Click Chemistry. *Langmuir* **2008,** *24*, 7625-7627.

(252) Mahapatro, A.; Johnson, D. M.; Patel, D. N.; Feldman, M. D.; Ayon, A. A.; Agrawal, C. M. Surface Modification of Functional Self-Assembled Monolayers on 316L Stainless Steel via Lipase Catalysis. *Langmuir* **2006,** *22*, 901-905.

(253) Rück-Braun, K.; Petersen, M. Å.; Michalik, F.; Hebert, A.; Przyrembel, D.; Weber, C.; Ahmed, S. A.; Kowarik, S.; Weinelt, M. Formation of Carboxy- and Amide-Terminated Alkyl Monolayers on Silicon(111) Investigated by ATR-FTIR, XPS, and X-ray Scattering: Construction of Photoswitchable Surfaces. *Langmuir* **2013,** *29*, 11758-11769.

(254) Hozumi, A.; Inagaki, M.; Shirahata, N. Vapor Phase Formation of a Well-Ordered Aldehyde-Terminated Self-Assembled Monolayer on a SiO_2 Surface and Formation of Silver Film on the Surface Based on the Silver Mirror Reaction. *Surf. Sci.* **2006,** *600*, 4044-4047.

(255) Schreiner, S. M.; Shudy, D. F.; Hatch, A. L.; Opdahl, A. Controlled and Efficient Hybridization Achieved with DNA Probes Immobilized Solely through Preferential DNA-Substrate Interactions. *Anal. Chem.* **2010,** *82*, 2803-2810.

(256) Niedziałkowski, P.; Bogdanowicz, R.; Zieba, P.; Wysocka, J.; Ryl, J.; Sobaszek, M.; Ossowski, T. Melamine-modified Boron-doped Diamond towards Enhanced Detection of Adenine, Guanine and Caffeine. *Electroanal.* **2016,** *28*, 211-221.

(257) Huang, C.-J.; Chang, Y.-C. In Situ Surface Tailoring with Zwitterionic Carboxybetaine Moieties on Self-Assembled Thin Film for Antifouling Biointerfaces. *Materials* **2014,** *7*, 130-142.

(258) Li, J.; Zhang, Y.; Yang, J.; Tan, H.; Li, J.; Fu, Q. Synthesis and Surface Properties of Polyurethane End-Capped with Hybrid Hydrocarbon/Fluorocarbon Double-Chain Phospholipid. *Journal of Biomedical Material Research A* **2013,** *101*, 1362-1372.

(259) Clements, J. H. Reactive Applications of Cyclic Alkylene Carbonates. *Ind. Eng. Chem. Res.* **2003,** *42*, 663-674.

(260) Feng, X.; Jiang, L. Design and Creation of Superwetting/Antiwetting Surfaces. *Adv. Mater.* **2006,** *18*, 3063-3078.

(261) Ghosh, A.; Beaini, S.; Zhang, B. J.; Ganguly, R.; Megaridis, C. M. Enhancing Dropwise Condensation through Bioinspired Wettability Patterning. *Langmuir* **2014,** *30*, 13103-13115.

(262) Park, K.-C.; Chhatre, S. S.; Srinivasan, S.; Cohen, R. E.; McKinley, G. H. Optimal Design of Permeable Fiber Network Structures for Fog Harvesting. *Langmuir* **2013,** *29*, 13269-13277.

(263) Bai, H.; Ju, J.; Sun, R.; Chen, Y.; Zheng, Y.; Jiang, L. Controlled Fabrication and Water Collection Ability of Bioinspired Artificial Spider Silks. *Adv. Mater.* **2011,** *23*, 3708-3711.

(264) Shirtcliffe, N. J.; McHale, G.; Newton, M. I. The Superhydrophobicity of Polymer Surfaces: Recent Developments. *J. Polym. Sci., Part B: Polym. Phys.* **2011,** *49*, 1203-1217.

(265) Yao, X.; Song, Y.; Jiang, L. Applications of Bio-Inspired Special Wettable Surfaces. *Adv. Mater.* **2011,** *23*, 719-734.

Appendix A.

Tabulated Contact Angle Measurements

This section outlines the numerical values of contact angle measurements performed throughout the thesis. The values of WCA include averages of advancing and receding contact angle values, standard deviation, as well as the hysteresis values.

A1. Tabulated WCA Measurements for Figure 3.1

1) **Native oxide** coated polished silicon substrates after a microwave induced reaction with 1-octanol. (Figure 3.1A)

Table A1.1. Water Contact Angle (WCA) Values before Soxhlet Extraction

microwave radiation time (min)	average advancing WCA (°)	standard deviation (°)	average receding WCA (°)	hysteresis (°)
1	100	1	96	4
3	106	2	101	5
5	108	2	103	5
10	111	1	109	2
20	109	2	108	1
30	111	1	107	4

Table A1.2. Water Contact Angle (WCA) Values after One Hour of Soxhlet Extraction

microwave radiation time (min)	average advancing WCA (°)	standard deviation (°)	average receding WCA (°)	hysteresis (°)
1	97	2	93	4
3	103	1	101	2
5	97	3	92	5
10	107	2	105	2
20	107	1	103	4
30	111	1	107	4

Table A1.3. Water Contact Angle (WCA) Values after Five Hours of Soxhlet Extraction

microwave radiation time (min)	average advancing WCA (°)	standard deviation (°)	average receding WCA (°)	hysteresis (°)
1	91	2	88	3
3	98	4	97	1
5	96	3	89	7
10	100	1	99	1
20	105	3	102	3
30	108	2	106	2

Table A1.4. Water Contact Angle (WCA) Values after Twenty Four Hours of Soxhlet Extraction

microwave radiation time (min)	average advancing WCA (°)	standard deviation (°)	average receding WCA (°)	hysteresis (°)
1	78	2	78	0
3	90	4	91	-1
5	84	3	82	2
10	95	2	92	3
20	99	2	100	-1
30	104	1	102	2

2) Polished silicon substrates with **100-nm thick oxide** after microwave induced reaction with 1-octanol. (Figure 3.1B)

Table A1.5. Water Contact Angle (WCA) Values before Soxhlet Extraction

microwave radiation time (min)	average advancing WCA (°)	standard deviation (°)	average receding WCA (°)	hysteresis (°)
1	100	1	97	3
3	103	3	100	3
5	103	2	97	6
10	106	2	102	4
20	105	1	98	7
30	108	1	105	3

Table A1.6. Water Contact Angle (WCA) Values after One Hour of Soxhlet Extraction

microwave radiation time (min)	average advancing WCA (°)	standard deviation (°)	average receding WCA (°)	hysteresis (°)
1	93	2	87	6
3	99	1	98	1
5	98	2	90	8
10	105	1	101	4
20	103	1	102	1
30	109	1	109	0

Table A1.7. Water Contact Angle (WCA) Values after Five Hours of Soxhlet Extraction

microwave radiation time (min)	average advancing WCA (°)	standard deviation (°)	average receding WCA (°)	hysteresis (°)
1	89	3	87	3
3	97	2	95	2
5	100	1	96	4
10	102	1	99	3
20	96	2	93	3
30	105	3	105	0

Table A1.8. Water Contact Angle (WCA) Values after Twenty Four Hours of Soxhlet Extraction

microwave radiation time (min)	average advancing WCA (°)	standard deviation (°)	average receding WCA (°)	hysteresis (°)
1	91	2	89	2
3	91	1	90	1
5	87	2	87	0
10	94	1	92	2
20	101	2	100	1
30	103	2	102	1

3) **Soda-lime glass** substrates after a microwave induced reaction with 1-octanol. (Figure 3.1C)

Table A1.9. Water Contact Angle (WCA) Values before Soxhlet Extraction

microwave radiation time (min)	average advancing WCA (°)	standard deviation (°)	average receding WCA (°)	hysteresis (°)
1	95	2	94	1
3	100	2	98	2
5	106	2	103	3
10	107	2	104	3
20	99	2	97	2
30	106	1	104	2

Table A1.10. Water Contact Angle (WCA) Values after One Hour of Soxhlet Extraction

microwave radiation time (min)	average advancing WCA (°)	standard deviation (°)	average receding WCA (°)	hysteresis (°)
1	67	2	70	-3
3	83	2	81	2
5	87	2	86	1
10	91	1	89	2
20	89	1	87	1
30	95	1	93	2

Table A1.11. Water Contact Angle (WCA) Values after Five Hours of Soxhlet Extraction

microwave radiation time (min)	average advancing WCA (°)	standard deviation (°)	average receding WCA (°)	hysteresis (°)
1	53	5	49	4
3	74	2	68	6
5	62	5	61	1
10	79	1	79	0
20	80	1	78	2
30	87	3	87	0

Table A1.12. Water Contact Angle (WCA) Values after Twenty Four Hours of Soxhlet Extraction

microwave radiation time (min)	average advancing WCA (°)	standard deviation (°)	average receding WCA (°)	hysteresis (°)
1	44	2	45	-1
3	65	4	63	2
5	63	5	62	1
10	75	4	75	0
20	72	2	73	-1
30	79	3	79	0

4) **Polished quartz** substrates after a microwave induced reaction with 1-octanol. (Figure 3.1D)

Table A1.13. Water Contact Angle (WCA) Values before Soxhlet Extraction

microwave radiation time (min)	average advancing WCA (°)	standard deviation (°)	average receding WCA (°)	hysteresis (°)
1	91	1	92	-1
3	93	7	87	6
5	104	1	104	0
10	108	1	107	1
20	110	2	106	4
30	109	1	109	0

Table A1.14. Water Contact Angle (WCA) Values after One Hour of Soxhlet Extraction

microwave radiation time (min)	average advancing WCA (°)	standard deviation (°)	average receding WCA (°)	hysteresis (°)
1	93	1	92	1
3	92	2	85	7
5	102	2	102	0
10	109	1	108	1
20	109	1	109	0
30	110	2	108	2

Table A1.15. Water Contact Angle (WCA) Values after Five Hours of Soxhlet Extraction

microwave radiation time (min)	average advancing WCA (°)	standard deviation (°)	average receding WCA (°)	hysteresis (°)
1	92	1	90	2
3	98	5	94	4
5	106	2	103	3
10	108	2	104	4
20	109	1	107	2
30	108	1	108	0

Table A1.16. Water Contact Angle (WCA) Values after Twenty Four Hours of Soxhlet Extraction

microwave radiation time (min)	average advancing WCA (°)	standard deviation (°)	average receding WCA (°)	hysteresis (°)
1	92	2	90	2
3	92	2	90	2
5	100	1	102	-2
10	108	2	106	2
20	109	1	107	2
30	108	1	108	0

A2. Tabulated Contact Angle Measurements for Figure 4.2 and 4.5

Results are tabulated below for contact angles corresponding to the data in Figure 4.2. The tabulated results include an average and a standard deviation of five advancing contact angle values, an average of four receding contact angle values and the calculated hysteresis.

Table A2.1. Water Contact Angle Values after the Microwave Reaction

compound	average advancing WCA (°)	standard deviation (°)	average receding WCA (°)	hysteresis (°)
1	91	1.6	91	0
2	90	3.1	87	3
3	109	1.5	108	1
4	102	3.0	101	1

Table A2.2. Toluene Contact Angle Values after the Microwave Reaction

compound	average advancing CA (°)	standard deviation (°)	average receding CA (°)	hysteresis (°)
1	35	3.2	34	1
2	48	2.9	45	3
3	78	3.2	77	1
4	32	1.1	31	1

Table A2.3. Hexadecane Contact Angle Values after the Microwave Reaction

compound	average advancing CA (°)	standard deviation (°)	average receding CA (°)	hysteresis (°)
1	50	2.2	49	1
2	55	3.0	53	2
3	78	2.5	79	-1
4	24	2.2	23	1

Results are tabulated below for the contact angles reported in Figure 4.5. The tabulated results contain an average of five advancing contact angle values, an average of four receding contact angle values, and the calculated hysteresis.

Table A2.4. Water Contact Angle Values after Microwave Reactions to Form Mixed Monolayers

molar ratio of compound 4 (%)	average advancing WCA (°)	standard deviation (°)	average receding WCA (°)	hysteresis (°)
0	109	1.5	108	1
20	109	1.9	105	4
25	110	1.5	108	3
33	108	1.7	109	-1
50	106	2	105	1
67	108	2.0	107	1
100	102	3.0	101	1

Table A2.5. Toluene Contact Angle Values after Microwave Reactions to Form Mixed Monolayers

molar ratio of compound 4 (%)	average advancing CA (°)	standard deviation (°)	average receding CA (°)	hysteresis (°)
0	78	3.2	77	1
20	49	4.5	45	4
25	53	2.4	52	1
33	52	1.3	51	1
50	45	1.5	45	0
67	46	2.0	45	1
100	32	1.1	31	1

Table A2.6. Hexadecane Contact Angle Values after Microwave Reactions to Form Mixed Monolayers

molar ratio of compound 4 (%)	average advancing CA (°)	standard deviation (°)	average receding CA (°)	hysteresis (°)
0	78	2.5	79	-1
20	55	1.6	54	1
25	54	2.7	52	2
33	53	2.3	52	1
50	44	1.8	43	1
67	41	1.9	40	1
100	24	2.2	23	1

A3. Tabulated WCA Measurements for Figure 6.4, 6.6, and 6.7

Results are tabulated below for the water contact angle values reported in Figure 6.4.

Table A3.1. Water Contact Angle Values for Silicon Oxide Surfaces after Reacting with 600 mM 1-Octanol in Propylene Carbonate at a Reaction Temperature of 50 °C

reaction time (h)	average advancing WCA (°)	standard deviation (°)	average receding WCA (°)	hysteresis (°)
1	58	1.5	54	4
3	70	1.5	64	6
5	82	3.1	78	4
24	102	2.7	99	3
48	107	1.9	105	2
72	110	1.5	108	2

Table A3.2. Water Contact Angle Values for Silicon Oxide Surfaces after Reacting with 600 mM 1-Octanol in Propylene Carbonate at a Reaction Temperature of 100 °C

reaction time (h)	average advancing WCA (°)	standard deviation (°)	average receding WCA (°)	hysteresis (°)
1	91	2.5	90	1
3	96	1.9	94	2
5	99	1.9	97	2
24	108	2.6	106	2
48	109	0.4	108	1
72	110	2.3	108	2

Table A3.3. Water Contact Angle Values for Silicon Oxide Surfaces after Reacting with 600 mM 1-Octanol in Propylene Carbonate at a Reaction Temperature of 120 °C

reaction time (h)	average advancing WCA (°)	standard deviation (°)	average receding WCA (°)	hysteresis (°)
1	49	1.6	45	4
3	75	11	65	10
5	73	2.9	65	8
24	92	1.2	74	18
48	91	1.9	80	11
72	88	3.9	76	12

Results are tabulated below for the water contact angle values reported in Figure 6.6A.

Table A3.4. Water Contact Angle Values for Silicon Oxide Surfaces after Reacting with 60 mM 1-Octanol in Propylene Carbonate at a Reaction Temperature of 100 °C

reaction time (h)	average advancing WCA (°)	standard deviation (°)	average receding WCA (°)	hysteresis (°)
1	58	2.1	49	9
3	73	0.8	70	3
5	83	2.0	79	4
24	98	1.1	96	2
48	98	3.8	94	4
72	99	1.5	94	5

Table A3.5. Water Contact Angle Values for Silicon Oxide Surfaces after Reacting with 6 mM 1-Octanol in Propylene Carbonate at a Reaction Temperature of 100 °C

reaction time (h)	average advancing WCA (°)	standard deviation (°)	average receding WCA (°)	hysteresis (°)
1	36	1.7	19	17
3	47	1.6	32	15
5	47	3.6	28	19
24	61	2.4	42	19
48	61	2.6	51	10
72	67	2.2	65	2

Results are tabulated below for the water contact angle values reported in Figure 6.6B.

Table A3.6. Water Contact Angle Values for Silicon Oxide Surfaces after Reacting with 600 mM 1-Octanol in Propylene Carbonate with the Additional of 0.6 M Water at a Reaction Temperature of 50 °C

reaction time (h)	average advancing WCA (°)	standard deviation (°)	average receding WCA (°)	hysteresis (°)
1	37	5.7	19	18
3	38	2.3	24	14
5	39	1.6	35	4
24	63	4.0	64	-1
48	94	1.5	94	0
72	95	1.6	92	3

Table A3.6. Water Contact Angle Values for Silicon Oxide Surfaces after Reacting with 600 mM 1-Octanol in Propylene Carbonate with the Additional of 6.0 M Water at a Reaction Temperature of 50 °C

reaction time (h)	average advancing WCA (°)	standard deviation (°)	average receding WCA (°)	hysteresis (°)
1	25	4.0	5	20
3	21	1.1	8	13
5	22	0.5	5	17
24	12	0.9	5	7
48	16	1.4	5	9
72	11	1.5	4	7

Results are tabulated below for the water contact angle values reported in Figure 6.7A.

Table A3.7. Water Contact Angle Values for Silicon Oxide Surfaces after Reacting with 50 mM 1-Dodecanol in Propylene Carbonate at a Reaction Temperature of 100 °C

reaction time (h)	average advancing WCA (°)	standard deviation (°)	average receding WCA (°)	hysteresis (°)
1	68	1.1	67	2
3	79	1.8	76	4
5	89	1.1	86	3
24	100	1.1	95	5
48	103	2.4	97	5
72	109	1.1	103	6

Table A3.8. Water Contact Angle Values for Silicon Oxide Surfaces after Reacting with 50 mM 1-Tetradecanol in Propylene Carbonate at a Reaction Temperature of 100 °C

reaction time (h)	average advancing WCA (°)	standard deviation (°)	average receding WCA (°)	hysteresis (°)
1	75	0.5	72	3
3	95	2.1	91	4
5	101	2.0	99	3
24	106	0.8	104	2
48	110	1.5	108	2
72	109	1.3	107	2

Table A3.9. Water Contact Angle Values for Silicon Oxide Surfaces after Reacting with 50 mM 1-Hexadecanol in Propylene Carbonate at a Reaction Temperature of 100 °C

reaction time (h)	average advancing WCA (°)	standard deviation (°)	average receding WCA (°)	hysteresis (°)
1	87	1.8	85	2
3	100	1.7	98	2
5	105	1.1	103	2
24	110	0.8	109	2
48	110	1.1	107	2
72	110	0.4	110	0

Table A3.10. Water Contact Angle Values for Silicon Oxide Surfaces after Reacting with 50 mM 1-Octadecanol in Propylene Carbonate at a Reaction Temperature of 100 °C

reaction time (h)	average advancing WCA (°)	standard deviation (°)	average receding WCA (°)	hysteresis (°)
1	98	4.0	93	5
3	103	2.1	99	5
5	105	2.1	103	3
24	111	1.2	111	1
48	110	0.9	109	1
72	111	1.1	111	0

Appendix B.

Improving Quality of Alcohol Based Monolayers on Soda-Lime Glass Substrates by Sol-Gel Based Deposition of Silica Films

Quality of monolayers are largely compromised on soda-lime glass substrates likely due to the presence of surface impurities. To improve the quality of these monolayers, the substrates were pre-coated with a layer of silica obtained through sol-gel processing. Briefly, piranha cleaned substrates were immersed in a solution containing 31.6 g of ethanol, 3.2 g of deionized (DI) water, 2.7 g of an aqueous ammonium hydroxide solution (29% by weight), and 1.5 g of tetraethyl orthosilicate (TEOS). The reaction was stirred for 2 h before adding another 1.5 g of TEOS. After an additional 2 h of vigorous stirring, the substrates were removed from solution, washed with ethanol and DI water, and dried under a stream of nitrogen gas. These dried substrates were processed in a microwave oven while immersed in a neat solution of 1-octanol for 10 min. Finally, WCA values were measured both before and after 24 h of Soxhlet extraction (see methods described in the main text). As a control, a set of substrates were also prepared without the sol-gel derived silica layer on the soda-lime glass. Each set of substrates were prepared in duplicate to evaluate the reproducibility of the results. As depicted in Figure B1, the WCA values before and after Soxhlet extraction for the soda-lime glass substrates (without the additional sol-gel layer) indicate that a significant amount of 1-octanol were physically adsorbed on their surfaces. The hydrophobicity of these monolayers were compromised upon Soxhlet extraction. In contrast, the WCA values for the substrates coated with 1-octanol SAMs supported on a layer of sol-gel based silica demonstrated a minimal change in their hydrophobicity following the solvent extraction. Survey spectra obtained from X-ray photoelectron spectroscopy analysis for the substrates with or without the sol-gel based silica coatings (Figure B2) indicate that the impurities present on soda-lime glass were not present in the sol-gel coatings. In summary, deposition of an additional silica film prior to the formation of the monolayers can improve the overall quality of the resulting monolayers prepared on soda-lime glass substrates.

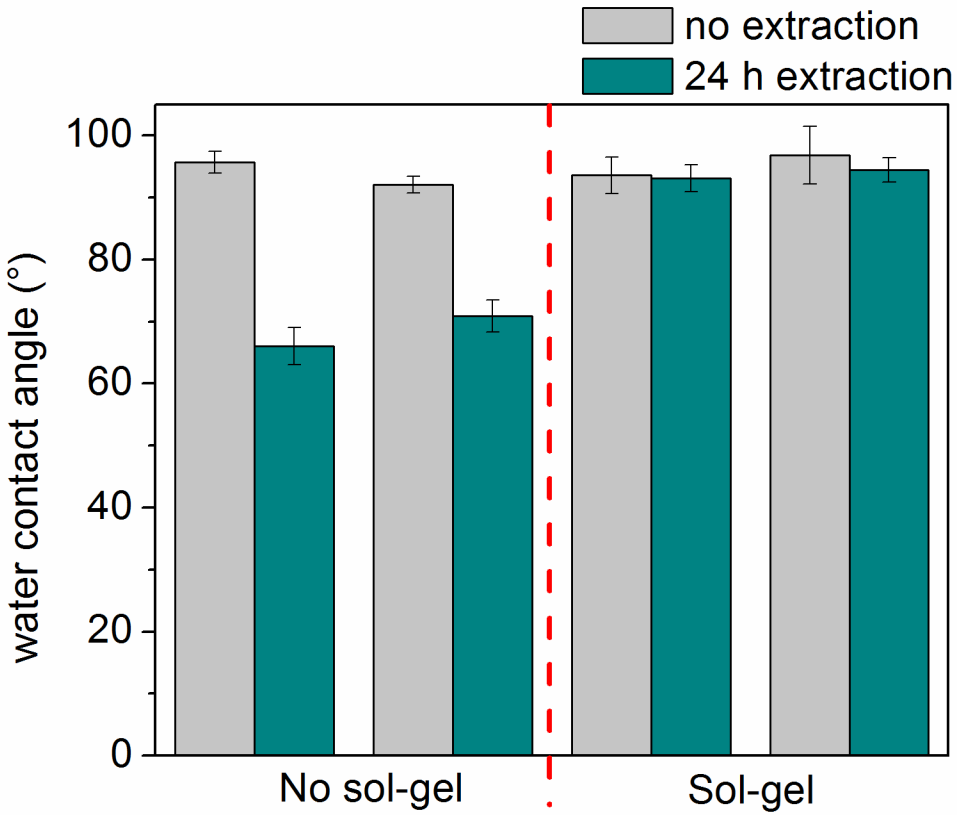

Figure B1. **Water contact angle (WCA) measurements performed on soda-lime glass substrates either (A) without or (B) with the addition of a sol-gel derived silica coating, each modified with a monolayer of 1-octanol. Reprinted with permission from Ref. [199] ©2016 American Chemical Society.**

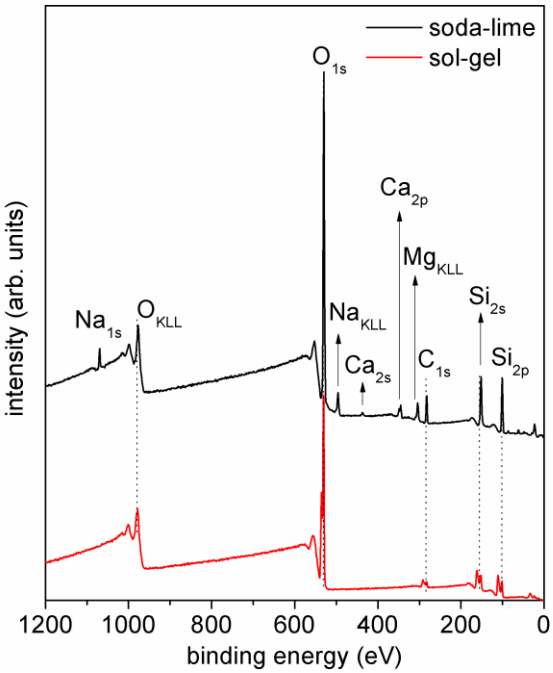

Figure B2. **Survey scans obtained by XPS analyses of soda-lime glass substrates either with or without the addition of a sol-gel derived silica coating. Reprinted with permission from Ref. [199] ©2016 American Chemical Society.**

Appendix C.

Insight into Thermal Degradation and Optimization of the Reaction Temperature

Microwave processing at high temperatures can induce thermal degradation. The change from a colorless, transparent solution to a light yellow, brown, or black coloration is an indication of thermal degradation of the reactant(s). Thermal degradation can lead to the deposition of white spots on the silicon substrates, which is another method of quickly discerning whether there was significant thermal degradation.

Initially, 180 °C was chosen as the reaction temperature, but there were multiple indications that the compounds were undergoing thermal degradation. For example, the color of the solution changed from clear to a transparent yellow. There were also white spots covering the surfaces of the substrates after the reaction. In addition, XPS analysis of the C_{1s} region showed unexpected peaks (Figure C1A) attributed to **C**=O and O**C**F_3. Lowering the reaction temperature to 150 °C reduced the observed thermal degradation with less color change to the solution and a lack of white spots on the substrates, but there was still at least one unexpected peak (e.g., C=O) observed in the XPS analyses (Figure C1B). The subsequent reaction temperature chosen for the Chapter 4 was 130 °C as the visual observations of the solutions and spectroscopic investigation of the substrates did not display any of the changes observed at the higher reaction temperatures.

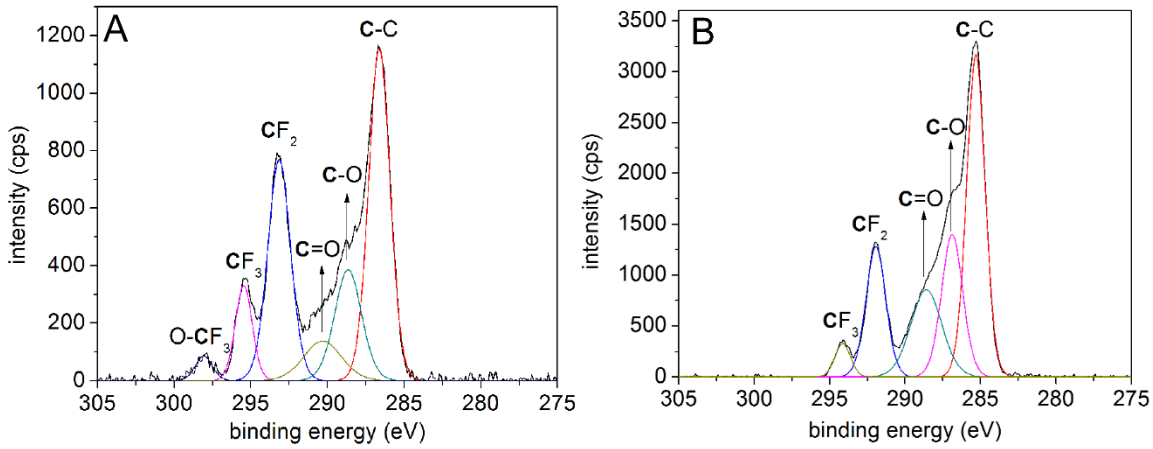

Figure C1. **High resolution C_{1s} XPS spectra of silicon substrates after a microwave assisted reaction of *1H,1H*-perfluoro-1-octanol at (A) 180 °C and (B) 150 °C. Reprinted with permission from Ref. [218] ©2016 American Chemical Society.**

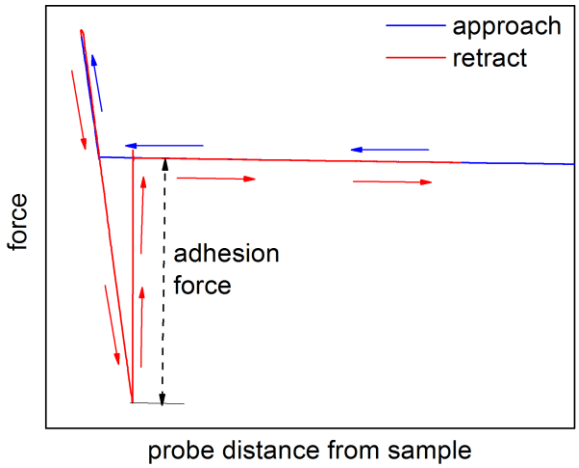

Figure C2. **A typical force-distance curve utilized for obtaining adhesion force measurements of the samples as determined from the interactions with the AFM tip.**

Appendix D.

Calculation of Molecular Lengths and ARXPS Measurements for Piranha Cleaned Silicon Substrates

The molecular chain lengths of each aliphatic alcohol was estimated from their molecular models projected in ChemDraw 3D (Figure D1). The Cartesian coordinates were determined for the oxygen atom and carbon atom at either end of these linear molecules (Table D1). The distance between these terminal atoms was calculated using the Pythagorean Theorem. Equation D.1 is the sample calculation for calculating the molecular length of 1-butanol.

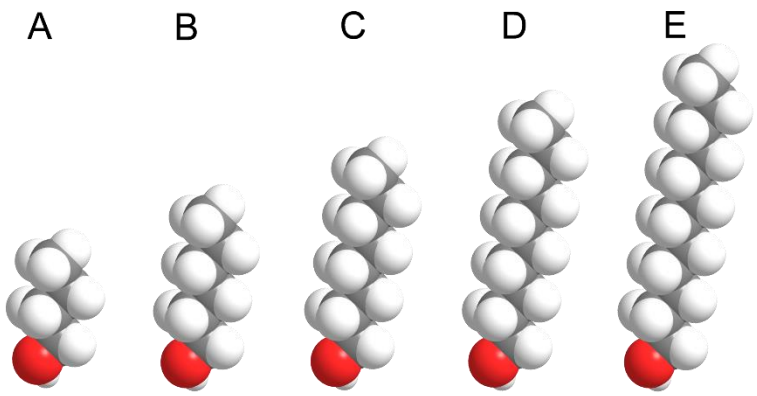

Figure D1. **ChemDraw models of (A) 1-butanol, (B) 1-hexanol, (C) 1-octanol, (D) 1-decanol, and (E) 1-dodecanol.**

Table D1. Coordinates and molecular length of the aliphatic alcohols used in the studies.

	Coordinates of O atom (Å)	Coordinates of C atom (Å)	Molecular length (Å)
1-butanol	(-15.32, -11.90, 0)	(-13.21, -16.30, 0)	4.9
1-hexanol	(-7.38, -6.93, 0)	(-4.07, -13.51, 0)	7.4
1-octanol	(0.63, -1.15, 0)	(4.82, -10.07, 0)	9.9
1-decanol	(7.34, 4.93, 0)	(12.57, -6.24, 0)	12
1-dodecanol	(-2.91,7.20, 0)	(3.36,-6.24, 0)	15

Sample calculation for determining the molecular length of 1-butanol is given by the following equation:

$$Distance = \sqrt{(x_O - x_C)^2 + (y_O - y_C)^2 + (z_O - z_C)^2}$$
$$= \sqrt{(-15.32 - (-13.21))^2 + (-11.90 - (-16.30))^2 + (0 - 0)^2} = 4.9\text{Å} \qquad \text{(D.1)}$$

where x_o, y_o, and z_o are the x,y, and z coordinates of the oxygen atom, respectively, and x_c, y_c, and z_c are the x,y, and z coordinates of the carbon atom, respectively.

Table D2. Angle resolved X-ray photoelectron spectroscopy (ARXPS) measurements for a piranha cleaned, polished silicon substrate covered with a native oxide film.

angle (°)	O_{1s} intensity (cps)	C_{1s} intensity (cps)	Si_{2p} intensity (cps)	Si/O ratio
0	233931.9	8620.0	165849.1	0.71
10	204169.6	8221.0	141901.0	0.70
20	171751.3	6670.0	109300.0	0.64
30	140306.9	5601.5	78981.5	0.56
40	110034.9	4387.7	53763.8	0.49
50	87770.0	2287.7	32150.1	0.37
60	70764.0	2598.5	20042.2	0.28
70	51195.6	2446.2	10242.6	0.20
80	18900.1	1110.8	2823.9	0.15

Table D3. Angle resolved X-ray photoelectron spectroscopy (ARXPS) measurements for a piranha cleaned, polished silicon substrate covered with a 100-nm thick thermally grown oxide film.

angle (°)	O_{1s} intensity (cps)	C_{1s} intensity (cps)	Si_{2p} intensity (cps)	Si/O ratio
0	695484.9	9529.2	129831.2	0.19
10	583210.8	6926.2	109547.6	0.19
20	462029.4	6037.7	89066.3	0.19
30	351603.7	4602.3	66096.4	0.19
40	261150.2	4148.5	47586.3	0.18
50	190976.6	4083.8	33532.1	0.18
60	133269.7	2822.3	23032.0	0.18
70	83385.2	2494.6	13655.1	0.16
80	30034.4	1256.2	4396.2	0.15

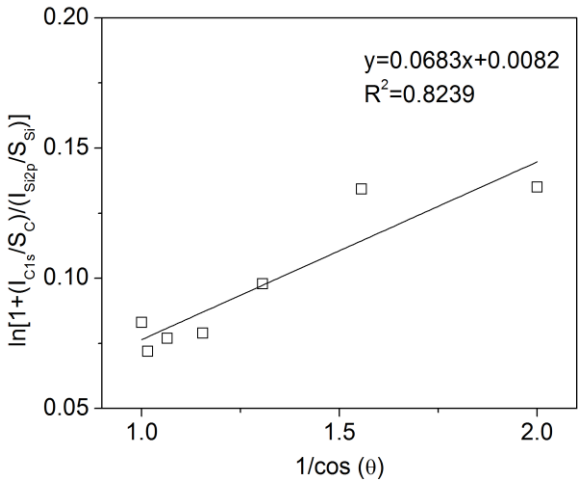

Figure D2. **The plot of $\ln(1+((I_{C1s}/S_C)/(I_{Si2p}/S_{Si}))$ vs. $1/\cos(\theta)$ for piranha cleaned silicon substrate covered with a 100-nm thick thermally grown oxide film. This data set was obtained from an ARXPS analysis between θ from 0° to 60° measurements taken at increments of 10°.**